WASM: Minerals, Energy and Chemical Engineering

Experimental and Numerical Study of Microwave Irradiation's Effect on Coal Petrophysical Property

Jinxin Huang

This thesis is presented for the Degree of
Doctor of Philosophy
of
Curtin University

August 2019

Declaration

To the best of my knowledge and belief this thesis contains no material previously published by any other person except where due acknowledgment has been made.

This thesis contains no material which has been accepted for the award of any other degree or diploma in any university.

This study does not have any human and animal ethics issue.

Signature:

Date: 13/08/2019

Acknowledgement

Studying as a PhD student in Curtin University was a memorable and meaningful experience to me. Many people provided precious support directly or indirectly during my PhD curriculum. Without their valuable help, it would be hardly possible for me to complete my PhD study in advance.

First of all, I would like to express my appreciation to my supervisor Dr. Guang Xu. Thanks for his great contribution in topic selection and paper revisions. I really appreciate his guidance in both academic career and daily life.

I would like to thank Prof. Guozhong Hu and China University of Mining and Technology for providing the experimental facilities in this study. I am grateful to postgraduate students Mr. Nan Yang, Mr. Chao Sun and Mr Jieqi Zhu for their assistance in my laboratory experiments.

I am extremely thankful to Prof. Mohammad Waqar Asad and Dr. Mehmet Cigla for providing me with TA positions. It was my great honour to work with you and to have your appreciation.

My special thanks to Revd. Dr. Elizabeth Smith and Mrs. Connie Klaassen for providing useful tips in improving my public speaking skills and for their great assistance in establishing WASM Speakers Club. I also thank the members of WASM Speakers Club for their regular attendance, and I wish they can keep it going after my departure.

Many thanks to my research group members, Dr. Xuhan Ding, Mrs. Yinping Chen, Mr. Ping Chang and Mr. Zidong Zhao for their assistance in both study and life. It was such a pleasure to have your company in Kalgoorlie. Thanks Dr. Bhrooz Rahimi for staying late at the office and keeping me from being alone.

I am also grateful to the staffs in WASM for their assistance in my PhD study. They are Prof. Sam Spearing, Prof. Chris Aldrich, Prof. Roger Thompson, Mrs. Raelene Newnham, Mrs. Lana McQueen, Mrs. Llesa Hawke, Ms Nichole Sik, Mrs. Avryl Pusey and Mrs. Debra Kerr.

I really appreciate the scholarship from Curtin University and the financial support from China Scholarship Council and Mining Education Australia. Thanks Mr. Wei Lin for offering me the job opportunity in Norton Gold Fields.

Finally, I would like to express my sincere gratitude to wife Jingsi Lin for her comprehension and support. I am really sorry for the three-year living apart. I will prove with the rest of my life that I am the one worth waiting for and the one makes her life full of love and happiness.

Abstract

Coalbed methane (CBM) is a clean energy source as well as a potential safety hazard in coal mining, and thus the exploitation of CBM is both necessary and meaningful. With the increase of mining depth, gas content increases while coal seam permeability decreases significantly, which causes big trouble to the gas extraction. Traditional methods in coal seam enhancement including hydraulic fracturing, enhanced coalbed methane recovery suffer from problems such as environmental pollution, high cost, low efficiency, low coverage and persistence. Therefore, an effective substitute method to enhance coal seam permeability is in a badly demand.

Recently, microwave heating is proposed as an alternative way to address this problem due to its benefits of environmentally friendly, wide applicable, selective heating and economical. Many researchers have investigated microwave irradiation's effect on coal petrophysical property. Laboratory experiments were conducted to observe the pore structure development under microwave irradiation using X-ray Computational Tomography (CT), Scanning Electron Microscope (SEM), and Nuclear Magnetic Resonance (NMR). It was found the pore size, pore number, connectivity and porosity of coal cores have obvious increase after microwave treatment. It was also found that microwave is extremely effective in coal dying and could be applied to deal with water blocking in coal reservoir. Numerical simulation was also introduced to study microwave's heating/fracturing effect on coal samples, whose influencing factors were made clear, such as microwave power, microwave frequency, and dielectric property of coal. However, there are still many limitations among previous studies. For laboratory experiments, few studies investigated moisture's effect on microwave heating/fracturing effect. Beyond that, most previous studies focused on the petrophysical variation after microwave treatment, while neglecting the microwave heating effect under various conditions. For numerical simulations, none of the previous numerical model for microwave heating of coal considered moisture vaporization, which do not represent the actual condition. Moreover, few numerical simulations studied microwave's effect on coal permeability at laboratory scale and field scale.

The aim of this thesis is to present comprehensive and in-depth study in microwave-assist coal seam enhancement. Firstly, a critical literature review is presented for coal permeability enhancement using microwave heating/fracturing. The mechanism and

advantages of microwave heating/fracturing were discussed in detail. Both experimental studies and numerical simulation in studying MI's effect on coal are summarized and reviewed. After studying the outstanding challenges for on-site application of microwave heating, the conceptual design of on-site microwave heating system is proposed. Then, a series of numerical simulations are carried out focus on the deficiency of previous models. A coupled electromagnetic irradiation, heat and mass transfer model for coal is proposed to consider moisture vaporization under microwave irradiation. Then, a coupled electromagnetic, thermal and mechanical model is established to study microwave's effect on coal permeability in laboratory scale and field scale. After that, a series of laboratory experiments are conducted to fill the research gap. The effect of microwave power, treatment time, and water saturation of coal on microwave fracturing effect are investigated with NMR and SEM. The microwave heating performance under various dielectric properties and water saturations of coal, and different microwave settings is also discussed in detail.

According to these studies, the mechanism of microwave heating/fracturing is made clear. The influence factors for microwave heating/fracturing are studies in detail. The innovative numerical models and detailed experiment results presented in this work could be very helpful to the field application of microwave-assist coal seam enhancement.

Abbreviations List

BET	Brunauer-Emmett-Teller
BVI	Bulk volume of irreducible
CBM	Coalbed methane
CPMG	Carr-Purcell-Meiboom-Gill
CT	Computational Tomography
ECBM	Enhanced coal bed methane
ICNIRP	International Commission on Non-Ionizing Radiation Protection
ISM	Industrial, scientific and medical
ITU	International Telecommunication Union
NMR	Nuclear Magnetic Resonance
MFPV	Macropore and fissure proportion variation
MH	Microwave heating
MI	Microwave irradiation
MICP	Mercury Injection Capillary Pressure
RF	Radiofrequency
SEM	Scanning Electron Microscope
TEGR	Thermally enhanced gas recovery
TII	Thermal Infrared Imagery
VMFP	Variation of macropore and fissure proportion
VRWP	Variation rate of water porosity
WHO	World Health Organization
XRD	X-ray diffraction

List of Publications Included in the Thesis

This thesis incorporates five journal papers and two conference papers. The copyright of these papers have been checked and they are applicable to be used in the thesis.

Journal Papers

1. Huang, J., Hu, G., Xu, G., Nie, B., Yang, N., & Xu, J. (2019). The development of microstructure of coal by microwave irradiation stimulation. *Journal of Natural Gas Science and Engineering, 66, 86-95.* https://doi.org/10.1016/j.jngse.2019.03.016
2. Huang, J., Xu, G., Hu, G., Kizil, M., & Chen, Z. (2018). A coupled electromagnetic irradiation, heat and mass transfer model for microwave heating and its numerical simulation on coal. *Fuel Processing Technology*, *177*, 237-245. https://doi.org/10.1016/j.fuproc.2018.04.034
3. Huang, J., Xu, G., Chen, Y., & Chen, Z. (2019). Simulation of microwave's heating effect on coal seam permeability enhancement. International Journal of Mining Science and Technology, 29(5), 785-789. https://doi.org/10.1016/j.ijmst.2018.04.017
4. Xu, G., Huang, J., Hu, G., Yang, N., & Zhu, J. (2019). Effective microwave heating of coal with various properties for thermally enhanced gas recovery. *Fuel* (Under review)
5. Huang, J., Xu, G., & Hu, G. (2019). Microwave heating applications in coal permeability enhancement—a review. *Science of the Total Environment.* (Preparing to submit)

Conference Papers

1. Huang, J., Xu, G., & Chang, P. (2019) Moisture content's effect on fracture development in coal under microwave irradiation. *Proceedings of the 17th North American Mine Ventilation Symposium*.

2. Huang, J., Xu, G., Chang, P., & Hu, G. (2019). A numerical model for coalbed methane reservoir enhancement using microwave heating. *Conference Proceedings - The Australian Mine Ventilation Conference 2019*.

Contents

List of Figures

List of Tables

1 Chapter 1

Outline

1. Background
2. Research Limitations and Objectives
3. Thesis Structure

1.1 Background

Coalbed methane is recognised as a promising cleaning fuel resource of worldwide importance and has already achieved commercial success in North America [1-3].

With the increase of mining depth, coal seam permeability decreases considerably due to the increasing effective stress, which makes big trouble to the coalbed methane exploitation. As enhanced permeability leads to higher coalbed methane production rate, lots of permeability enhancement methods have been applied on-site, including hydraulic fracturing [4], hydro-slotting [5, 6], blasting [7, 8] and so on. However, these methods cannot meet the production requirement due to their disadvantages: hydraulic fracturing is banned in some countries and regions because of environmental contamination [9]; hydro-slotting is not commonly used as it can only be applied in near-bore area and may result in water block; blasting is not economic and may cause gas explosion when hole sealing is ineffective. Enhanced coal bed methane (ECBM) recovery is another technique, which replaces coalbed methane with injected CO_2 or N_2 [10]. CO_2-ECBM is especially popular due to the additional benefit of sequestering huge amount of CO_2, which reduces the greenhouse effect and prevents global warming [11]. However, ECBM is only suitable for the coal seams with high initial permeability [12]. Many alternative methods were proposed to increase the coal seam permeability recently, including liquid nitrogen cooling[13], electrochemical treatment [14], ultrasonic wave excitation [15], partial coal pyrolysis [16], microbial stimulation [17], geothermal enhancement [18]. However, these methods suffer from problems such as high cost, low efficiency, low coverage and persistence.

Nowadays, interest was devoted to microwave heating to overcome these problems. Microwaves are electromagnetic waves ranged from 300 MHz to 300 GHz (wavelength ranging from 1 to 300 mm) [19, 20]. In the mid-1980s, researchers started to investigate microwave radiation on minerals [21]. Now, it has been widely used in coal pre-treatment and processing. The main purpose of coal permeability enhancement using microwave heating is to heat the coal reservoir and thus increase its permeability for coalbed methane. Coal is expected to be selectively heated under microwave irradiation (MI) due to its heterogeneous dielectric properties. The selective heating not only promotes coalbed methane desorption, but also induces thermal fractures.

In recent years, lots of laboratory experiments have been carried out to investigate the petrophysical variation of coals under microwave treatment. It was concluded that coal

permeability increased significantly for all the coals after microwave irradiation. However, few studies have investigated the moisture's effect on microwave heating of coal. To find suitable microwave parameters for field applications, numerical simulations were introduced to optimize the microwave power and frequency. However, none of these numerical models considered moisture vaporization and few of these models studies the variation of permeability under microwave irradiation. Moreover, most of these models simulated microwave heating of coal samples in microwave ovens, while simulations at field scale can be hardly found. Even though microwave heating is proved to be effective in the lab, it could be totally different when applying on-site. One of the major issues need to be addressed is that the penetration depth of microwave is very limited within coal reservoir, which means microwave attenuate quickly after entering coal body.

1.2 Research limitations and objectives

1.2.1 Research Limitations

Previous numerical simulations have the following major problems.

a. Previous numerical models in studying microwave heating of coal ignored phase change of moisture content and its latent heat of evaporation, which do not represent the actual condition.

b. Previous numerical models of microwave heating of coal neglected the accompanying thermal stress and its influence on coal seam permeability.

c. Most of the previous numerical simulations for microwave heating of coal were conducted in small scale. Few numerical simulations have been conducted to study the microwave heating effect on coal reservoir.

Previous laboratory experiments have the following major problems.

a. Few experiment studies have discussed the influence of coal's saturation conditions on its microwave heating/fracturing effect.

b. Few experiment data are available for microwave heating effect of coal core under various experiment conditions to verify the numerical models.

1.2.2 Objectives

Microwave heating is an alternative method to enhance coal seam permeability and thus gas productivity. Before applying this technology on-site, it is crucial to find out what factors may influence the microwave heating effect. To address this, numerical simulations and laboratory experiments were introduced to investigate the microwave heating/fracturing effect under different conditions in this study.

The objectives for numerical simulation are listed below.

a. Establish a 3D model coupling electromagnetic, heat and mass transfer for microwave heating of coal, which takes the moisture content into consideration.
b. Establish a coupled electric, heat transfer and mechanics model to study the microwave's heating effect on coal samples and to investigate the accompanying thermal stress's effect on permeability.
c. Establish a coupled electromagnetic, thermal and mechanical model for coal reservoir and study microwave's effect on coal seam permeability in large scale.

The objective for experimental studies is to fill the research gap in studying the microwave heating/fracturing effect under various coal conditions and microwave parameters, as listed below.

a. Conduct experiments to investigate the effects of microwave radiation on the microstructure of coal samples with different saturations under different microwave powers and microwave irradiation (MI) times.
b. Conduct experiments to study the influence factors for effective microwave heating of coal, including dielectric property and saturation of coal samples, microwave power and irradiation time.

1.3 Thesis structure

There are 9 chapters in this thesis. Chapter 1 presents the background, research limitations and the objectives of this study. Each chapter from Chapter 2 to chapter 8 is

developed by an independently published journal paper, a conference paper, a paper being under reviewed or a paper prepared to be submitted. In Chapter 9, the main findings from chapter 2 to chapter 8 were summarized. Limitations in current studies are discussed in detail and research focus for future works are proposed. The scheme of this thesis is as shown in Figure 1.

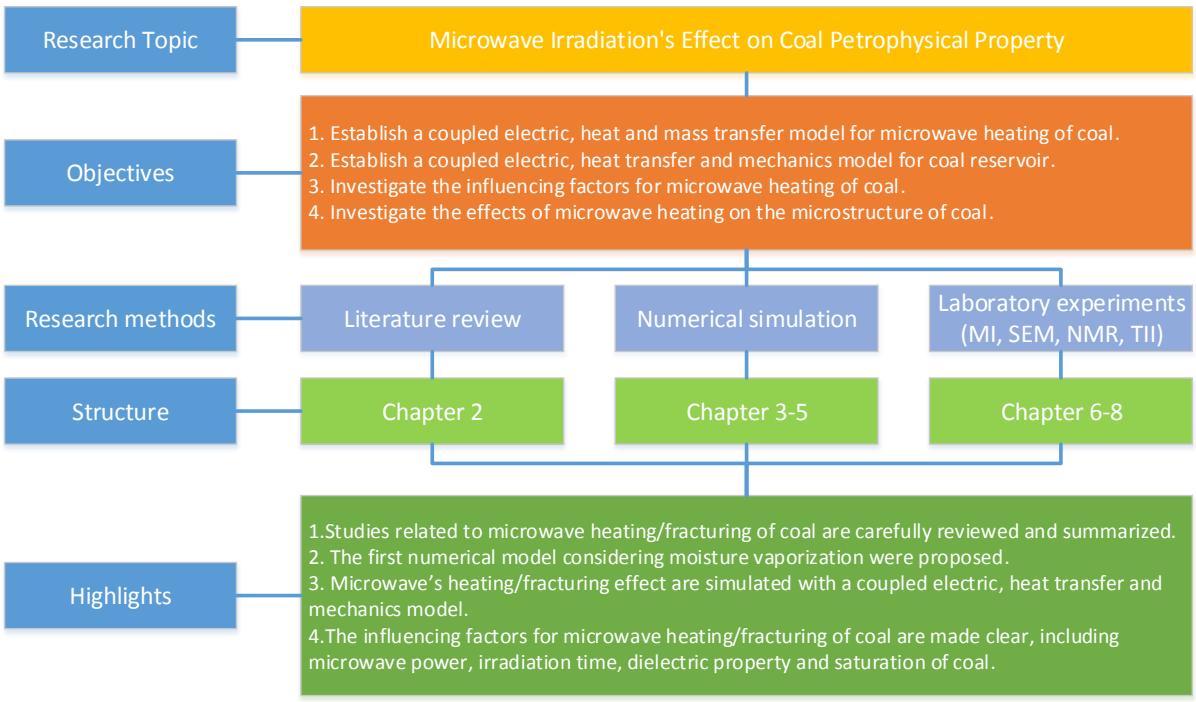

Figure 1. The flow chart of the thesis

Chapter 2 presented a critical review of the current studies of coal permeability enhancement using microwave heating/fracturing and discusses the feasibility of its on-site application. The mechanism and advantages of microwave heating/fracturing were explained in detail. Both experimental studies and numerical simulation in studying MI's effect on coal were summarized and reviewed, following by the discussion about the influencing factors on microwave fracturing effects. Finally, the outstanding challenges for on-site application of microwave heating were presented, and the conceptual design of on-site microwave heating system was proposed.

Chapter 3 to chapter 5 are numerical studies in microwave heating of coal, whose main content are summarized as follows: Chapter 3 proposed a coupled electromagnetic, heat and mass transfer model in studying microwave heating of coal. This microwave heating model firstly takes the moisture vaporization into consideration. After verified with previous experiment data, the temperature and electric field distribution of coal samples were analysed

in detail under different microwave frequencies, microwave powers and coal's moisture capacity.

Chapter 4 proposed a coupled electric, heat transfer and mechanics model in studying microwave heating of coal. The aim of this study is to investigate the accompanying thermal stress's effect on permeability under microwave irradiation.

Chapter 5 proposed a modified electromagnetic, thermal and mechanical model for coal reservoir. Based on the simulation results, the effect of microwave power on reservoir heating effect and the effect of treatment time on reservoir permeability development were made clear.

Chapter 6 to chapter 8 are laboratory experiments in studying the fissure development and heating effect under microwave irradiation, whose main content is summarized as follows: Chapter 6 investigated the effects of microwave irradiation on the pore development of coal samples with different saturations under various microwave powers and treatment times. NMR and SEM were conducted to compare the microstructure of coal before and after microwave treatment.

Chapter 7 studied water saturation's effect on fissure development of coal under microwave irradiation. High-resolution images were taken for the coal cores with different saturations (0%, 25%, 50%, 75% and 100%) before and after MI. The surface fissure areas were calculated and analysed through image processing.

Chapter 8 investigated the influencing factors for effective microwave heating of coal. Infrared thermal image system was applied to study the effect of dielectric property and saturation of coal samples, microwave power and irradiation time on microwave heating effects.

2 Chapter 2

Improving coal permeability using microwave heating technology —a review

This chapter is prepared to be submitted to Science of the Total Environment. It was written by Jinxin Huang and revised by Prof. Guang Xu.

Please cite this paper as:

Huang, J., & Xu, G. (2019). Improving coal permeability using microwave heating technology —a review. *Science of the Total Environment.*

Chapter 2 is devoted to provide a general idea of current research status, research limitations and future works in microwave-assist permeability enhancement of coal for other researchers. The chapter mainly focused on the following aspects:

a. The mechanism of microwave heating/fracturing.
b. Experiment and numerical studies in microwave fracturing of coal.
c. Influencing factors on microwave fracturing.
d. Outstanding challenges for field application.
e. Potential field applications.

2.1 Abstract

Microwave heating is a promising non-aqueous technology in coal seam enhancement. Recently, it has been considered as an alternative technology to hydraulic fracturing and Enhanced Coal Bed Methane recovery, which may be inapplicable due to environmental and geological restrictions. In this paper, a critical review of microwave heating applications in coal permeability enhancement is presented. The mechanisms of both microwave heating and microwave-induced permeability enhancement are discussed in detail. Most of the experimental studies and numerical simulations in the related area are reviewed. After discussing the challenges in applying microwave on-site, potential field applications were suggested. As no field application is reported till now, further studies, especially experiments in field-scale are in badly demand to test its technical and economic feasibility.

2.2 Introduction

Coalbed methane, mostly exists in the micropores of coal body, is recognised as a promising cleaning fuel resource of worldwide importance and has already achieved commercial success in North America [1-3]. Deeper coals generally have higher gas content and thus have greater commercial value. However, with the increase of mining depth, coal seam permeability decreases considerably due to the increased effective stress, which makes it hard to extract [22].

The current gas recovery enhancing methods can be divided into two categories according to whether they increase the permeability of coal seam. Enhanced coalbed methane recovery (ECBM), which replaces coalbed methane with injected CO2 or N2, is a typical

technique to enhance gas recovery without increasing the permeability of coal seam [10]. CO2-ECBM is especially popular due to the additional benefit of sequestering the huge amount of CO2, which reduces the greenhouse effect and prevents global warming [11]. However, ECBM is only suitable for the coal seams with high initial permeability [12]. Most methods enhance the coalbed methane production rate by increasing the permeability of the coal seam [22]. Traditional permeability enhancement methods including hydraulic fracturing, hydro-slotting [5, 6] and blasting [7, 8] have been applied on-site. However, these methods have negative environmental impacts and thus are restricted in some countries and regions [9]. Many alternative methods were proposed to address this problem, including liquid nitrogen cooling [13], electrochemical treatment [14], ultrasonic wave excitation [15], partial coal pyrolysis [16], microbial stimulation [17], and geothermal enhancement [18]. However, these methods suffer from problems such as high cost, low efficiency, low coverage and persistence.

Nowadays, interest was devoted to microwave heating (MH) to overcome these problems because of its advantages of non-contact volumetric heating, economical and environmentally friendly. The main purpose of microwave heating is to selectively heat the coal seam, which not only promotes coalbed methane desorption but also induces thermal fractures. Microwaves are electromagnetic waves ranged from 300 MHz to 300 GHz (wavelength ranging from 1 to 300 mm) [19, 20]. In the mid-1980s, researchers started to investigate microwave radiation on minerals [21]. Now, it has been widely used in coal pre-treatment and processing, including drying [20, 23], coking [24], desulfurization [25], flotation [26], pyrolysis [27, 28], grindability enhancement [29] and so on.

Although successful research results were achieved on investigating the petrophysical variation of coals under microwave treatment, the studies in this area still remain in the preliminary stage. Most of the laboratory experiments were conducted using commercial microwave ovens with a fixed frequency of 2.45 GHz as higher frequencies are not very safe due to the possible interference with other instruments in the laboratory. Even though numerical simulations have been conducted to investigate influencing factors for microwave heating/fracturing, most of these numerical models either have unrealistic assumptions or haven't been fully verified due to the lack of experimental data. Most importantly, on-site applications or field tests were not found in the literature. Even though microwave heating is proved to be effective in the lab, it could be totally different when applying on-site as the penetration depth of microwave is very limited within the coal reservoir.

The aim of this article is to review the studies of coal permeability enhancement using microwave heating and to discuss the feasibility of its on-site applications. At first, the mechanism of microwave heating/fracturing was presented, and the advantages of microwave heating were highlighted. Then, the literature review of both experiments and numerical simulations in studying MH's effect on coal was presented, following by the influencing factors on microwave fracturing effects. After discussing the outstanding challenges for on-site applications of MH, the conceptual design for potential field applications was proposed. This paper not only reviewed the current research status of microwave-induced permeability enhancement but also discussed the weakness of present studies and provided new angles for future research. Therefore, this work provides comprehensive knowledge in microwave-assist coal seam enhancement technology for other researchers, which could be very helpful for developing microwave applications in coalbed methane exploitation.

2.3 Microwave induced permeability enhancement

2.3.1 Mechanism

2.3.1.1 Microwave heating

Microwaves can be transmitted, reflected or absorbed, depending on the material's dielectric properties (Figure 2) [30]. The dielectric properties of a material are described with complex permittivity ε, which is expressed in real and imaginary parts:

$$\varepsilon = \varepsilon' - j\varepsilon'' \tag{1}$$

where ε' is real permittivity (F/m) that represents the material's capacity to store electromagnetic energy, ε'' is imaginary permittivity (F/m), which reflects the amount of energy dissipated into heat.

Insulators are transparent to microwave and therefore can transmit microwaves with no energy conversion. Metals with high conductivities, which has no significant heating effects under MH, reflect microwaves. Materials with median conductivities, especially from 1 to 10 S m^{-1}, can be effectively heated under MH [31].

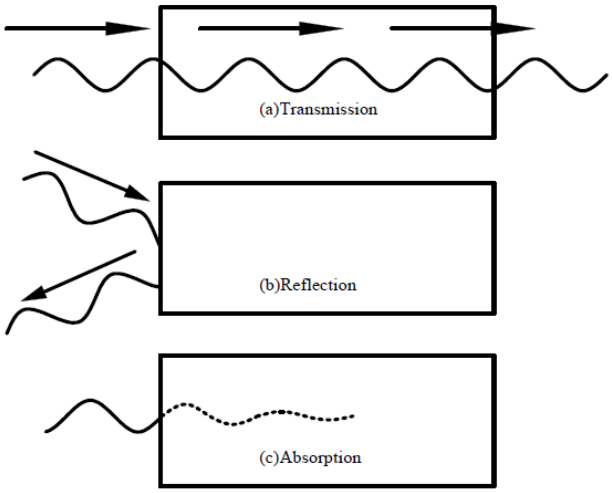

Figure 2. The behavior of materials under microwave irradiation (modified from [30])

Dipolar polarization is considered as the most important mechanism in microwave heating [32]. When polar molecules are exposed under an oscillating electric or magnetic field, molecules attempt to keep in phase with the electromagnetic field [33]. However, this motion is restricted by the inter-particle and inter-molecular resistance, which effect on the motion of molecules [33]. As the electromagnetic field is oscillating, polar molecules are always in random motion, which further results in friction and heat loss. The key factor for dipolar polarization is the microwave frequency. The appropriate frequency range for oscillating polar molecules is from 0.3 to 30 GHz. If the frequency is too low, polar molecules have enough time to align with the field and therefore no random movement will occur. If the frequency is too high, inadequate interaction will occur as intermolecular forces will stop the polar molecule in the electromagnetic field.

Interfacial polarization also induces microwave heating. It occurs in a non-conducting medium with conducting material dispersed in it [33]. This applies to coal as only the minerals in it absorb microwave radiation. Affected by an external electromagnetic field, the charge build-up occurs at the interface of coal and minerals [34]. This interfacial polarization results in heat losses in coal.

The increase of coal temperature enhance the extraction of coalbed methane in two ways: On one hand, higher temperature accelerates gas's molecular thermal motion and thus facilitates its transformation from the adsorbed state into the free state [35]. Pan [36] found methane adsorption capacity has an inverse relationship with the temperature at a certain pressure for all types of coal. Specifically, it was reported adsorption capacity of bituminous

coals decrease 1 m^3/t for every 10 ℃ temperature rise [37, 38]. On the other hand, some high activity materials decompose easily due to the thermal effect, including methylene, methylene, methoxyl, and carboxyl [39]. With the increase of temperature, more activity materials and volatiles were decomposed, and the decomposition and release of little organic compound expand the pores and fissures. It was observed with X-ray CT that moisture and minerals bound in coal gradually disappear under MH [40]. As a result, the original fractures extend, and new fractures are formed. It was also confirmed the pyrolysis of oxygenic function groups and some volatile at 450℃ creates new pores less than 3 mm [41]. In conclusion, increasing coal temperature facilities desorption and diffusion of gas and gives rise to pore expansion due to pyrolysis.

2.3.1.2 Microwave induced thermal stress

Due to selective heating, components such as pyrite heat much faster in the electromagnetic field compared to the surrounding coal matrix, which leads to a thermal gradient between the heated phase and the coal matrix [42, 43]. In this case, differential expansion rates of gangue minerals would be expected and structural embrittlement of coal will occur consequently [21]. The extent of embrittlement depends on the mineral dielectric constant, the quantity of mineral and the position within the coal structure [44]. In a similar manner, moisture heats up and imparts thermal stresses, which further promotes the generation of new fractures and changes at the grain level [45, 46]. Moreover, it was speculated the rapid expansion of moisture during evaporation induces mechanical stresses and facilitates the formation of the cracks [29]. However, it is still unclear whether it is the bulk water in macropores and micro-fractures or the bound water resided in micropores that gives rise to the fracturing [47].

2.3.1.3 Microwave drying

Water in coal greatly influences gas storage and flow behaviour [48, 49]. The moisture within the coal matrix block the coal pore structure and thereby reduce gas adsorption capacity, gas diffusivity and coal permeability [50]. It was found that the permeability of coal decreases significantly with rising moisture content under pressure from 0 to 10 MPa. For dried coal sample, an increase of 7% moisture content results in more than 50% permeability drop. It was also reported the initial gas production rate improves nearly 4 times when the relative humidity decreases from 99% to 73% [51]. Another study result suggests the moisture content has a significant influence on gas diffusivity, which controls

the gas production rate. Both the macro-diffusivity and micro-diffusivity for CH_4 decreased by more than 82% from dry coal to saturated coal [50].

Microwave heating is especially effective in water removal due to volumetric heating and selective heating [19]. Due to such benefit, it has been applied to deal with water blocking in gas reservoir [52]. Moisture within gas reservoir rapidly absorbs microwave energy and evaporates. Vaporization of liquid phase and gas expansion drives pore fluid flow from closed internal space to open shaft [53]. During this process, the moisture that blocks the pores and fissures evaporate, dissolved gas is freed from water and flow out together with the vapour. The coal seam permeability and gas production thus increase significantly with the reduction of moisture content.

2.3.2 Advantages

Due to the unique feature of the microwave, microwave heating has the following advantages over conventional heating.

1. Rapid, non-contact and volumetric heating:

Most traditional heating methods rely on convection, where heat is applied to the surface and gradually transferred to the inner part [54]. However, microwave heating is realized via the conversion of electromagnetic energy to heat. With great penetrating capacity, microwaves can heat materials volumetrically, which greatly improves the heating rate and energy efficiency.

2. Selective heating:

For an object with heterogeneous dielectric properties, the microwave will selectively heat the adsorbing phase while passing through the transparent phase unaffected. The loss factor of coal as a bulk material is less than 0.25 at 2.21 GHz and 25 ℃ [30]. Due to this mechanism, the moisture and minerals within coal body are selectively heated under MH.

3. Massive moisture loss:

Resulted by the volumetric heating and selective heating, significant internal evaporation occurs for water-bearing materials, which results in additional moisture transport during MH [20]. It was reported that removing the same amount of moisture requires 22.5 times higher energy consumption for thermal heat than by MH [41]. The quantitative experiments suggest microwave drying is an order of magnitude more efficient than thermal

heating for fine coal slurry sample [55]. Therefore, microwave heating is an efficient and energy-saving drying method for coal.

4. Wide applicability

Microwave heating is widely applicable to all the coal seams with different geology conditions. For the coal seam with low moisture content, microwave showed great fracturing effects [56]. As for the coal seam with high moisture content or even with serious water blocking, the microwave is a very effective drying method to remove the water from the coal seam.

5. Environmentally friendly

Microwave stimulation does not consume a huge amount of water to generate steam to heat the reservoir, nor contaminate the underground water system. Beyond that, less amounts of greenhouse gas will be emitted using MH [57].

6. Easy to control

Unlike traditional heating methods, microwave can be switched on and off instantly, and its thermal effect will not continue once turned off [58]. This feature makes it possible to precisely control the temperature of the targeted coal seam in field application [59].

7. Economical

Microwave energy can be derived from electrical energy, which is easily accessible. It can be transported through a hollow non-magnetic metal tube (waveguide) without the requirement for storage [60]. Moreover, MH is more energetically efficient compared to other aqueous thermal heating methods [57].

2.3.3 Experiment studies

Experimental studies of microwave-assisted coal permeability enhancement are conducted through comparing pore structure before and after MH. The methods in determining pore structure in coal can be generally divided into two categories, direct and indirect experimental techniques (Figure 3). The direct methods include X-ray Computational Tomography (CT), Scanning Electron Microscope (SEM), X-ray diffraction (XRD) and Optical microscope; the indirect methods include Nuclear Magnetic Resonance (NMR), Mercury Injection Capillary Pressure (MICP) and N_2/CO_2 adsorption experiment [40, 52, 59, 61, 62].

As shown in Figure 3, MICP and XRD are destructive methods and thus not applicable to evaluate pore structure evolution after MH. Optical microscope and N_2/CO_2 adsorption experiment are less commonly used due to their limited aperture range. The most commonly used methods in studying fissure development of coal under MH are NMR, CT and SEM. As shown in Figure 4, NMR has the widest aperture range and is able to detect micro-pore, mesopore, macrospore and fissures. However, NMR is an indirect method that cannot provide information about the position or distribution of the pores and fissures. CT can not only provide general information of the fissure network system but also reconstruct the internal structure and texture of the coal sample. Nevertheless, it cannot be used to observe details of microstructures due to its low resolution. SEM, on the contrary, enables a close look to the coal surface but not able to detect internal structures or provide general information. Therefore, NMR, CT scanning and SEM are complementary technologies to provide not only overall but also detailed information about pore structure.

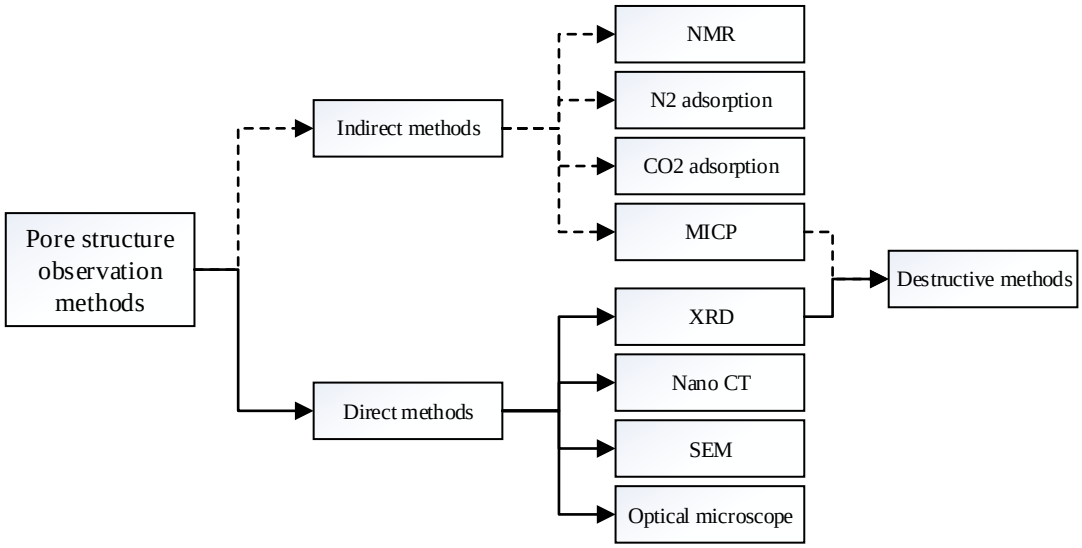

Figure 3. Pore structure observation methods

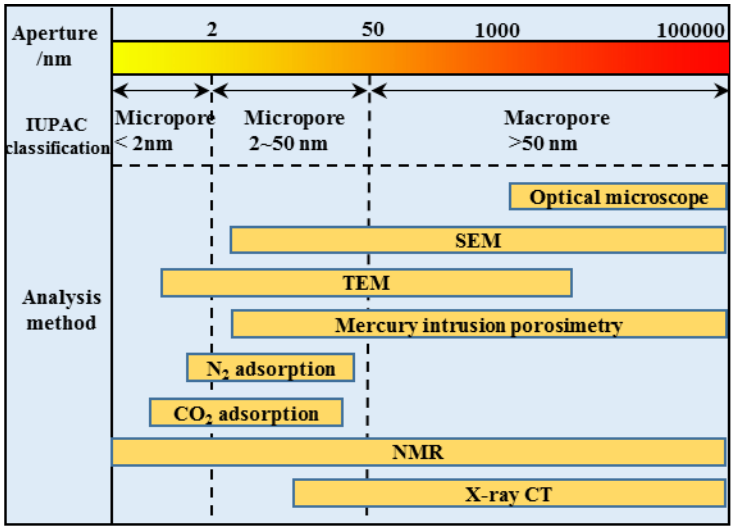

Figure 4. Aperture ranges for coal petrophysical characterization methods (modified from [40]).

2.3.3.1 NMR

NMR is a frequently used technique with the advantages of non-destructive, less time-consuming and wide aperture range (see Figure 5). It is a physical phenomenon that the spin nuclei absorb external RF field energy in the strong magnetic field. After full saturation of samples, pore volume is obtained from detecting the NMR signals of water within the pore and fissures [63]. A typical NMR result (T_2 spectrum) is shown in Figure 5. The transversal relaxation T_2 reflects pore size and the amplitude correlated with the pore number.

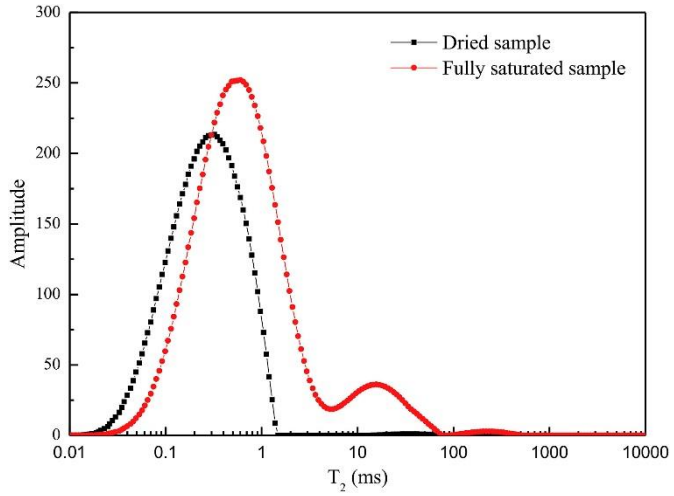

Figure 5. T_2 spectrum of a dried and saturated coal sample [56]

As long as water fills in all the pores and fissures within coal samples, NMR is capable to obtain their full range of pore size distribution. With the benefit of non-destructive and wide aperture range, NMR has become the most frequently used method in comparing coal structure before and after MH under various experimental conditions, including

microwave power, irradiation time, coal rank, water saturation. Meaningful results were drawn from these NMR experiments and the effect of these influencing factors on MH were made clear, which will be discussed in detail in chapter 3.

It is worth to note that, NMR can only accurately detect pore structure when it is saturated with water. For instance, macropores with residual water on the wall will be mistaken as micropores when using NMR to measure the irreducible water existed in coal fissure. In a similar manner, NMR is not suitable to measure large cracks and gaps where water cannot be reserved under gravity.

2.3.3.2 X-ray CT

X-ray CT is a non-destructive technique that has been widely used to investigate the internal structure of coal [64-67]. Through CT scanning, the internal structure and texture of the sample can be reconstructed. Even though its resolution is too low to observe details of microstructures, it can easily identify the existence of micro-fracture and provide general information of the whole sample [52]. A representative study was conducted by Kumar, who reconstructed the fissure system of coal core before and after microwave using X-ray CT, as shown in Figure 6 [47]. Cleat frequency and distribution of bituminous coal cores with and without application of isotropic stress were evaluated. For both un-stressed and isotopically stressed core, it was confirmed that new fractures generate and existing cleat apertures increase under MH: fracture volume increased by 1.8-16.1% for non-stressed and 0.5-5.5% for the stressed coal cores [47].

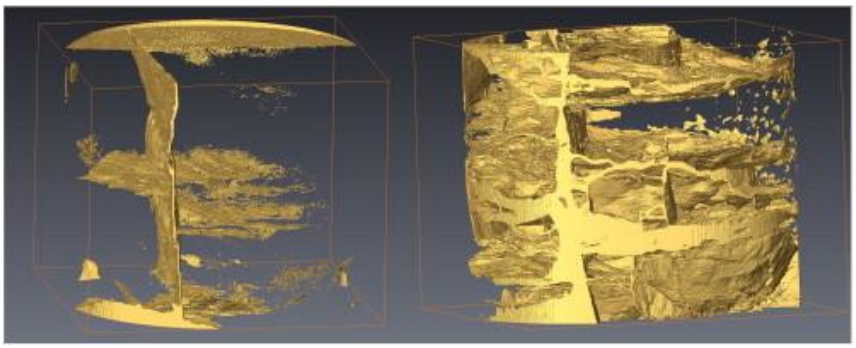

Figure 6. Fracture reconstruction of the unconfined coal core before (left) and after (right) MH

2.3.3.3 SEM

SEM is a method to observe small surface features and structures through scanning a high energy electron beam on the surface of samples [68]. The most advanced SEM can magnify as much as 1 million times and can observe features smaller than 1 nm.

SEM experiments have been applied to compare the surface micro-topography of coal before and after MH, whose results suggest that MH smoothens coal surface, induces fissures and alter the angularity and surface properties of coal particles [69]. Sahoo [70] monitored the structure of coal core before and after MH using SEM. SEM results suggest that coal surface become smooth and fissures become prominent after MH. It was also found the cracks and fissures developed along grain boundaries under MH. Similar experiments were conducted by Liu [62] and Huang [56]. As shown in Figure 7, many small particles representing fine pore network were observed to cover and accumulate on the surface of raw coal, while no visible fissures can be found before microwave treatment [62]. On the contrary, fissures appear while the accumulated small particles decreased after MH, which indicates that the fine pore networks expand and connect into coarse pore network under MH. Zhou [69] analysed pulverized lignite under MH with SEM. It was found the particles enlarge and their surface hardens with the increase of microwave time. Zhou believes the continuous moisture evaporation and decomposition of oxygen functional groups result in the collapse of pores and the shrunk of lignite particles, which harden the surface particles. During this process, new crosslinking surfaces were created in the closed pores and thus increase the size of particles.

Even though SEM provides detailed information on coal samples, it has several major weaknesses. Firstly, it is almost impossible for SEM to capture the exact same spot again after removing the sample from the device. Even though the SEM images were taken for the same sample before and after MH, the images are most likely from different positions due to the challenges of identifying the exact spot. As coal is anisotropic, the conclusions drawn from the comparison of different spots before and after microwave treatment is not solid. Secondly, SEM images can only be taken on the surface, while not able to provide any information about the internal structures. Finally, as SEM only focus on a very small part of the surface, it cannot be used as a quantitative analysis to determine microwave's effect on fissure development.

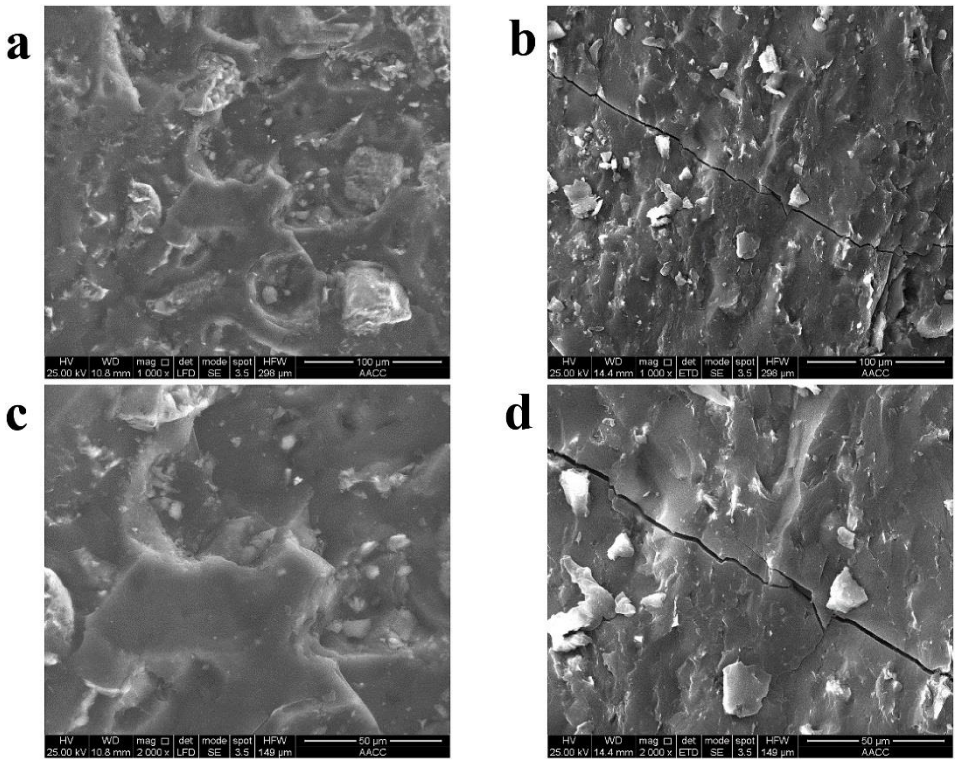

Figure 7. SEM images of coal samples before (a,c) and after(b,d) MH [56]

2.3.3.4 N2 adsorption

N_2 adsorption determines the pore size distribution and specific surface area of coal using a theoretical model and measured equilibrium adsorption capacity [71]. However, N_2 adsorption experiments are not suitable for evaluating pore structure variation under MH. First of all, its limited aperture range can only cover a small part of micropores and most part of mesopores, which is too narrow to determine the pore structure. Secondly, N_2 adsorption/desorption experiments can only perform with coal powders instead of coal cores. The original pore structure for coal powders is damaged when the raw samples were crushed and milled for analysis, thus cannot reflect the true characteristics.

Due to the above-mentioned limitations, the use of N_2 adsorption for investigating microwave heating of coal is not suggested. Past studies have shown inconsistent findings. For example, in one study [39], the pore structure for brown coal was investigated using the N_2 adsorption measurements before and after microwave heating. Brunauer-Emmett-Teller (BET) equation was used to determine the surface area, whereas the pore size distribution and volume were calculated using the Barret-Joyner-Halenda (BJH) model. It was found the surface area and total pore volume increased, while average pore diameter decreased after MH treatment. This was explained that it was due to macropores broke and developed into

micropores regions. However, this speculation is untenable as N_2 adsorption measurements are not able to detect macropore: the measured pore size in this study ranges from 0 to 30 nm, whereas macropore ranges from 50 to 100 nm. Another N_2 adsorption/desorption experiments, which were performed at 77K for lignite, also suggest total pore volume increased after MH [62]. However, the experiments also report that the specific surface area decreases and the average pore diameter increases after MH, which is contradictory to the first experiment results. This experimental result is also questionable as the pore structure will change significantly under 77K. It is impossible to distinguish the pore structure variation contributed by MH from that changed due to low temperature. Finally, another similar N_2 adsorption experiments suggest the specific surface area distribution of Shenhua coal remains almost unchanged after treated by microwave heating [41]. In the study, various levels of microwave power and treatment period were applied to coal samples. The specific surface area distributions of coal samples were determined with Quantachrome Autosorb-1-C N_2 adsorption porometer. The results suggest that the specific surface area distribution of the coal samples (pore diameter mainly ranges from 3-4.5 nm and peaks at 3.7 nm) remains almost unchanged with increasing microwave power and time. The author claimed the microwave directly penetrates the inner particles and therefore has little effect on the pore structures of coal.

2.3.4 Numerical simulations

Numerical models were first established to study microwave heating on coal in the early 1990s. These 2D models made it possible to simulate the electromagnetic and thermal field distribution of coal sample as a function of microwave power, frequency and irradiation time. However, these preliminary models were simplified to reduce computation time and none of these models was verified with experiment results. Chatterjee [72, 73] developed a 2D electromagnetic and thermal model and calculated the electromagnetic energy absorption of coal under microwave irradiation. The coal model is represented by an array of 12×12 cells, each cell consists of different percentages of coal, water, mineral matters, pyrite and air pockets. The volume-averaged dielectric constant and conductivity of each cell are calculated from the measured values and percentage of individual constituents. The method of moments is used to solve the electromagnetic model to obtain the absorbed electromagnetic energy distribution. The corresponding temperature distribution is then calculated by solving the heat conduction equation. In a similar attempt, Clemens [74] proposed a coupled 2D electromagnetic and thermal model to evaluate the influence of specimen size and electrical

properties on microwave absorption and electric field patterns. The electromagnetic model is developed based on Maxwell's equations using finite-difference time-domain method and the heat transport model is established via transient finite difference method. The results suggested when the distance between the sample edges and the cavity walls is less than $\lambda/2 = 6.13$ cm, microwaves tend to propagate around the sample and are thus significantly attenuated. It was also reported that a slight variation of microwave frequency leads to a significant change in electrical intensity distribution in an empty cavity. Similar 2D models were built by Peng [75], who investigated the influence of electrical properties on microwave heating using an explicit finite difference approach. It was reported that microwave heating at 915 MHz exhibits better heating uniformity than 2450 MHz because of longer penetration depth.

Finite element analysis software including COMSOL Multiphysics and ANSYS are the current mainstream research software in simulating microwave systems [52, 76-79]. With all kinds of modules (such as Electromagnetics, Fluid flow & heat transfer and Structural mechanics), this software can easily couple different physical and chemical reactions and thus enables investigating moisture vaporization, stress and strain distribution in simulating microwave heating of coal. Hong and Lin [80, 81] developed a coupled electromagnetic and heat transfer model with COMSOL Multiphysics. The model was verified with experiment results and then applied to investigate the influencing factors for microwave heating on coal. These models considered the permittivity of coal as a fixed value during microwave treatment. The coal's ability to absorb microwave energy is thus the same and its temperature increases linearly with time. However, the heating rate of coal decreases over time due to moisture vaporization and minerals decomposition. Further development was made by Huang [35], who took the mass transfer (moisture migration) into account and proposed a coupled electromagnetic irradiation, heat and mass transfer model. It was reported microwave power has little effect on the average temperature of coals with the same energy input. Higher power, however, is more effective in increasing permeability of coal seam as higher power give rise to larger maximum temperature difference. It was also reported that coal sample with 5% specific moisture capacity within 0-10% has the best heating effect at 1 kW and 2.45 GHz.

Even though COMSOL Multiphysics is powerful in simulating microwave heating, it has a major limitation in establishing large-scale reservoir models. COMSOL requires extensive memory when solving models with a large grid numbers and therefore difficult to

simulate the large model with very high grid numbers [82]. However, to ensure simulation accuracy, the mesh size for microwave heating is generally defined as no more than one-fifth of the wavelength, which leads to huge grid number and almost impossible to handle with COSMOL. Recently, a fully coupled electromagnetic-thermal-mechanical model was proposed for coal reservoir stimulation. To avoid the problem mentioned above, the geometric model was simplified as a 2D coal reservoir model to reduce calculation time. Considering coal deformation, gas flow and transport, the cumulative gas production before and after microwave heating were simulated on a real size reservoir model. Their reports suggested that through promoting gas desorption and seepage, microwave heating enhances the cumulative gas production by 37.8% after 100 days, 41.4% after 200 days and 43.9% after 300 days [83]. These simulation results suggest microwave heating is a promising technology in stimulating coal reservoir. However, this model still requires verification by the use of on-site experiment data.

ANSYS is a similar finite element software, which requires more complicated operations but has the capability to handle the model with large grid numbers. Therefore, ANSYS is more suitable for simulating microwave heating in reservoirs. Wang [84] established a numerical model of microwave heating for tight gas sand reservoirs with ANSYS Multiphysics and STARS-CMG. The electric field and thermal field distribution of a natural gas reservoir were first simulated with ANSYS Multiphysics, whose results were imported into CMG to obtain the relative permeability, water saturation and production rate of the reservoir. The simulation results show that the cumulative gas production increased from 4.0×10^6 m^3 to 4.4×10^6 m^3 in 90 days after applying microwave heating [84]. Moreover, when severe formation damage happens and the well fails to produce gas, the application of microwave make the water saturation drop from 0,8 to 0 in the near bore area, thereby increasing the relative permeability from almost 0 to nearly 1. Even though meaningful results were achieved in this paper, the reliability of this model is questionable as the geometry dimension of the model is not the same size as the real reservoir. When building the geometry model on a scale, the simulated penetration depth of microwave will certainly change according to the geometry scale. However, penetration depth should be constant under given microwave frequencies instead of affected by geometry scale. In this case, the simulation exaggerates the penetration depth and therefore overestimate the microwave heating effect on the reservoir.

Numerical models have also been developed to simulate microwave-assisted breakage. Whittles [85] developed the first coupled electric, thermal and mechanical model to study microwave fracturing on calcite host with randomly scattered pyrite particles. He first calculated the thermal energy transformed from microwave energy, followed with the calculation of transient heat conduction during microwave heating. The thermally generated strain and stress were then calculated using Hoek's law for isotropic elastic behaviour [86]. Finally, thermal damage associated with material failure and strain softening was modelled and unconfined compressive strength tests were simulated on the damaged samples. In an attempt to describe the mechanism of thermal expansion, thermal fracturing, thermal volatilization and gas adsorption/desorption, Teng [87] proposed a thermally sensitive permeability model to describe the coal-gas interactions under various temperatures. After verified by experiment data in previous literature, they reported that temperature has a significant impact on the mechanical and transport properties of coal. They suggested permeability evolution with temperature can be divided into four stages according to four primary factors: thermal expansion, thermal volatilization, thermal fracturing and crack coalescence.

2.4 Influencing factors on microwave heating/fracturing

2.4.1 Factors related to microwave properties

2.4.1.1 Power level

The volumetric adsorption of microwave energy (in units of W/m^3) is proportional to the electric strength within the material, and higher heating rates will lead to more significant formation of cracks in coal [43]. Therefore, higher microwave powers or electric field strengths have better microwave heating effects, which further lead to better microwave drying and fracturing effects.

Higher power level is not only more effective but also more energy efficient in microwave fracturing. Simulations were conducted under different microwave powers but at the same energy input to compare the energy efficiency of various microwave power [35, 81]. It was found the average temperatures are similar with the same energy input. However, the maximum temperature increases while the minimum temperature decreases with microwave power, which suggest increasing power contributes to the thermal heterogeneity. As temperature difference facilitates the expansion of existing fissures and formation of new

fissures, larger microwave power seems to have better performance in fracturing. The experiment results basically agree with this conclusion. In a recent study, the normalized increment of the water porosity of coal samples was measured under different microwave powers and irradiation times at the same energy input [88]. It was found that the microwave has better fracturing performance under higher powers when total energy input reaches a certain amount, before which no obvious pattern was observed. Moreover, higher power level also seems to be more energy efficient in microwave drying. It was reported that the microwave drying effect for coal samples under 1200W is 7.8 times as fast as that under 217W after 3 minutes [20].

Even though larger microwave power is more efficient and economical, it is worth to mention that large microwave power leads to a rapid temperature rise in the nearby coal seam. The heat conductivity of coal is extremely low (especially for coal with low saturations) and thus not able to transfer heat rapidly to adjacent areas, which may result in overheating and causes fire. Therefore, due to safety concerns, suitable microwave power is vital to on-site applications for preventing overheating. Before application, a safe microwave power level needs to be determined based on the measured microwave heating rate and the heat transfer rate of the specific coal seam.

2.4.1.2 Frequency

The industrial, scientific and medical (ISM) radio bands are limited to certain frequencies as powerful emission of microwave energy may disrupt radio communication using the same frequency. International Telecommunication Union (ITU) designated the following frequencies for ISM, including 6.78, 13.56, 27.12, 40.68, 433.92, 915, 2450, 5800 MHz and 24.125, 61.25, 122.5, 245 GHz [89]. However, uses of the ISM bands are also governed by governments around the world, which means the allowed frequency range for microwave heating differs in different countries. Currently, the frequency of 915 and 2450 MHz are most commonly used in microwave heating, while there are other options if necessary.

Microwave frequency affects MH performance in three ways: First of all, different microwave frequencies lead to various electromagnetic field distribution in a confined space, which is vital for microwave oven performance. Numerical simulation has shown that different microwave frequencies create diverse electric field distributions within the microwave oven [35]. Therefore, the thermal field distribution of coal largely depends on its

position in the oven. For instance, if the coal sample happens to locate at a high electric intensity zone under a certain frequency, its MH performance will be much better compared to other frequencies [80, 81]. In practical applications, the microwave oven achieves the uniform heating effect through rotating the plate.

Secondly, microwave frequency may influence the dielectric properties of coal and thus changes its microwave adsorption capability [90]. However, it was found the effect of microwave frequency on coal dielectric property is negligible within the current industrial microwave frequency band [30] [91]. Marland [30] found this variation is small and thus did not regard microwave frequency as a major factor influencing microwave adsorption capability of coal. The dielectric constant of Chinese bituminous coal samples was measured with Agilent E5071C vector network analyser and confirmed the dielectric property of bituminous coal remains stable within 0.915 to 5.0 GHz.

Finally, microwave frequency determines its penetration depth in coal, which further influences the effective range of microwave heating. This factor is insignificant in the microwave oven but especially crucial for large-scale on-site applications. The discussion regarding microwave frequency's effect on penetration depth will be further elaborated in section 2.5.1.

2.4.1.3 Treatment time

Coal temperature increase under MH can be divided into two stages. In the first stage, the temperature increases rapidly to a certain value (almost linearly with time). In the second stage, the heating rate decrease over time because of vaporization and decomposition, and the temperature remain constant after reaching a certain point. It was found with the increase of load of mass, the heating rate decrease significantly, and it takes much longer time for the first stage of microwave heating. Till now, no field experiment in microwave-assisted coal seam enhancement was reported. However, it can be speculated that the heating rate of coal seam is very limited when applying MH on-site and the temperature of coal seam will increase linearly with treatment time for a long period. With the extension of time, the thermal conduction, convection and radiation of coal body and pore liquid can achieve effective heating on a large scale [53].

Most researchers believe microwave has more significant fracturing effect on coal with longer treatment time. Experimental studies have shown that porosity and permeability increase with microwave treatment time for all types of coal samples [40, 56, 70]. However,

it was reported the microwave fracturing effect decreases with treatment time at a certain stage [88]. The study suggested the coal matrix expansion, which may close part of pores, have a more obvious effect than thermal stress before absorbing enough microwave energy. A turning point of 100 KJ was observed, after which thermal stress induces fractures significantly.

2.4.2 Factors related to coal properties

2.4.2.1 Coal rank

Coal rank affects the moisture, volatile matters and fixed carbon content, which will ultimately influence the capability of coal to absorb microwave power [30]. It is widely acknowledged that the dielectric constant of higher-ranked coal is more steady under MH However, whether low-rank coals or high-rank coals have larger dielectric constants remains controversial.

Some researchers believe the dielectric constant increases with coal rank [30, 92]. In a representative study, dielectric constants of coals with various ranks were measured before and after drying [30]. To reduce the influence of mineral, coals of various ranks with low mineral matter were used for these experiments. The results show the highest dielectric constants belongs to high (F-1 to F-3) and low (F-6 to F-8) rank coals before drying. After drying, lower-ranked coal shows the least dielectric constant and the largest change in dielectric constant due to moisture removal. Whereas high ranked coals exhibit the least variation in dielectric constant and greatest values [30]. On the contrary, there is one study suggest lower-ranked coals have larger dielectric constant, which is possible because of their higher moisture contents [50].

2.4.2.2 Moisture content

Water's loss factor is as high as about 12 at 25℃ and 2.45 GHz, which is considerably higher than most materials within the coal body [43]. Even though the loss factor of water decreases with rising temperature (reduces to 3 at 85℃ and 2.45 GHz), it is still much higher than the other phase in the coal body [43]. Under MH, water is firstly heated up and gradually driven off the coal body due to phase change. Because of moisture removal, a substantial reduction in both real and imaginary permittivity values was observed between 80 and 180 ℃ [30], which means coal body becomes less susceptible to MH. Moisture content has both a positive and negative effect on microwave-assist permeability enhancement. On the one

hand, it increases coal's ability in absorbing microwave energy, which leads to a better microwave heating effect. On the other hand, moisture blocks the passage for gas flow and thus significantly decrease the permeability for gas. Moreover, large moisture content results in uniform heating of coal, which mitigates the effect of microwave fracturing.

The moisture within coal matrix block the coal pore structure and thereby reduce gas adsorption capacity, gas diffusivity and coal permeability. However, both numerical simulations and experiment results suggest microwave have better fracturing effect for the coal with low moisture saturation compared to the dried coal. For coal seam with low moisture content, moisture is unevenly distributed within the coal body. Heated moisture imparts thermal stress, which further promotes the generation of new fractures and changes at the grain level. It was found the total porosity after MH increases exponentially with water contents from 1% to 15% [32]. When the water content is 1%, where most of the water exists in super-macropores or micro-fractures, the irradiated water has little effect on the pore distribution. With the increase of water content, more water is irradiated in smaller pores, resulting in corresponding pore enlargement. Moisture's effect on microwave heating of coal was investigated with a coupled 3D electromagnetic, heat and mass transfer model [35]. The simulation results suggest the average temperature increases with moisture content and achieve the highest value at 5% specific moisture capacity under MH of 2.45 GHz and 1.0 kW. It can be speculated that for each microwave setting, there is an optimal moisture content to achieve the best microwave heating/fracturing effect.

However, moisture is not always beneficial to microwave heating. With the continuous increase in saturation, more and more pores and fissures are filled with water, leaving little space for gas to flow. The increase in the saturation of the reservoir may result in water blocking and lead to diminished gas production [53]. It was also found that microwave can hardly generate new fissure for the coal with high moisture content, before its saturation drop to a certain point. The reason is the interconnected water content makes the coal uniformed heated under MH, where thermal fractures are hard to form [56]. Under such circumstances, microwave's effect is mainly reflected in drying. Massive water evaporates and flows from closed internal space to open shaft under MH, which clears the water blocked space and provides channels for gas flow. Meanwhile, the absorbed gas and dissolved gas are also freed into the open space with the temperature increase and moisture evaporation.

2.4.2.3 Mineral composition

Minerals in coal is another major absorber of microwave energy. The heating effect of a number of minerals and reagent grad inorganic compounds under 2450 MHz microwave irradiation were investigated by the US Bureau of Mines [93, 94]. It was found that most of the metals oxides have a great heating effect, such as NiO, MnO_2, Fe_3O_4, Co_2O_3, CuO and WO_3. In contrast, gangue minerals including quartz, calcite and feldspar did not heat [60]. The test results also revealed that most of the metal sulphides heated well, but did not have a consistent heating pattern. For instance, pyrite in coal decomposes following $FeS_2 \rightarrow Fe_{1-x}S \rightarrow FeS$ under MH [31]. As the decomposition product $Fe_{1-x}S$ and FeS are significantly more magnetic comparing to FeS_2, pyrite has inconsistent heating pattern under MH [95].

Many scholars have found fractures are easily induced in samples containing good microwave absorbers in a poor absorbing matrix. Rapid heating of ore minerals in the non-heating gangue matrix can effectively produce flaws and caused embrittlement [45]. Through SEM-EDX elemental analysis, it was observed micro-cracks started to form in the ferrum-rich zone under MH [96]. The dielectric properties of ferrum are higher than other surrounding mineral component, which proves that the rapid heating of ferrum in a microwave transparent matrix create micro-fissures along ferrum boundaries. Therefore, gangue minerals have little effect on MH of coal as they barely absorb microwave energy. In contrast, metallic minerals within the coal matrix heat up rapidly and undergo differential thermal expansion under MH. This expansion generates stress within the lattice, which induces fractures at the grain boundary [97].

2.5 Outstanding challenges

2.5.1 Penetration depth

Coal exhibited great attenuations of microwave propagation, especially for that with high moisture content [52]. Microwave is severely hampered travel through such coal body and therefore the penetration depth is limited [91]. Even though microwave can penetrate further when the water saturation decreases, the short penetration depth is still a major problem need to be addressed.

Penetration depth (D_p) is defined as the distance from the surface to the point where the power drops to e^{-1} of the value at the surface [98], given as:

$$P_A = 2\pi f \varepsilon_0 \varepsilon'' |E|^2 \quad (2)$$

$$D_p = \frac{\lambda_0}{2\pi(2\varepsilon')^{1/2}}\left[(1 + \left(\varepsilon''/\varepsilon'\right)^2)^{1/2} - 1\right]^{-1/2} \quad (3)$$

where P_A denotes the absorbed power per unit volume, f is the microwave frequency, E is the root mean square internal electric field, ε_0 and λ_0 represent the permittivity and wavelength of free space respectively, ε' is dielectric constant and ε'' is the loss factor.

Equation (3) indicates that the penetration depth is directly proportional to the wavelength, thereby inversely proportional to the microwave frequency. Experiments were carried out to verify the relation between penetration depth and microwave frequency. A laboratory experiment indicates the penetration depth in pyrite decreased from 14 cm to 4 cm when the frequency increased from 615 MHz to 2.21 GHz [99]. Field measurement of penetration depth for heavy oil reservoir was performed with 8 microwave frequencies ranging from 13.54 to 2450 MHz [100]. Although the resulted fitted curve suggests the penetration depth decreases with increasing microwave frequency (see in Figure 8), the relationship was not inversely proportional. This may be resulted by the different dielectric responses under various microwave frequencies.

Comparing to the heavy oil reservoir, coal seam has a relative larger dielectric constant and thus has even smaller penetration depth. When applying microwave heating on coal reservoir, microwave mainly effects on the surface layer of coal as microwave attenuate quickly after entering coal body. With the increase of temperature of the surface layer, the heat gradually transfers to the inner part. Therefore, in contrast with the instant heating of the microwave oven, it takes a long time for microwave heating to take effect on reservoirs. To achieve a larger effective heating range, lower microwave frequency seems to be more suitable for on-site application. The lower frequency is also more competitive from the perspective of energy efficiency. It was reported that the conversion efficiency from electricity to microwave energy is about 50% for 2450 MHz but increases to 85% for 915 Hz [60]. It is also worth mentioning that lower frequency microwaves carry less energy, which

results in longer times to achieve the same heating effect [33].

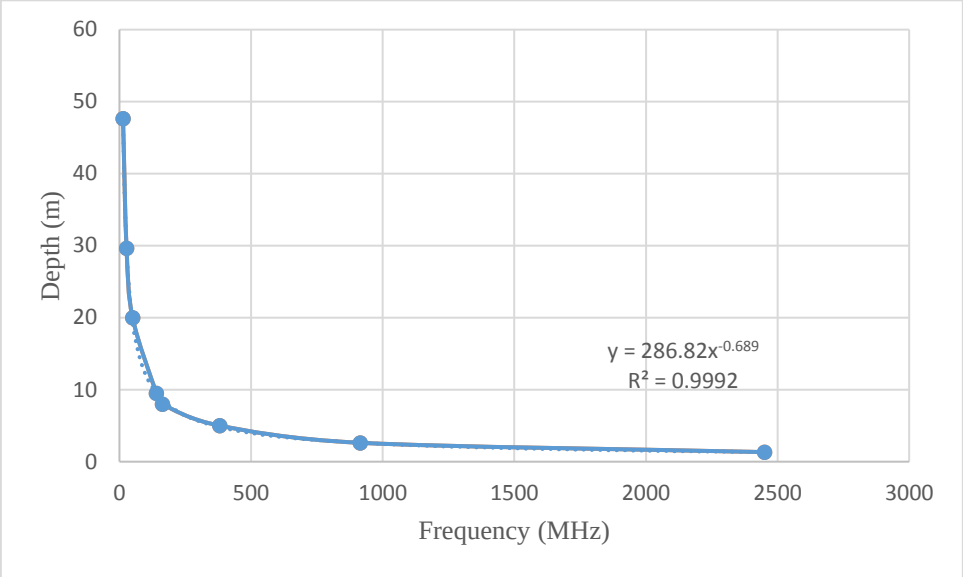

Figure 8. Penetration depth (Dp) in heavy oil reservoir measured at 100 °F for various frequencies (modified from [100])

2.5.2 Safety and environmental issues

As most of the main rock-forming minerals are insensitive to microwave, its application to coal seam should have little impact on the stability of roadways. However, human tissue is very sensitive to microwave and thus must be protected against over irradiation. Till now, there is no universally adopted regulation for exposure to radiofrequency (RF) radiation. Guidelines proposed by International Commission on Non-Ionizing Radiation Protection (ICNIRP) is recognised as an international standard and has been widely accepted by lots of countries and organizations, including the European Union, New Zealand and the World Health Organization (WHO) [101]. According to its latest guidelines, the basic restrictions for electromagnetic field exposure is shown in Table 1 [102]. The potential hazard can be managed by using a waveguide to confine the microwave and transport it to the targeted coal seams. And the underground application of microwave energy has no impact on people on the surface as the RF field intensity decreases to 0 within a few meters of the coal seam and rock formation. However, electromagnetic protection measures should be taken in a microwave activated area to protect underground miners.

Table 1 Basic restrictions for electric, magnetic and electromagnetic field exposure (≥ 6 minutes) [102]

Exposure Scenario	Frequency Range	Whole body average SAR (W kg^{-1})	Local head/torso SAR (W kg^{-1})	Local limb SAR (W kg^{-1})
Occupational	100kHz-6 GHz	0.4	10	20
General public	100kHz-6 GHz	0.08	2	4

As for the environmental impact, although MH does not have any polluting by-products, it may still have damage to the ecosystem depending on the electromagnetic field strength, frequencies, modulation and duration of exposure [103]. Due to its thermal and nonthermal effect, the microwave is a potential threat to microorganism and plants [104, 105]. Microwave can resonate the cellular membranes of trees and thus interrupt the water circulation [106]. Studies on the microwave bio-interaction also found the microwaves induce genetic changes in biosystem [103]. However, these impacts are believed to be minimal negative effects are minimal if the application of microwave is properly managed.

2.6 Potential field applications

Microwave heating has been studied and applied in the petroleum industry since the early 1970s [33, 107-110]. The main aim is to heat the oil reservoir with microwave energy and thus reduces its viscosity or increases its pressure, which promotes oil flow [110]. Based on these researches, conceptual designs of on-site microwave heating system were proposed for coal seam enhancement. It can be divided into two categories base on the application location: underground borehole or surface well, as shown in Figure 9 and Figure 10. Both systems consist of three sub-systems:

i. A microwave heating system consists of a microwave radiator, a control system, a waveguide and several antennas.
ii. A gas extraction system composed of a floral tube, a gas extraction tube and a pump.
iii. A safety guarantee system consists of a monitoring sensor, a casing pipe, a sealing for electromagnetic shielding.

Microwave can deal with the regular problems in borehole such as “borehole blocked” and “borehole full of water”. In Australia, extensive gas drainage boreholes were

drilled in gassy seams prior to production. However, the gas drainage efficiency is low in coal seam with high water saturation [111]. MH was proposed to heat and dry the coal seam through situating microwave antenna in these boreholes [47]. As depicted in Figure 9, microwave radiator was proposed to set on the upwind of roadways. CBM will release to the borehole after microwave treatment, which will then be extracted with a pump and emitted to the downwind or stored in a gas tank [88]. It is worth to mention that the underground applications are much more complicated and dangerous. This system needs to be designed and operated without radiation hazard to the operator [55] and the methane concentration must also be monitored to prevent gas explosion.

Microwave can also address the water blocking in the near-wellbore area, which has huge damage to gas production [52]. As shown in Figure 10, a microwave radiator is set on the surface. Microwave is transmitted with a waveguide and emitted through antennas closed to the coal seam. The microwave will remove the water from coal seams and enlarge their connectivity and permeability. The CBM is then released to the wellbore together with moisture vapour and extracted with a pump.

There were other potential on-site applications based on microwave's fracturing characteristics. It can potentially reduce the drill diameter and still achieve the same production by using microwave fracturing, thus reducing the drilling cost [47]. Another potential application is to apply microwave heating together with CO_2-ECBM. As CO_2-ECBM is not feasible for coal seam with small permeability, microwave can be applied in increasing permeability prior to CO_2 injection.

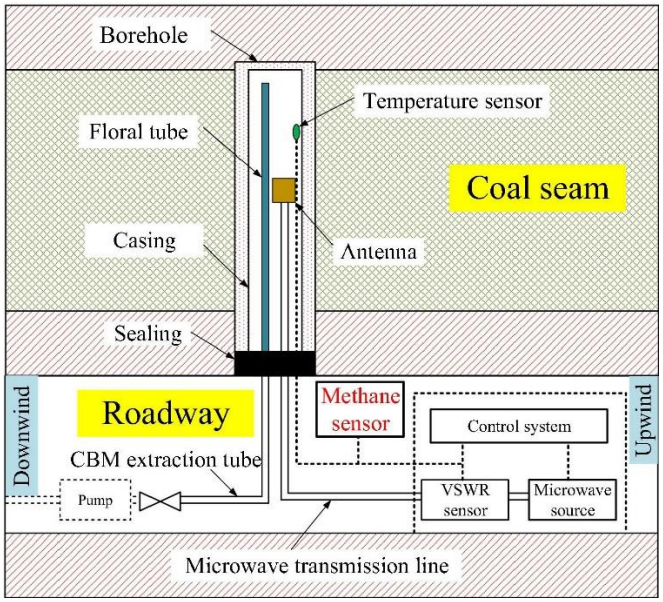

Figure 9. Microwave heating system for underground borehole (modified from [88]).

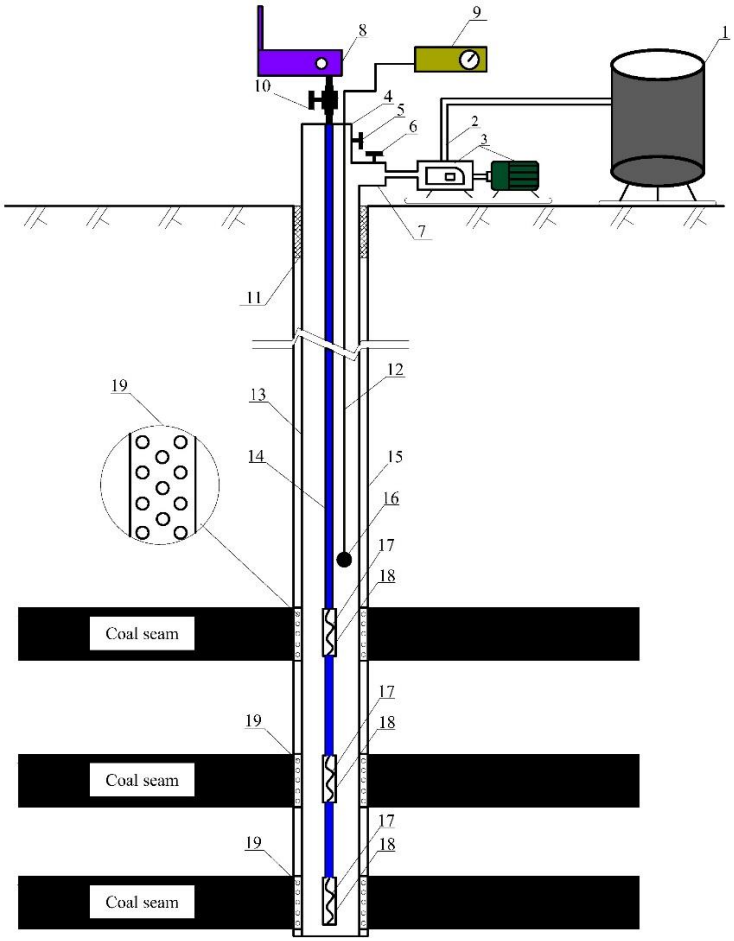

Figure 10. Microwave heating system for surface well 1-gas storage tank; 2-gas extraction tube; 3-extraction pump; 4-monitoring window on MWR; 5-monitoring window valve on MWR; 6-extraction pipeline valve; 7-extraction window; 8-microwave radiator; 9-monitoring devices; 10-waveguide valve; 11-cementing section; 12-signal transmission line; 13-casing pipe; 14-waveguide; 15-wall of surface well; 16-sensor; 17-microwave radiating antenna; 18-microwave radiating windows; 19-high-strength non-metal sieve tube [59].

2.7 Discussion and conclusions

A critical review concerning microwave heating in coal permeability enhancement was provided in this paper. Numerical simulations and experimental studies have suggested that microwave heating is a feasible and promising technology for coal seam enhancement. To assist researchers in understanding current research status, Table 2 and Table 3 summarized previous experimental and numerical studies of microwave heating and fracturing of coal.

Experimental studies suggest that microwave has a great influence on the petrophysical property of coal, whose pore size, pore connectivity, permeability and porosity increase significantly after MH. However, it still remains controversial whether microwave fracturing increases the number of pores in coal or not. Some researchers believe macropores collapse into the micropore system under the shrinkage forces caused by the rapid evaporation of the inherent moisture in the brown coal [39, 88, 112]. However, other experiments found the moisture vaporization break the pore structure and connect the micropores into larger pores, which leads to the decrease in pore number [41, 52, 56, 62]. It requires further studies to make clear the opposite result in pore number variation and whether the variation of pore number depends on the coal petrophysical property.

To optimize the energy efficiency and to achieve the best microwave heating/fracturing effect, microwave parameters require custom design based on the dielectric properties and geological conditions of the specific coal seams. Firstly, the mono-mode microwave system that generating specific frequency and power has much higher energy efficiency comparing to the multimode microwave systems. It was reported that the energy efficiency of a pilot and full-scale mono-mode type systems are over 80%, while the efficiency for multimode type applicator can be as low as 40% [97]. Secondly, microwave heating/fracturing effect is very sensitive to microwave parameters and therefore need to be determined after prudent consideration: lower microwave frequency has larger penetration depth but carries less energy; low microwave power leads to low heating rate, while large operating power may result in overheat of the surface layer. Finally, the same microwave device may have totally different heating/fracturing effect on various coal seam. Previous studies suggested high-rank coals have better and more constant microwave heating effect. And microwave achieves the best fracturing effect in coal with low moisture and high metallic minerals content.

The main research shortage in microwave-assisted coal seam enhancement is the lack of on-site experiment and field applications. As encouraging laboratory experimental results cannot ensure good performance on-site, further field-scale experiments are required before the on-site application of microwave heating. Numerical models for coal reservoirs also need to be modified or verified based on the field test.

Table 2. Literature on laboratory experiments of MI's effect on the petrophysical property of coal

Authors	Experimental object	Microwave power	Subject of study	Experiment methods	Main findings
Kumar et al. [47]	Coal cores (50mm diameter and 54mm height)	15 kW	Determining the pre- and post-microwave fracture network under both ambient conditions and simulated overburden stress	X-ray CT, Optical microscopy	Cleat/fracture volume increased from 1.8% to 16.1% for unconfined and 0.5% to 5.5% for confined coal core after MI.
Sahoo et al. [70]	Small coal (19.05-12.7 mm)	900 W	The influence of microwave pre-treatment on the grindability of coal	Grindability tests, SEM, XRD	The grindability increased significantly with the specific rate of breakage increasing by an average of 15% after MI.
Ge et al. [39]	Coal powder (< 0.074 mm)	1 kW	The effect of MI on the combustion characteristics of low-rank coals and the improvement of coal rank	N2 adsorption, FTIR, TGA	MI treatment is an upgrading process, which significantly increases the fixed carbon content and calorific value.
Liu et al. [62]	Coal powder (< 0.149 mm)	0.4-0.9 kW	The effect of drying temperature, microwave power and drying time on the pore structure of lignite	N2 adsorption, SEM	The specific surface area of microwave-treated lignite differently decreased, whereas the average pore diameter and total pore volume differently increased. Microwave power and drying time have more remarkable effects than drying temperature on the pore structure of lignite.
Zhu et al. [113]	Coal powder (< 0.154, 0.154-0.6, 0.6-1, 1-1.7 mm)	0.3-1 kW	Investigating microwave-drying characteristics of lignite and analysing moisture migration during the drying process	Microwave drying	The lignite's equilibrium moisture decreased with increasing microwave power and with decreasing particle size.
Hong et al. [88]	Coal cores (50mm diameter and 60mm height)	2, 4 and 6 kW	The effect of microwave irradiation on the porosity of coal samples	NMR	The porosity obviously increases after microwave heating, whose growth rate decreases at first then increases with microwave energy.

Hong et al. [112]	Coal cores (50mm diameter and 60mm height)	2, 4 and 6 kW	Effect of microwave irradiation on fractal features of coals	NMR	MI decreases the fractal dimension of coal cores.
Li et al. [40]	Coal cores (50mm diameter and 60mm height)	2 kW	Evolution of pore structure under MI for four different coals (lignite, subbituminous, bituminous, and anthracite)	NMR, X-ray CT, P-wave, TI	Porosity improvement decreases with coal rank.
Hu et al. [59]	Coal powder (0.177 - 0.250 mm)	0.7, 1 kW	Determining the influence of MI on the desorption capacity, diffusion and gas penetrability in coal	Methane adsorption and diffusion tests, Indirect gas penetrability test	The desorption capacity for methane, diffusion and gas penetrability property of coal increase after MI.
Li et al. [32]	Coal cores (50mm diameter and 60mm height)	2-10 kW	Evolution of pore structure under MI for coal with water saturation from 1% to 15%	NMR, X-ray CT, P-wave	The porosity grows exponentially with the increase of water contents.
Li et al. [114]	Cylindrical coal cores	1-8 kW	The effect of microwave power on the drying behaviour of coal	LF-NMR	Drying capacity increases by 125.3% and the maximum drying rate increases by 257.5% when increases the microwave power from 1 to 8 kW.
Huang et al. [56]	Coal cores (50mm diameter and 50mm height)	0.8-2 kW	The effects of microwave radiation on the microstructure of coal samples with different saturations under different microwave powers and microwave irradiation (MI) times	NMR, SEM	Pore size, water porosity and moisture loss increase with rising microwave power and irradiation time. Microwave fracturing has the best performance when water saturation is between 25% and 50%.

Table 3. Literature on numerical simulations of microwave heating of coal

Name	Numerical methods	Numerical models	Simulation software	Numerical parameters	Main findings
Chatterjee and Misra [72, 73]	Method of moments	Coupled 2D electromagnetic and thermal model	NA	12*12 cells: 2.45 GHz, 663 W, 955 W	The energy absorption efficiency is about 51% under both incident powers
Clemens and Saltiel [74]	Finite difference method	Coupled 2D electromagnetic and thermal model	NA	Microwave oven: 2.205, 2.45 and 2.695 GHz, various dielectric constants.	A slight variation of microwave frequency leads to a significant change in electrical intensity distribution in an empty cavity
Whittles et al. [85]	Finite difference method	Coupled 2D electromagnetic, thermal and mechanical model	FLAC V3.3	15*30 mm: Various microwave power (2.6 and 15 kW) and irradiation time (1, 5, 15 and 30 s).	By increasing the power density, significantly greater stresses are created for much lower energy inputs.
Peng et al. [75]	Finite difference method	Coupled 2D electromagnetic and thermal model	Mathematica 7.0	0.2*0.2 m: Various microwave powers (0.5-4 MVm-2), frequencies (0.915 and 2.45 GHz) and irradiation time (1-600 s).	Heating homogeneity is improved by reducing microwave frequency and object dimension.
Hong et al. [80]	Finite element method	Coupled 3D electromagnetic and thermal model	COMSOL Multiphysics	Microwave oven (270*267*188 mm): Various microwave powers (0.5-3 kW), frequencies (2.4-2.5 GHz) and sample positions	Microwave frequency, power and sample position affected the temperature and heating behaviour of the coal sample.

Li et al. [83]	Finite element method	Coupled 3D electromagnetic, thermal and mechanical model	COMSOL Multiphysics	Coal reservoir (20*6 m): Various microwave powers (20-120 W), frequencies (0.915, 2.45 and 5.8 GHz)	Microwave heating promotes the cumulative gas production by 37.8% after 100 days, 41.4% after 200 days, and 43.9% after 300 days.
Lin et al. [81]	Finite element method	Coupled 3D electromagnetic and thermal model	COMSOL Multiphysics	Microwave oven (630*650*660 mm): Various microwave powers (0.5-6 kW), frequencies (2.4-2.5 GHz), coal sizes and permittivity.	Larger microwave power contributes to better thermal heterogeneity. The energy efficiency and temperature increase while the thermal heterogeneity decreases with the increase of loss factor.
Huang et al. [35]	Finite element method	Coupled 3D electromagnetic, heat and mass transfer model	COMSOL Multiphysics	Microwave oven (267*270*188 mm): Various microwave powers (0.5-2 kW), frequencies (1.95-3.7 GHz) and specific moisture capacity (0.5-10 %).	Moisture increases coal sample's ability to absorb microwave energy, while evaporation takes away the absorbed energy. The coal with low water saturation has the best microwave heating effect.
Huang et al. [115]	Finite element method	Coupled 3D electromagnetic, thermal and mechanical model	COMSOL Multiphysics	Microwave oven (267*270*188 mm): 2.45 GHz, 500 W and various treatment time (0-300 s).	The average permeability increased by 2.2 times under 2.45 GHz and 500 W microwave radiation after 300 s.

3 Chapter 3

A coupled electromagnetic irradiation, heat and mass transfer model for microwave heating and its numerical simulation on coal

This chapter was published in Fuel Processing Technology. It was written by Jinxin Huang and revised by Prof Guang Xu, Dr Guozhong Hu, Dr Mehmet Kizil and Dr Zhongwei Chen.

Please cite this paper as:

Huang, J., Xu, G., Hu, G., Kizil, M., & Chen, Z. (2018). A coupled electromagnetic irradiation, heat and mass transfer model for microwave heating and its numerical simulation on coal. *Fuel Processing Technology*, *177*, 237-245.

https://doi.org/10.1016/j.fuproc.2018.04.034

After reviewing the previous studies, it is noted that there are research gaps in both numerical and experimental studies. For instance, none of the previous numerical models considered moisture vaporization in microwave heating of coal. Chapter 3 proposed a coupled electromagnetic, heat and mass transfer model in studying microwave heating of coal. The temperature and electric field distribution of coal samples were analysed in detail under different microwave frequencies, microwave powers and coal's moisture capacity.

3.1 Abstract

As hydraulic fracturing as a means to enhance coal bed methane was banned in some countries due to possible negative environmental impacts, the microwave heating was proposed as an alternative approach to enhance coal permeability and thus gas productivity. One of the mechanisms on improving coal permeability using microwave irradiation is that thermal stress caused by microwave heating generates fractures. To study the influence of microwave settings to the heating effect of coal samples, a coupled mathematical model for electromagnetic, heat and mass transfer in the process of microwave heating is proposed and is numerically implemented using a finite element method. This coupled model for microwave heating have considered heat and mass transfer, and is validated by comparison with experimental results. Then it is used to simulate the influence of frequency, power and moisture capacity on microwave heating. The simulation results show that microwave heating of coal is highly sensitive to excitation frequency. Frequencies around 3.45 GHz contribute to significant thermal heterogeneity. With the same energy input, different powers do not influence the overall heating effect, but higher powers cause greater thermal heterogeneity. Moisture capacity also has great effect on microwave heating and thermal distribution pattern. Under 2.45 GHz and1.0 KW, the coal sample with moisture capacity of 5% has the best microwave heating effect.

Keywords: Coal permeability enhancement; Microwave heating; Numerical simulation

3.2 Introduction

Coalbed methane (CBM) exist in coal seam in four ways: adsorbed in micropores, trapped in matrix porosity, dissolved in ground water and as free gas in fissures [1]. It needs to be extracted prior to as well as during underground mining operations to avoid methane outburst and explosion accidents [2]. Beyond that, CBM exploitation has potential economic benefit and great environmental benefit [2, 3]. CBM extraction can be divided into underground drainage and CBM drainage using surface vertical wells [4, 5]. Underground drainage has been used extensively and achieved good effects despite of the difficulties in the collection, transmission and utilization of low-concentration gas [4]. CBM extraction from surface wells overcomes these challenges, while the gas production of most wells is low and therefore not so economical.

With the increase of mining depth, the gas content generally increases while the coal permeability decreases, which makes it harder to drain the gas. The most commonly used technologies to increase coal permeability for methane are hydraulic fracturing and CO2 injection enhanced coalbed methane (CO2-ECBM) recovery [6, 7]. However, hydraulic fracturing is banned in some countries and regions due to potential environmental concerns [8], and ECBM is restricted by in-situ conditions and therefore not suitable for some of the coal mines[7]. Heat injection has also been applied as an alternative means to recover coal bed methane. However, this method is also restricted by geological conditions as hot liquid cannot arrive in certain area [9]. To address this, microwave heating was proposed to replace hot liquid. It is worth to mention that microwave heating is not only limited to coalbed. It can also be applied in stimulating shale and oil sand reservoir to assist or even replace traditional methods [10-14].

Microwave is an electromagnetic radiation with frequencies between 300MHz and 300GHz, which has been broadly used in industrial, scientific, medical and instrumentations applications [15]. It also has been widely applied in the field of coal processing areas, such as drying [16], coking [17], pyrolysis [18-20], flotation [21], increasing grindability [22, 23], and magnetic removal [24]. The theory of using microwave to increase coal permeability is that moisture within coal body evaporate under microwave irradiation, and the accompanying vapour pressure

together with the heating effect expand pores and fissures of the coal [25, 26]. Meanwhile, the heat effect of microwave accelerates coal bed methane's (CBM) molecular thermal motion and therefore promotes its transformation from adsorbed state to free state [27]. As the dielectric loss factor of coal is negligible comparing to the moisture and metalliferous mineral within the coal body, heating effect is non-uniform and therefore results in thermal fractures [23, 28]. Experiments have been conducted to investigate microwave's effect on microstructures of coal. Hong [29] measured water porosity of 20 coal samples before and after irradiation and found the average water porosity increased by 22.49%. Nuclear Magnetic Resonance (NMR) was the most common used tool to compare the petrophysical characterization of coal before and after microwave treatment. The results showed that pore size, throat size and pore numbers all increase significantly with microwave energy [29-31]. By using analysis techniques, such as low-temperature nitrogen adsorption experiments, Computational Tomography (CT), Scanning Electron Microscope (SEM) and Mercury Injection Capillary Pressure (MICP), studies have concluded that microwave irradiation enlarges pore size and increases coal permeability substantially, and therefore it has the potential to be applied in coal bed methane stimulation [32-35].

As the effectiveness of coal permeability enhancement is determined by the microwave's heating behaviour, it is vital to find out what factors may influence the microwave's heating behaviour on coal before applying this technology on-site. It is reported that microwave heating effect entirely depends on the electric field distribution in the oven, with larger electric intensity results in better heating effect. Therefore, it is critical to investigate the electric field and thermal field distribution within the coal samples. As the electric field and temperature distribution are hard to measure, numerical experiments were introduced to simulate the microwave heating process. In previous studies, coupling electromagnetic and thermal field, numerical models were built with COMSOL Multiphysics to investigate microwave heating under various conditions [9, 36]. However, these models assumed there is no phase change or mass transfer and ignored moisture contents within the coal samples and its latent heat of evaporation, which do not represent the actual condition.

The aim of this paper is to study the heating and drying effect of microwave on coal samples by using a coupled electromagnetic, heat and mass transfer model.

To address this, a 3D model coupling electromagnetic, heat and mass transfer was established with COMSOL Multiphysics. The electromagnetic and thermal field were coupled with microwave heating effect. The electromagnetic field affects the mass transfer through affecting moisture conductivity and mass transfer coefficient. And the thermal field and flow field are connected with the latent heat of evaporation. The model was then verified through comparing with data from previous articles. Finally, temperature and electric field distribution of coal samples were analysed in detail under different microwave frequencies, microwave powers and coal's moisture capacity.

3.3 Governing Equations

3.3.1 Assumptions

The following assumptions are made in the model to simplify the complex problem and save computational cost:

1) The initial coal sample is homogeneous and isotropic.
2) There is no microwave heating or heat transfer in the glass plate.
3) Heat capacity, dielectric constant, moisture conductivity and mass transfer coefficient of coal sample remain constant under various temperatures and frequencies.
4) Dielectric constant is proportional to moisture concentration.
5) Chemical reaction is not considered.
6) The movement of water molecule in the magnetic field and electric field is simplified as a constant mass transfer.
7) Only latent heat of vaporization is considered in the phase change, while the vapour pressure is ignored.
8) The effect of moisture vapour on the coal pore structure is not considered.

3.3.2 Electromagnetic Field

Maxwell's equation is the most commonly used equation to describe electromagnetic propagation. In this paper, the governing equation is given as [37]:

$$\nabla \times \mu_r^{-1}(\nabla \times E) - k'^2\left(\varepsilon_r - \frac{j\sigma}{\omega\varepsilon_0}\right)E = 0 \quad (1)$$

where μ_r is the relative permeability (N/A^2), E denotes the electric field intensity (V/m), ε_r represents relative permittivity, j is imaginary unit, σ is the electrical conductivity (S/m), ω represents the angular frequency and ε_0 is the permittivity of free space (8.85×10^{-12} F/m) [9]. The wave number in the vacuum k' is given as:

$$k' = \frac{\omega}{c'} \tag{2}$$

where c' is the speed of light in vacuum (2.998×10^8 m/s).

3.3.3 Heat Transfer Equation

Heat transfer is only solved in the coal sample domain. The microwave heat and phase change heat are coupled in *Fourier's* law of heat conduction, given as below [38]:

$$\rho C_p \frac{\partial T}{\partial t} + \rho C_p \boldsymbol{u} \cdot \nabla T + \nabla \cdot \boldsymbol{q} = Q_{vap} + Q_{ted} \tag{3}$$

where ρ is the density of the coal sample, C_p denotes the specific heat capacity, T is the temperature, Q_{vap} represents the latent heat of moisture vaporization, Q_{ted} is the microwave heat. Heat flux **q** is expressed as:

$$\mathbf{q} = -\mathrm{k}\nabla\mathrm{T} \tag{4}$$

where k is the thermal conductivity ($\mathrm{W}/(\mathrm{m}^2 \cdot \mathrm{K})$)

Latent heat of vaporization Q_{vap} is given as:

$$Q_{vap} = \lambda \frac{dc}{dt} \tag{5}$$

where c denotes concentration, λ is the molar latent heat of vaporization (*J/mol*).

3.3.4 Mass Transfer Equation

Similar to the heat transfer, the mass transfer is only solved in the coal sample domain as well, expressed as [38]:

$$\frac{\partial c}{\partial t} + \nabla \cdot (-D\nabla c) = R \tag{6}$$

where D is moisture diffusivity, R is molar production rate.

The moisture diffusivity is calculated according to equation (7), given as:

$$D = \frac{k_m}{\rho C_m} \tag{7}$$

where D is the diffusion coefficient, k_m represents moisture conductivity, ρ is density of coal sample, and C_m is specific moisture capacity.

3.3.5 Boundary Conditions

For the electromagnetic field, the walls of waveguide and oven are defined as impedance boundary condition and solved in the frequency domain, given as the following equation [39]:

$$\sqrt{\frac{\mu_0 \mu_r}{\varepsilon_0 \varepsilon_r - j\sigma/\omega}}\, n \times H + E - (n \cdot E)n = (n \cdot E_s)n - E_s \tag{8}$$

where μ_0 is the permeability of free space ($4\pi \times 10^{-7} N/A^2$), H is magnetic field intensity (A/m), E_s denotes electric field source which is 0 in this case.

The symmetry boundaries are described as perfect magnetic conductor, which is expressed as:

$$\boldsymbol{n} \times \boldsymbol{H} = \mathbf{0} \tag{9}$$

The port boundary is excited by a transverse electric wave. The wave, which has no electric field component in the direction of propagation, is controlled by a propagation constant β, which is presented as [39]:

$$\beta = \frac{2\pi}{c}\sqrt{v^2 + {v_c}^2} \tag{10}$$

where v represents the microwave frequency, v_c is the cutoff frequency, given as:

$$v_c = \frac{c'}{2}\sqrt{(\frac{m}{a})^2 + (\frac{n}{b})^2} \tag{11}$$

where *m* and *n* are the mode numbers, *a* and *b* denote the lengths of rectangular cross section (a=78 *mm* and b=18 *mm*). In this case, TE_{10} mode (*m=1*, *n=0*) is the only propagating mode for frequencies between 1.95 *GHz* and 3.70 *GHz*.

For the thermal field, the bottom and symmetry face are defined as thermal insulation boundary conditions, which are written as[40]:

$$\mathbf{n} \cdot (-\mathrm{k}\nabla \mathrm{T}) = 0 \tag{12}$$

As for the other surfaces of coal sample, the boundary conditions for the heat transfer interfaces are given as [40]:

$$\mathbf{n} \cdot (\mathrm{k}\nabla \mathrm{T}) = h_T(T_{air} - T) \tag{13}$$

where h_T is the heat transfer coefficient, and T_{air} is the air temperature in the microwave oven.

For the mass transfer field, the bottom and symmetry face are defined as no flux boundary condition, which is expressed as equation (14), while external forced convection is applied to the other surfaces of coal sample, given as equation (15) [38, 40].

$$\mathbf{n} \cdot (-\mathrm{D}\nabla \mathrm{c}) = 0 \tag{14}$$

$$\mathbf{n} \cdot (-\mathrm{D}\nabla \mathrm{c}) = k_c(c_b - c) \tag{15}$$

where D denotes the moisture diffusion coefficient in the coal sample, given as equation (7), and c_b refers to the air moisture concentration. k_c is the mass transfer coefficient, presented as follows [38]:

$$k_c = \frac{h_m}{\rho C_m} \tag{16}$$

where h_m refers to the mass transfer coefficient in mass units of coal sample.

3.3.6 Numerical Implementation in COMSOL Multiphysics

3.3.6.1 Geometry and Meshing

The model geometry is established based on the microwave oven model in COMSOL Multiphysics application gallery [39], as shown in Figure 11. The microwave oven and waveguide are filled with air. The coal sample sits on a fstationary cylindrical glass plate at the bottom centre of the oven. Both the plate and coal sample are stationary during the simulation. To reduce the model size, a symmetry model was adopted. The detailed geometry parameters are shown in Table 4.

Table 4. Global model parameters

	Width (mm)	**Depth (mm)**	**Height (mm)**	**Radius (mm)**
Microwave oven	267	270	188	—
Waveguide	50	78	18	—
Glass plate	—	—	6	113.5
Coal sample	—	—	60	25

The physics-controlled mesh is enabled, and the maximum mesh size was set to 1/5th of the wavelengths. The meshes of the coal sample are customized with 0.005 m maximum element size, while the rest meshes are predefined as finer meshes. There are 40365 elements in the entire geometry with averaged element quality of 0.74, as shown in Figure 12. This proves the mesh quality is accurate enough to obtain reliable results.

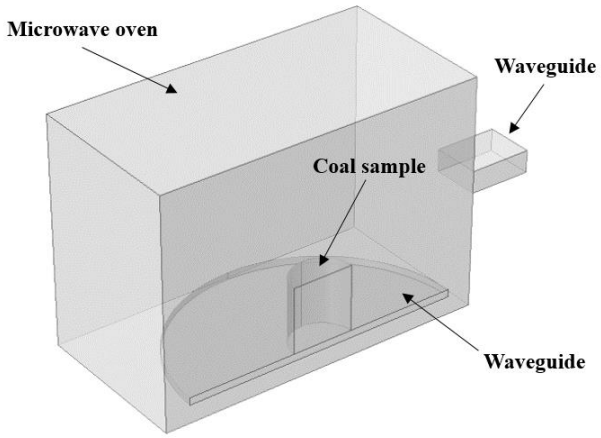

Figure 11. Geometry of microwave heating model

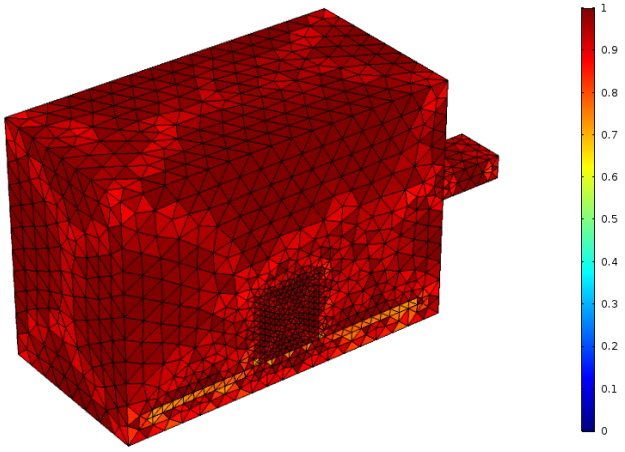

Figure 12. Mesh quality evaluation

3.3.6.2 Parameter Determination and Initial Conditions

Moisture conductivities and mass transfer coefficients of coal samples are two critical parameters in microwave drying simulation. However, such data are not available in the literature and therefore needed to be calculated indirectly. As mentioned in the assumptions, moisture conductivities and mass transfer coefficients of coal samples are assumed constant in each individual simulation. In previous studies, 5g coal samples with various particle size were used to investigate microwave drying characteristics [16, 41]. It was found that the drying rate increased approximately proportionally with the increasing output power level. We adopted one of the experiment data and obtained a fitting curve, which reflects the relationship between the output power and moisture loss. Based on the reported 55.5% moisture loss after 8 min of 650 W microwave irradiation [42], we achieved the same result with $h_m = 5.8 \times 10^{-4}\ kg/(m^2 \cdot s)$ and $k_m = 6.59 \times 10^{-5}\ kg/(m \cdot s)$ by trial and error through adjusting the moisture conductivity and mass transfer coefficients. Combining the fitting curve and the data under 650W, the moisture conductivity and mass transfer coefficients under 0.5, 1.0, 1.5, 2.0, 2.5, and 3.0 kW were calculated, as shown in Table 5.

Table 5. Moisture conductivity and mass transfer coefficient under various powers

Power (W)	Moisture conductivity 10^{-5} kg/(m · s)	Mass transfer coefficient 10^{-4} kg/(m^2 · s)
500	4.17	4.74

1000	9.59	10.90
1500	15.02	17.06
2000	20.44	23.22
2500	25.86	29.38
3000	31.28	35.54

Relative permittivity (real permittivity ε' and imaginary permittivity ε'') of coal plays a vital role in microwave heating and drying as imaginary permittivity (or loss factor) determines how much energy dissipates from the electric field [43]. Comparing to water (with loss factor of 12 at 25℃ and 2.45GHz), bulk material of coal has negligible loss factor (less than 0.25) [22, 44, 45]. The permittivity (including real and imaginary permittivity) of coal samples with different moisture capacities from Shanxi China were measured, as shown in Figure 13 [44]. According to the fitting curve, the ε' and ε'' of coal samples with specific moisture capacity of 0.5%, 1%, 2%, 3%, 4%, 5%, 6%, 7%, 8%, 9%, 10% were calculated, as shown in Table 6. It is reported that the dielectric constant of coal decreases with increasing temperature, which is primarily resulted from moisture loss [46]. To address this, the relative permittivity of coal samples was estimated using the following equation:

$$\varepsilon_r = (\varepsilon' + \varepsilon'') * (c/c_0) \quad (18)$$

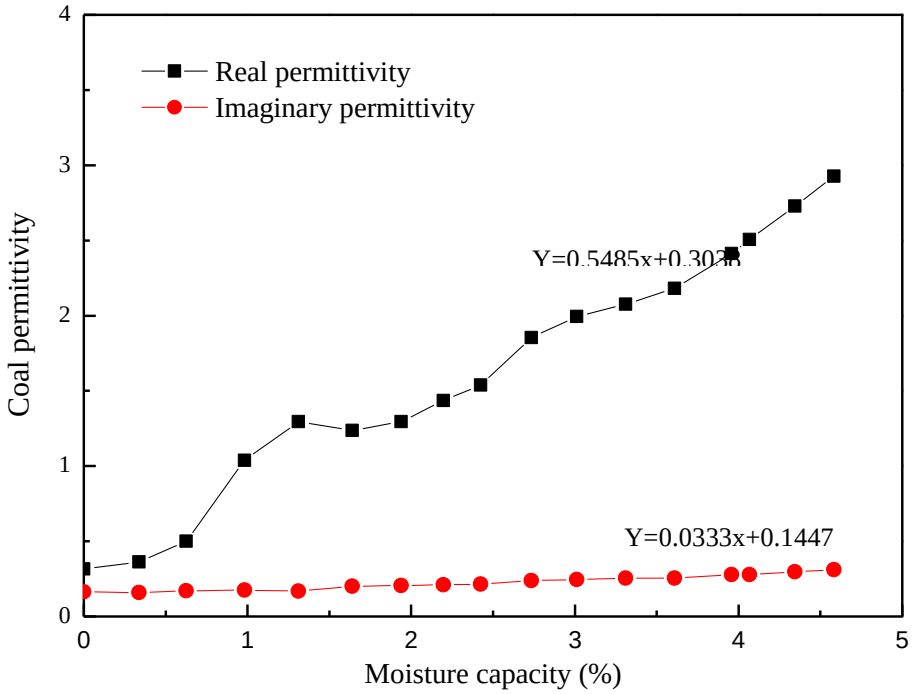

Figure 13. The relationship between moisture capacity and coal permittivity

Table 6. Real permittivity and imaginary permittivity of coal samples with different specific moisture capacity

Specific moisture capacity (%)	ε′	ε″	Specific moisture capacity (%)	ε′	ε″
0.5	0.578	0.161	5.0	3.046	0.311
1.0	0.852	0.178	6.0	3.595	0.345
2.0	1.401	0.211	7.0	4.143	0.378
3.0	1.949	0.245	8.0	4.692	0.411
4.0	2.498	0.278	9.0	5.240	0.444
4.7	2.882	0.301	10.0	5.789	0.478

The initial conditions and other parameters of the model are list in Table 7.

Table 7. Initial conditions and global parameters [36, 39]

Name	Description	Expression

c_{air}	Air moisture concentration	0.5 [mol/m^3]
c_0	Initial moisture concentration of coal sample	3394.4 [mol/m^3]
T_0	Initial temperature of the coal sample and air	298.15 [K]
E_0	Initial electric field intensity in all domain	0
ρ	Coal density	1300 [kg/m^3]
k	Thermal conductivity	0.478 [$W/(m \cdot K)$]
h_T	Heat transfer coefficient	25 [W/($m^2 \cdot K$)]
λ	Molar latent heat of vaporization	41400 [J/mol]

3.3.7 Comparison with Experimental Results

The established model considers heat and mass transfer, and thus both microwave heating and drying are simulated. Its heating and drying effects need to be verified before conducting further simulations. The microwave heating effect of this model was verified through comparing to the microwave heating experiments done by Lin et al [36]. As shown in Figure 14, the simulated temperature of the upper coal surface was recorded and compared with the experimental results. It is shown that the simulation results agree well with the experiment results except for some parts that the simulated temperatures are lower than the measured ones. This may be due to the fact that the moisture conductivity and mass transfer coefficient are set as constant in the model. These values are initially larger than the actual situation, which will result in more moisture vaporization and larger latent heat of vaporization and therefore lead to lower temperature. In addition, the dielectric constant in this model is assumed only sensitive to moisture concentration, while the temperature effect is neglected. This may also lead to the difference between the simulation and experiment results. Considering that the moisture conductivities and

mass transfer coefficients of coal samples are deduced from different microwave drying experiment results, the microwave drying effect of this model is considered accurate enough to perform further simulations.

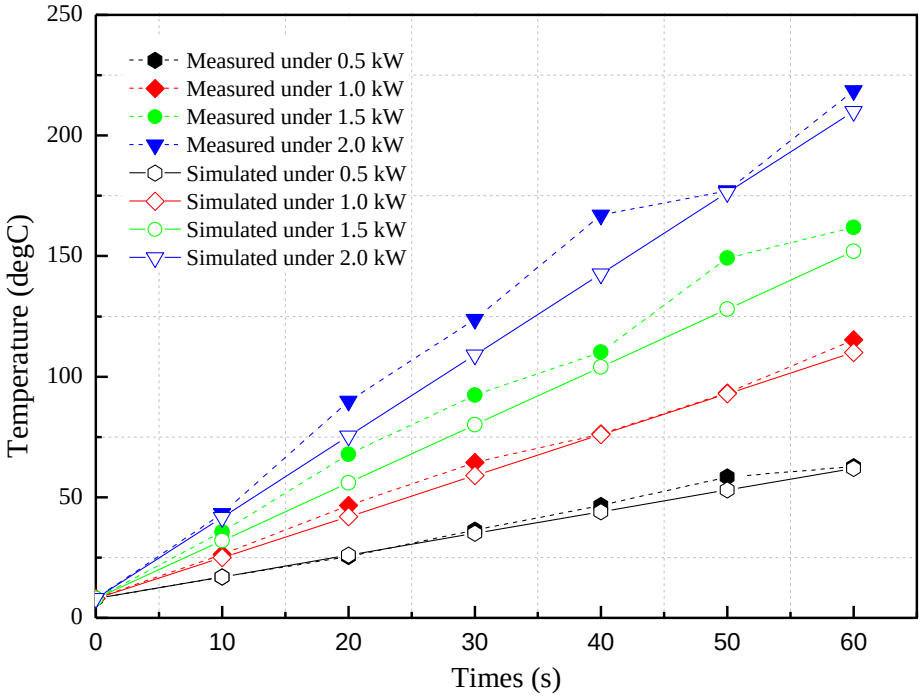

Figure 14. Measured and simulated temperature of upper coal surface

3.4 Results and Discussion

3.4.1 Effect of Microwave Frequency

The frequency of microwave has significant impact on electric field distribution, and thus influence its heating behaviour. Other studies have only investigated microwave frequency within 2.4 GHz to 2.5 GHz [36, 47]. This range is too narrow to see any substantial impact due to the change of frequency. For industrial application, the applied frequency can be extended to a broader range. Thus, in this study, simulations were conducted with excitation frequencies ranging from 1.95 GHz to 3.70 GHz, with 0.25 GHz increments. All the microwave powers were set to 650 W and the specific moisture capacities were defined as 4.7%.

It is worth mentioning that the simulation objects in this paper are coal samples, which are small enough to be easily penetrated by all microwave with frequencies between 1.95 GHz and 3.70 GHz. However, penetration depth is one of the most significant issues needs to be investigated before applying microwave on-

site. Clark and Sutton [48] defined penetration depth (D_p) as the distance from the surface to the material where the power drops to e^{-1} of the initial value, given as

$$\mathrm{D}_p = \frac{\lambda_0}{2\pi(2\varepsilon')^{1/2}}\left[(1+\left(\varepsilon''/_{\varepsilon'}\right)^2)^{1/2}-1\right]^{-1/2} \quad (1)$$

where λ_0 is the wavelength of free space, ε' and ε'' are the dielectric constant and loss factor respectively.

It is obvious from equation (1) that the penetration depth is in direct proportion to the wavelength, thus inversely proportional to the microwave frequency [49]. However, no field test in coal seam has been conducted to verify the proposed theory. Considering microwave has been tested by theoretical models, laboratory experiments and field trial researches in the recovery of heavy oil reservoirs, it should have great application prospect in coal seam as well [50-53].

In general, different microwave frequencies result in substantially different electric field distributions in the microwave oven and coal samples, which result in the difference in the thermal field distribution in the coal samples. As displayed in Figure 15, (a) shows the electric field distribution in the microwave oven (front view), (b) illustrates the electric field distribution in coal samples, and (c) presents the thermal field distribution in coal samples. Due to the limitation of space, only results for frequency 2.70 GHz and 3.45 GHz are provided, and the results are at 600s after microwave applied. It can be seen that under some frequencies (e.g. 2.70 GHz) the electric field are more evenly distributed than others (e.g. 3.45 GHz), which causes more evenly distributed thermal field in coal samples. The frequencies that cause even thermal distribution may not be preferred in enhancing coal permeability as only large differential heating generates new fractures [54] (i.e. uneven expansion induced fractures). In addition, comparing the thermal field distribution for different frequencies (Figure 15 (c)), the location of the maximum heated area in the coal sample is different. For practical application, it seems plausible that by using more than one microwave frequencies alternately will improve the permeability enhancing effectiveness as more areas can be heated.

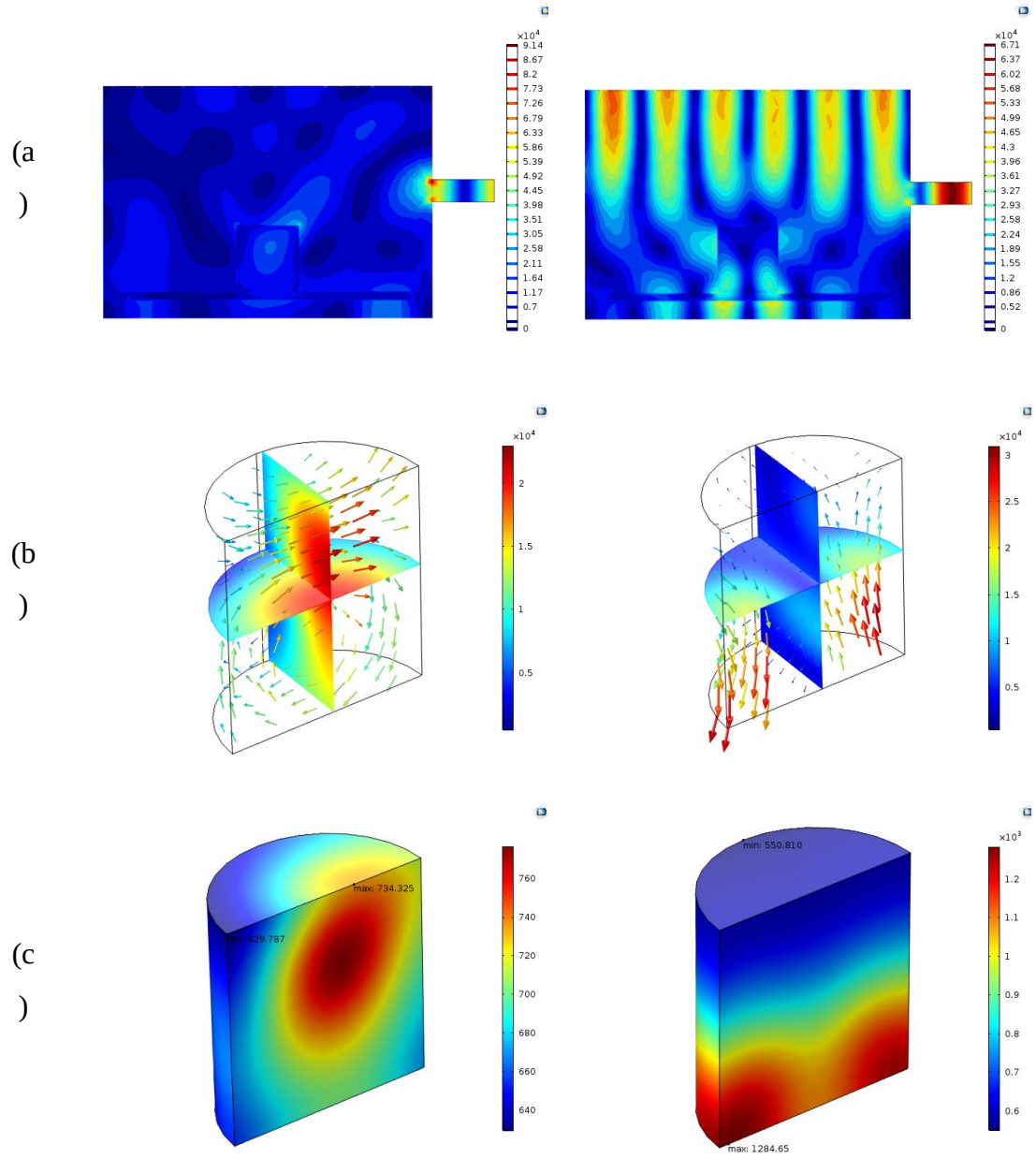

Figure 15. Electric (a, b) and thermal field (c) distributions at 650 W after 600s

For each simulated frequency, the average electric field intensity, average temperature, and the maximum temperature difference in the coal samples at 650W and 600s are displayed in Figure 16. As can be observed, for nearly all the frequencies, the change trend of the average electric field intensity curve and the average temperature curve are consistent. This means a higher electric field intensity causes higher average temperature in coal samples. However, the maximum temperature difference within the coal sample does not necessarily increase with

higher frequencies. It is because the electric field distribution varies under different frequencies, which result in various thermal distribution pattern. In this case, the maximum temperature difference reaches maximum at 3.45 GHz frequency. As higher maximum temperature difference causes more inhomogeneous expansion that creates thermal stresses and fractures, we could infer that a frequency around 3.45 GHz works better in enhancing the permeability of coal sample.

For application in thick coal seam, frequency of 2.45 GHz or even lower could be a good working frequency in stimulating coal bed methane, as lower microwave frequencies lead to larger penetration depth. The best working frequency for different coal seam thicknesses should be investigated in the further study. Using more than one microwave frequencies alternately could be an effective way to achieve great fracturing effect and long penetration depth at the same time.

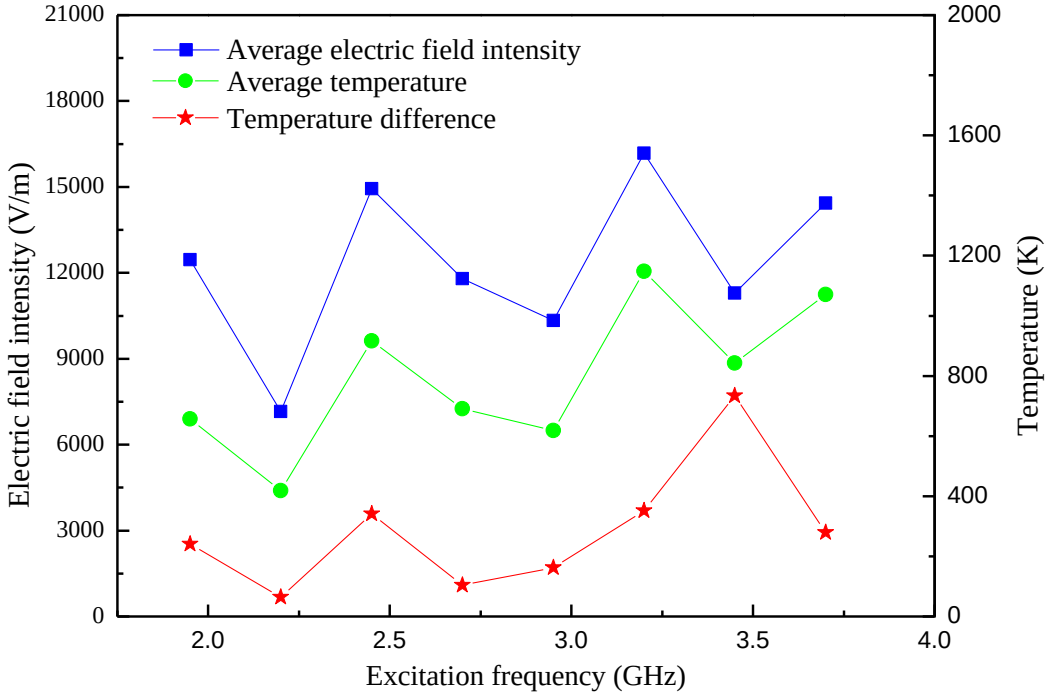

Figure 16. The effect of excitation frequency on electric field intensity and temperature of coal samples

3.4.2 Effect of Microwave Power

It is obvious that larger power results in larger electric field intensity, which further contributes to better microwave heating and drying effects within the same time period. However, economic benefit should also be considered in industrial applications. In this study, the power effect comparison was made at the same energy

input of 300 KJ. Thus, microwave heating and drying effects were compared with the same energy input and specific moisture capacity of 4.7% under frequency of 2.45GHz. The simulation results (0.5 KW at 600 s, 1.0 KW at 300 s, 1.5 KW at 200 s, 2.0 KW at 150 s, 2.5 KW at 120 s, 3.0 KW at 100 s) were presented in Figure 17. The figure indicates that the temperature and concentration distributions have similar characteristics, with the hot spots and high moisture regions in roughly similar locations.

To investigate the difference between different power patterns in detail, the average moisture concentration, average temperature, maximum temperature, minimum temperature and maximum temperature difference were calculated and depicted in Figure 18. Although the average temperature remains approximately constant with the same energy input, higher power lead to larger temperature difference. It is found that the maximum temperature of coal sample increases with rising input power, while its minimum temperature decreases. Considering both effects, the temperature difference increase continuously with increasing input power. It indicates that the larger input power contributes to more nonuniform temperature distribution (the time of microwave heating shortens with the increase of microwave power, while the thermal conductivity remains the same), which is better for enhancing permeability of coal seam. It is also found that higher input power contributes to better microwave drying effect, but the difference is insignificant when the input power is above 1 KW.

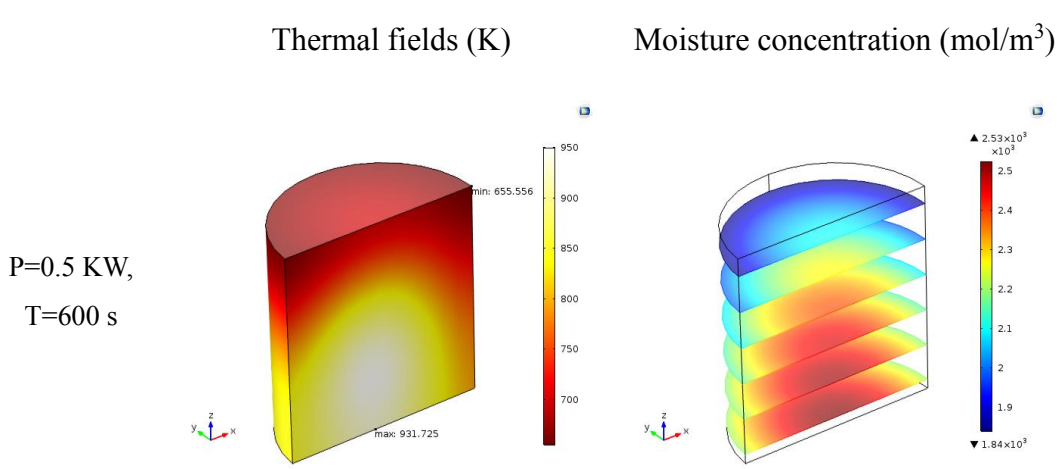

P=1.0 KW,
T=300 s

P=2.0 KW,
T=150 s

P=3.0 KW,
T=100 s

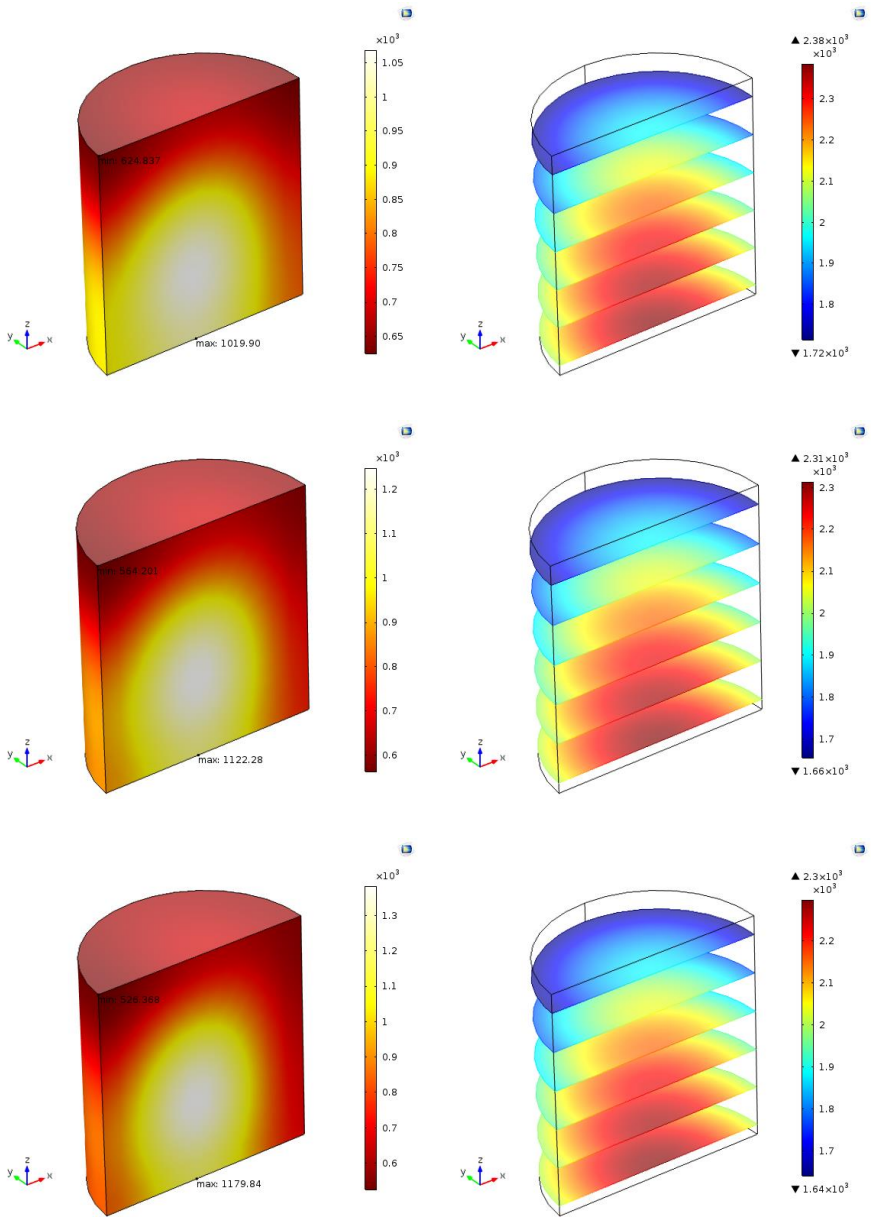

Figure 17. The thermal and concentration distributions of coal samples under various input powers

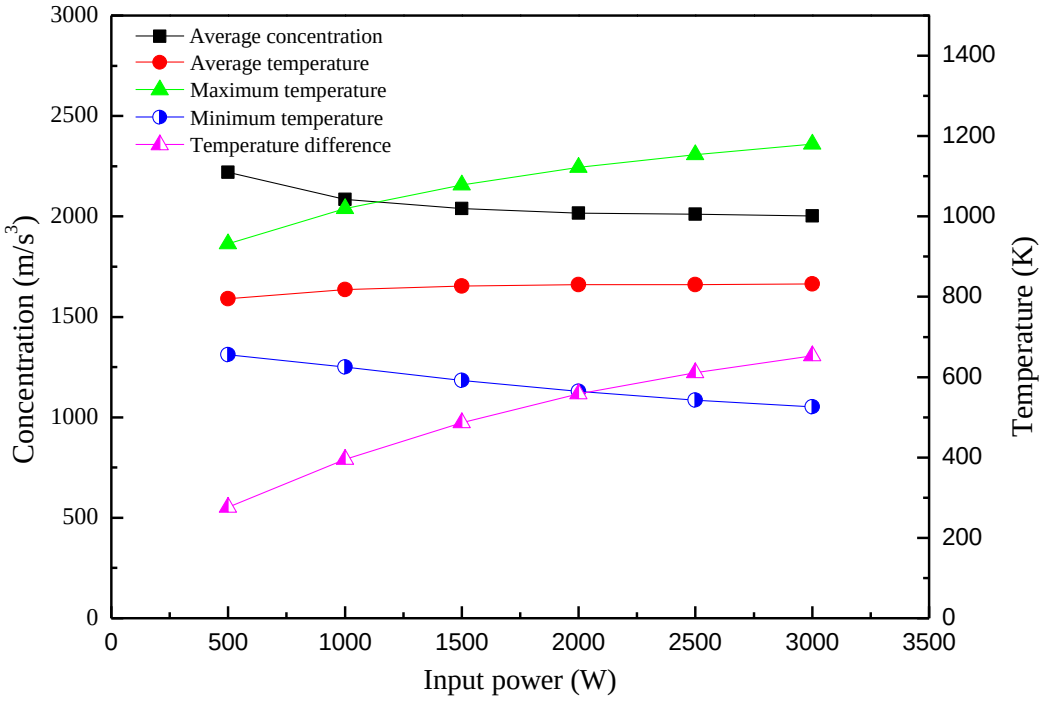

Figure 18. Effect of power on temperature and concentration with the same energy input

3.4.3 Effect of Specific Moisture Capacity

To study the effect of moisture capacity, simulation experiments were carried out respectively with specific moisture capacity ranged from 0.5% to 10% under 2.45 GHz and 1.0 KW. Some representative results are shown in Figure 19.

As revealed in Figure 19, the specific moisture capacity has remarkable influence on electric and thermal field distribution. The moisture within coal sample affects microwave heating in two ways. On one hand, the moisture content increases coal sample's dielectric constant (as shown in Tab.3) and thus enhances its ability in absorbing microwave energy. On the other hand, larger moisture content requires more energy for each degree rise in temperature. Moreover, it also leads to greater latent heat of moisture vaporization, and the moisture takes energy away from coal sample as the vapor evaporates into the air. Unlike the effect of microwave power, the temperature distributions have diverse characteristics. For specific moisture capacities between 0.5% and 2%, the hot spot is located at the top left corner and the spot with the minimum temperature situate in the bottom right corner. And the hot spot moves to the bottom left corner when the specific moisture capacity is 3%.

Then, as it increases from 3% to 10%, the hot spot gradually shifts from bottom left corner to the bottom centre of the coal sample.

The average electric field norm and average temperature of coal sample were calculated and depict in Figure 20. It is shown that for the input of 2.45GHz and 1.0 KW, the average electric field norm and temperature increase exponentially with increasing specific moisture capacities from 1% to 5%. It then decreases with rising specific moisture capacity until it reaches 9%. It can be concluded that under 2.45 GHz and 1.0 KW, the coal sample with specific moisture capacity of 5% has the best microwave heating effect. As explained before, the moisture increases coal sample's ability to absorb microwave energy, and evaporation takes away the absorbed energy. The first effect dominates when the specific moisture capacity is less than 5%. Then, as the specific moisture capacity continues to increase, the rate of evaporation overcomes that of the rate of microwave absorption. This is the reason the microwave effects differ for coal with different specific moisture capacities. However, the specific moisture capacity that leads to the best microwave heating effect may differs if conditions are changed, such as microwave frequencies, microwave powers and geological conditions. Therefore, before applying microwave heating on site, simulations should be conducted according to the field data to find the most suitable microwave frequency and power.

Moisture capacity (%)	0.5	2	5	10
Electric field (V/m)	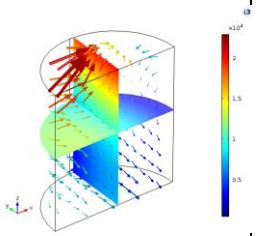	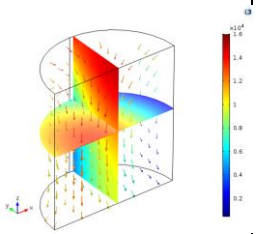	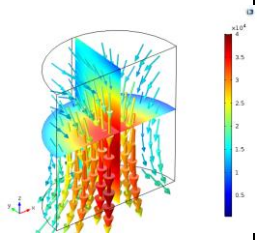	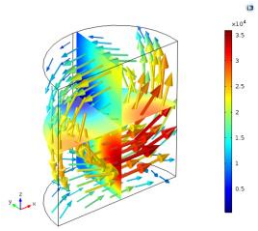
Thermal field (K)	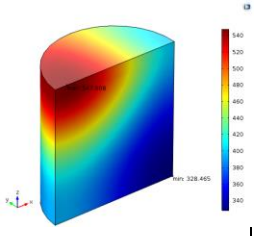	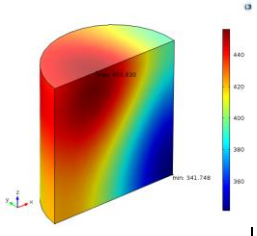	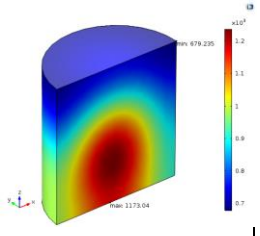	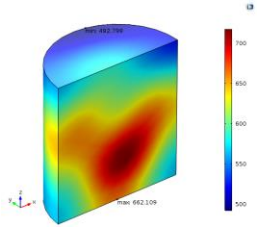

Figure 19. The electric and thermal distributions of coal samples with various specific moisture capacity at 1000W of 2.45GHz after 300s

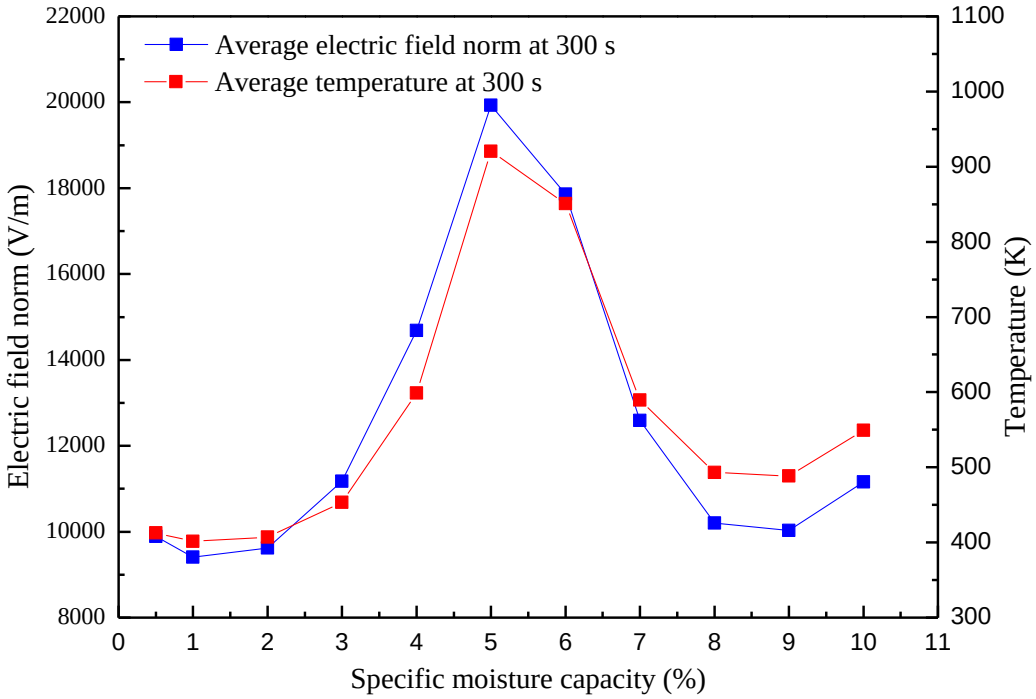

Figure 20. The effect of specific moisture capacity on electric field intensity and temperature of coal samples

3.5 Conclusions

Prior work has simulated the microwave heating effects of coal samples under various circumstances. For example, the influencing factors of microwave frequency, power, coal permittivity and coal size on microwave heating were studied with a coupled electromagnetic and heat transfer model [36]. However, these models did not consider the phase change and mass transfer of moisture contents within the coal sample. Thus, the ignorance of latent heat of evaporation cannot reflect the real situation.

In this study, we established a coupled electromagnetic, heat and mass transfer model with COMSOL Multiphysics, which approximates more closely to the real condition. After verification, simulations were conducted to study the effects of microwave power, frequency and coal's moisture capacity. We found that microwave heating is extremely sensitive to microwave frequency as different frequencies lead to various electric field and thermal distributions. It was also found

that coal sample under 3.45GHz has the largest temperature difference and therefore should be an ideal work frequency for enhancing the permeability of coal sample. Microwave power, on the other hand, has little effect on the average temperature of coal samples with the same energy input. However, higher power increases the maximum temperature difference in the treated coal, which is better for enhancing the permeability of coal seam. As for the effect of specific moisture capacity, it was found that moisture capacity has great influence on microwave heating. An optimal microwave heating performance exists for a certain moisture capacity. In the current study, microwave settings of 1 KW at 2.45 GHz result in the best heating effect for coal samples with 5% specific moisture capacity.

Although assumptions were made to determine moisture conductivity and mass transfer coefficient, and only one microwave setting was investigated for various moisture capacity, the findings in this paper fill the research gap in considering the effect of coal sample's moisture in microwave heating model. It could be very helpful in determine microwave working frequency and power when applying microwave on-site to improve permeability of coal seam. To better reflect actual situations and improve the model accuracy, further experiments will be done to obtain the change of moisture conductivity and mass transfer coefficient during coal sample heating. Beyond that, coal will be defined as an initial nonhomogeneity material to study the thermal stress and fissure development in coal samples under microwave irradiation.

3.6 Acknowledgements

This project is supported by the National Natural Science Foundation of China (Grant No. 51774279), the Petrochemical Joint Funds of National Natural Science Foundation of China and China National Petroleum Corporation (Grant No. U1762105), the Independent Research Projects of State Key Laboratory of Coal Resources and Safe Mining, CUMT (SKLCRSM15KF01), and the Mining Education Australia Collaborative Research Grant Scheme (2017). The research stipend support from China Scholarship Council is acknowledged.

4 Chapter 4

Simulation of microwave's heating effect on coal seam permeability enhancement

This chapter was published on International Journal of Mining Science and Technology. It was written by Jinxin Huang and revised by Prof Guang Xu, Mrs. Yinping Chen and Dr Zhongwei Chen.

Please cite this paper as:

Huang, J., Xu, G., Chen, Y., & Chen, Z. (2019). Simulation of microwave's heating effect on coal seam permeability enhancement. International Journal of Mining Science and Technology, 29(5), 785-789.

https://doi.org/10.1016/j.ijmst.2018.04.017

On the basis of previous models, this chapter proposed a coupled electric, heat transfer and mechanics model in studying microwave heating of coal. This model makes it possible to investigate the thermal stress, strain and permeability distribution of coal under microwave irradiation.

4.1 Abstract

As hydraulic fracturing was forbidden in some countries due to possible negative environmental impacts and enhanced coal bed methane (ECBM) was restrict by in-situ conditions, microwave heating was proposed to enhancing coalbed permeability. One of the mechanisms of improving coal permeability with microwave irradiation is that thermal expansion caused by microwave heating. To study the influence of microwave's heating effect of coal samples, the simulations were conducted using a coupled electromagnetic, thermal and mechanical model in this paper. The temperature, Von-Mises stress and strain distribution of coal sample are recorded every 10 s. The permeability distribution is also obtained based on the relationship between strain and permeability from articles. It was found that volume average temperature, stress, strain and permeability increase almost linearly with time. The average permeability increased from 1.65×10^{-16} m^2 to 3.63×10^{-16} under 2.45 GHz and 500 W microwave radiation after 300 s. The significant increase proved microwave to be effective in coal seam permeability enhancement.

4.2 Introduction

Gas drainage has been widely adopted in mine production. The exploitation of coal bed methane (CBM) is not only considerable to coal mine safety production, but also significant to energy conservation and environment protection [116-119]. The enhancement of coal seam permeability is one of the most crucial problems in gas drainage. The most commonly used method to achieve permeability enhancement is hydraulic fracturing and enhanced coalbed methane (ECBM). However, hydraulic fracturing is environmentally harmful, and ECBM is restricted by field conditions and not effective for certain cases. Therefore, alternative methods were sought to address this problem as well. In recent years, microwave was proposed to enhance coal seam permeability due to its penetrability and heating effect.

Several experiments were carried out to study microwave's effect on coalbed permeability enhancement. Li's NMR tests indicated that pore size of coals, as well as the total pore volume, increase under microwave irradiation [40]. Kumar found that cleat volume of unconfined coal sample increased from 1.8% to 16.1% and concluded that microwave can be applied in enhancing the connection between wellbore and fracture system in coal seams [47].

Beyond that, numerical simulations were also introduced to microwave's heating effect on coal sample [80]. Lin investigated the influence of microwave frequency, microwave power, coal permittivity and coal size on coal's microwave heating effect [81]. However, all these models only studied the microwave heating effect of coal sample, while neglecting the accompanying thermal stress and its influence on coal seam permeability.

The aim of this paper is to study the microwave's heating effect on coal samples and to investigate the accompanying thermal stress's effect on permeability. A coupled electric, heat transfer and mechanics model was built with COMSOL Multiphysics. The electric field and thermal field were coupled with microwave heating effect. The thermal field distribution and thermal stress of coal sample were obtained when microwave frequency and power determined. Then, the permeability of coal sample can be calculated using the relations between stress and permeability. The results show that microwave has significant effect on enhancing permeability of coal.

4.3 Model formulation

4.3.1 Assumptions

To reduce simulation time and difficulty, the following assumptions are made:

1. The coal sample is homogeneous and isotropic initially.
2. The microwave heating, heat transfer and thermal expansion only happen within the coal sample.
3. Heat capacity, dielectric constant, coefficient of thermal expansion of coal sample remain constant during the simulation.
4. The coal sample is assumed as linear elastic material.

5. Chemical reaction is neglected.

4.3.2 Geometry and Meshing

Based on the microwave oven model in COMSOL Multiphysics application gallery, the model geometry is established, as shown in Figure 21. The cavity of microwave oven and waveguide are filled with air. The coal sample sit on a cylindrical glass plate at the bottom centre of the oven. To reduce the model size, a symmetry model was adopted. The detailed geometry parameters are shown in Table 8.

Table 8. Global model parameters

	Width (mm)	Depth (mm)	Height (mm)	Radius (mm)
Microwave oven	267	270	188	-
Waveguide	50	78	18	-
Glass plate	-	-	6	113.5
Coal sample	-	-	60	25

The physics-controlled mesh is enabled and the maximum mesh size was set to 1/5th of the wavelengths. The meshes of the coal sample are predefined as extra fine meshes, while the rest are chosen as finer meshes. There are 12962 elements in the entire geometry with averaged element quality of 0.716, as shown in Figure 22. The meshes of coal sample have very good quality and is accurate enough to obtain reliable results.

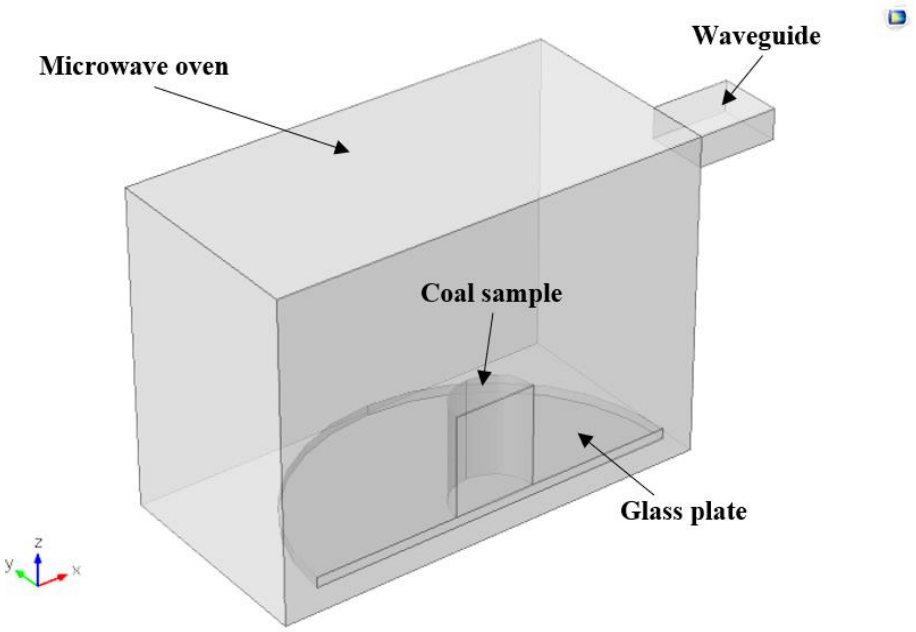

Figure 21. Geometry model of microwave heating.

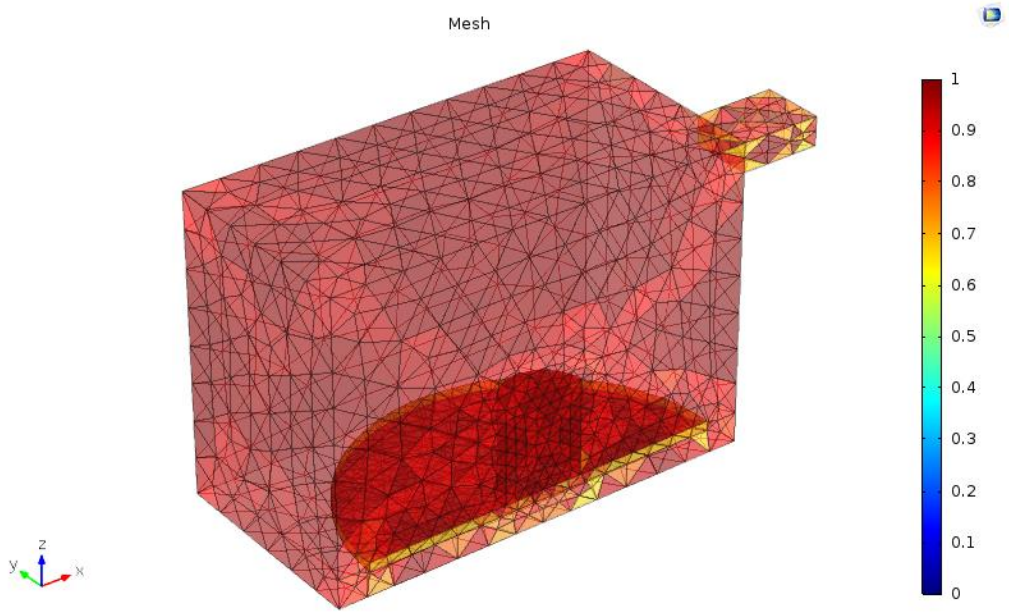

Figure 22. Mesh quality evaluation.

4.3.3 Governing Equations

4.3.3.1 Electromagnetic Field:

Maxwell's equation is one of the most commonly used equations to describe electromagnetic propagation. In this paper, the governing equation is given as [120]:

$$\nabla \times \mu_r^{-1}(\nabla \times E) - k'^2\left(\varepsilon_r - \frac{j\sigma}{\omega\varepsilon'}\right)E = 0 \tag{4}$$

where μ_r denotes the relative permeability, E is the electric field intensity, ε_r is relative permittivity, σ represents the electrical conductivity, ω is the angular frequency and ε' is the permittivity of free space (8.85×10−12 F/m). The wave number in the vacuum k' is expressed as:

$$k' = \frac{\omega}{c'} \tag{5}$$

where c' is the speed of light in vacuum (2.998×108 m/s).

4.3.3.2 Heat Transfer:

Heat transfer is only solved in the coal sample domain. The microwave heat and phase change heat is coupled in Fourier's law of heat conduction, expressed as below:

$$\rho C_p \frac{\partial T}{\partial t} + \rho C_p \boldsymbol{u} \cdot \nabla T + \nabla \cdot \boldsymbol{q} = Q_{ted} \tag{6}$$

where ρ is the coal sample density, C_p denotes the specific heat capacity, T is the temperature, Q_{ted} denotes the microwave heat. Heat flux $\boldsymbol{q}$ is given as:

$$\mathbf{q} = -\mathrm{k}\nabla\mathrm{T} \tag{7}$$

4.3.3.3 Thermal Stress, Strain and Permeability:

As stated in assumption, the coal sample is considered as linear elastic material. The governing equation for linear elastic motion is given as [121]:

$$\nabla \cdot \mathbf{S} + \mathbf{F} = \frac{\mathrm{d}^2 \boldsymbol{u}}{dt^2} \tag{8}$$

where *S* is the strain tensor, $\boldsymbol{F} = (\mathrm{F}_1, \mathrm{F}_2, \mathrm{F}_3)^T$ denotes the external force on coal sample and $\boldsymbol{u} = (\mathrm{u}_1, \mathrm{u}_2, \mathrm{u}_3)^T$ is displacement vector.

As stated in assumption, the coal sample is assumed homogeneous and isotropic. The strain tensor $\boldsymbol{S}$ for isotropic homogeneous media is given by [121]:

$$\mathbf{S} = \lambda \mathrm{tr}(\varepsilon)\mathrm{I} + 2\mu\varepsilon \tag{9}$$

where λ is the Lamé's constant, μ represents the shear modulus, *I* is identity matrix, and ε is stress tensor that given as [121]:

$$\varepsilon = \frac{1}{2}(\nabla \mathbf{u} + \nabla \mathbf{u}^T) = \alpha \Delta \mathrm{T} \tag{10}$$

where α is temperature expansion coefficient.

The relation between permeability and volumetric strain of coal is approximately linear and given as [122]:

$$\eta = \eta_0 + \lambda \mathbf{S} \tag{11}$$

where η_0 is the initial permeability and λ is given as:

$$\lambda = \frac{d\eta}{d\mathbf{S}} \tag{12}$$

Based on the experiment results, $\eta_0 = 1.756 \times 10^{-16}$ and $\lambda = 2.361 \times 10^{-14}$. The equation (12)) can be further express as:

$$\eta = 1.756 \times 10^{-16} + 2.361 \times 10^{-14}\, \varepsilon_v \tag{13}$$

4.3.3.4 Boundary Conditions

For the electromagnetic field, the walls of waveguide and oven is described as impedance boundary condition, given as:

$$\sqrt{\frac{\mu_0 \mu_r}{\varepsilon_0 \varepsilon_r - j\sigma/\omega}}\, \boldsymbol{n} \times \boldsymbol{H} + \boldsymbol{E} - (\boldsymbol{n} \cdot \boldsymbol{E})\boldsymbol{n} = \mathbf{0} \tag{14}$$

where $\boldsymbol{E}$ is the electric field intensity (V/m) and $\boldsymbol{H}$ is the magnetic field intensity (A/m)

The symmetry boundaries are defined as perfect magnetic conductor, given as:

$$\boldsymbol{n} \times \boldsymbol{H} = \mathbf{0} \tag{15}$$

The port boundary is excited by a transverse electric wave. The wave, which has no electric field component in the direction of propagation, is controlled by a propagation constant β, which is presented as:

$$\beta = \frac{2\pi}{c}\sqrt{v^2 + {v_c}^2} \tag{16}$$

where v represents the microwave frequency, v_c is the cutoff frequency, which is given as:

$$v_c = \frac{c'}{2}\sqrt{\left(\frac{m}{a}\right)^2 + \left(\frac{n}{b}\right)^2} \tag{17}$$

where *m* and n are the mode numbers, *a* and *b* denote the lengths of rectangular cross section (*a*=78 mm and *b*=18 mm). In this case, TE_{10} mode was chosen for simulation (*m*=1, *n*=0).

For the thermal field, the bottom and symmetry face were defined as thermal insulation boundary conditions, which were written as[123]:

$$\mathbf{n} \cdot (-\mathrm{k}\nabla \mathrm{T}) = 0 \tag{18}$$

As for the other surfaces of coal sample, the boundary conditions for the heat transfer interfaces are given as [123]:

$$\mathbf{n} \cdot (\mathrm{k}\nabla \mathrm{T}) = h_T(T_{air} - T) \tag{19}$$

where h_T is the heat transfer coefficient, and T_{air} is the air temperature in the microwave oven.

For mechanical field, the bottom of coal sample was fixed. The displacements in *x*, *y* and *z* direction were prescribed as 0. All other boundaries were defined as free boundaries.

2.5. Parameter determination and initial conditions

To study the thermal expansion effect of coal sample under microwave, relative permittivity, thermal conductivity, heat capacity, coefficient of thermal expansion and so on are required in the model. Such parameters are available in separate studies, while no complete set of parameters for a specific coal sample can be found. Therefore, based on several studies, the basic parameters of coal sample are shown in Table 9 [124-126]:

Table 9. Basic parameters of coal sample.

Name	Description	Expression
ε'	Real permittivity	2.86
ε''	Imaginary permittivity (j)	0.17

k	Thermal conductivity ($W/(m \cdot K)$)	0.189
Cp	Heat capacity ($J/(kg \cdot K)$)	4.187×10^3
E	Yong's modulus (Pa)	1.998×10^9
nu	Poisson's ratio	0.4
T_0	Initial temperature of the coal sample and air	298.15
ρ	Coal density (kg/m^3)	1310

The initial conditions and global parameters are shown in Table 10.

Table 10. Initial conditions and global parameters.

Name	Description	Expression
E_0	Initial electric field intensity	0
T_0	Initial temperature of the coal sample and air (K)	298.15
v	Microwave frequency (GHz)	2.45
P	Microwave power (W)	500

4.4 Results and Discussion

After all the parameters and initial conditions defined, the electric field was solved in frequency domain, followed by applying stationary solver in thermal and mechanical field. The coupled electric, thermal and mechanical model run 300 s, simulation results were recorded every 10 s.

The normal electric field distributions of the oven with coal sample under 2.45 GHz and 500 W at 300 s is shown in Figure 23. As dielectric constant of coal sample is assumed to be stable, the normal electric field distributions remain unchanged during the simulation. It can be seen from Figure 23 that electric field is not uniformly distributed. The reflection of microwave by the copper wall results in low and high energy zone in the electric field [81]. It is obvious there is a high energy zone in the bottom middle of the coal sample. As shown in Figure 24, the thermal field distribution follows the same pattern. Therefore, it can be concluded that higher electric field intensity causes higher temperature in coal samples.

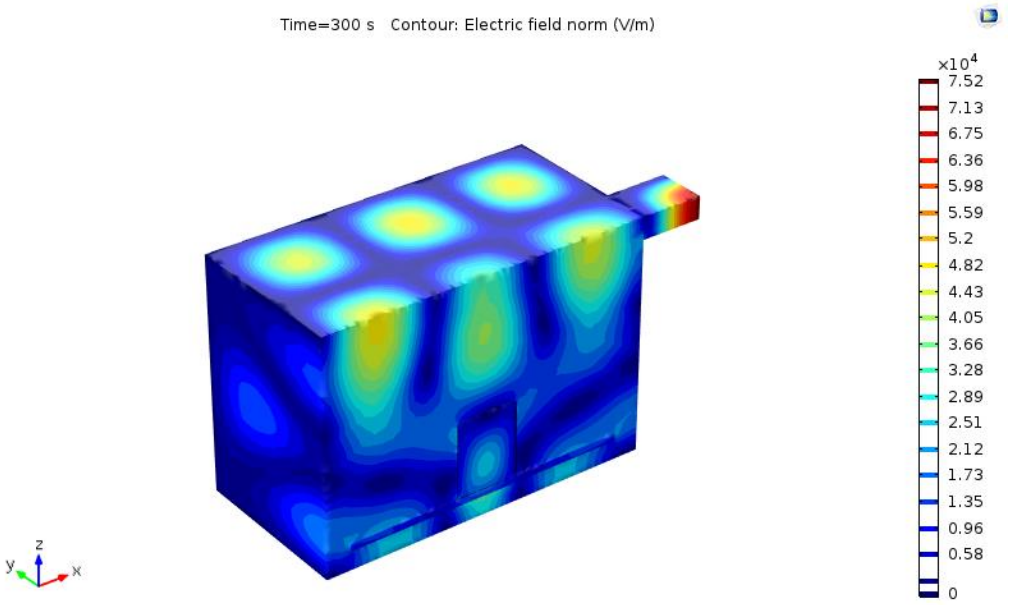

Figure 23. Electric field distribution of microwave oven.

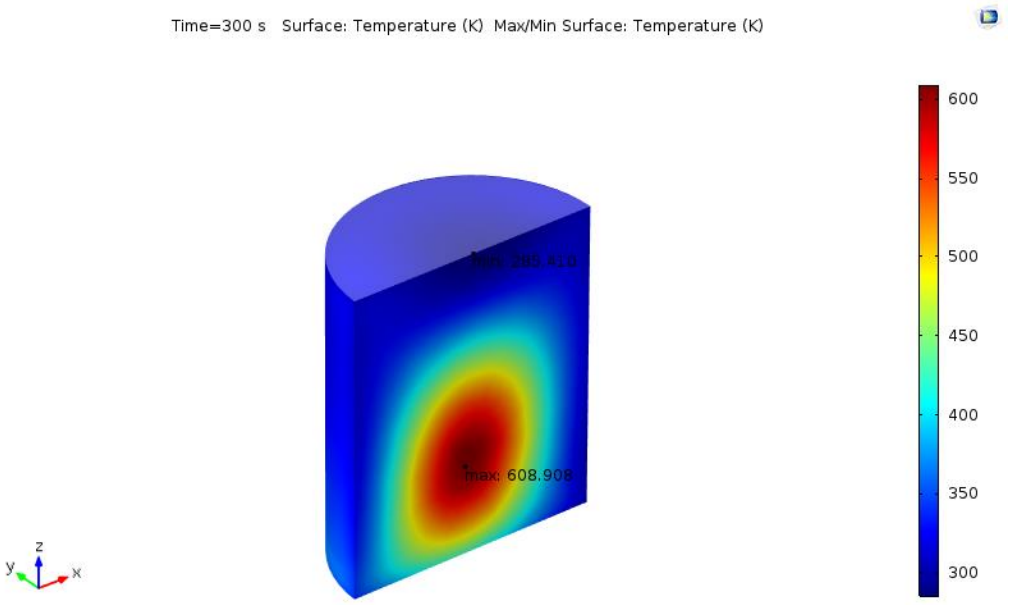

Figure 24. Thermal field distribution of coal sample.

The Von-Mises stress and strain distribution of coal sample are also obtained, as shown in Figure 25 and Figure 26. As the bottom of the coal sample is fixed, the thermal expansion result in stress concentration at the bottom.

Similar to the Von-Mises stress, the maximum strain occurs at the bottom of the coal sample. However, the strain distribution differs a lot from that of Von-Mises

stress. It can be seen from slice map, Figure 25, strain in the center of the coal sample is significantly larger than that of exterior, while for Von-Mises stress, this pattern is not so obvious.

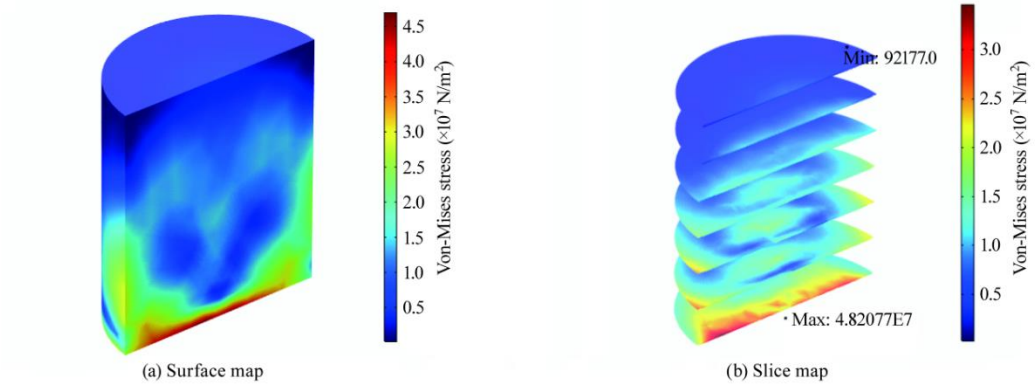

Figure 25. Von-Mises stress distribution at 300 s.

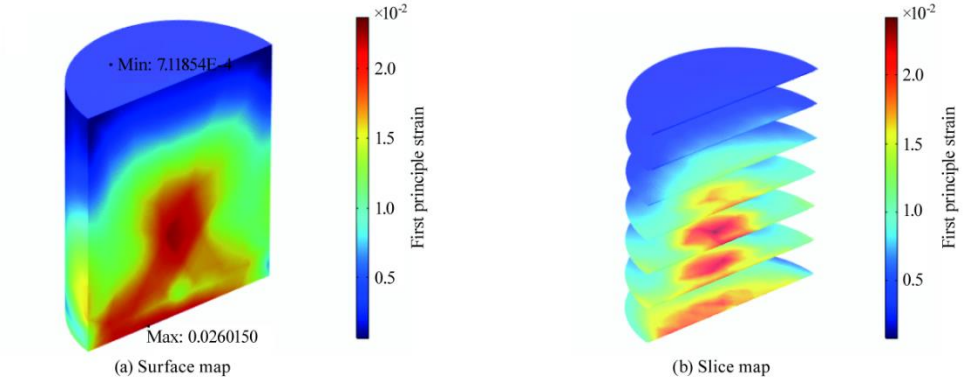

Figure 26. Strain distribution at 300 s.

To study the relationship between temperature, stress, strain and permeability, the volume average of these parameters over time are calculated and depict in Figure 27 and Figure 28. It can be concluded that volume average temperature, stress, strain and permeability increase almost linearly with time. The average strain and permeability decrease at the beginning and increase steady afterwards.

The average permeability increased by 2.2 times (from 1.65×10^{-16} m^2 to 3.63×10^{-16}) under 2.45 GHz and 500 W microwave radiation after 300 s. The significant increase proved microwave to be effective in coal seam permeability enhancement.

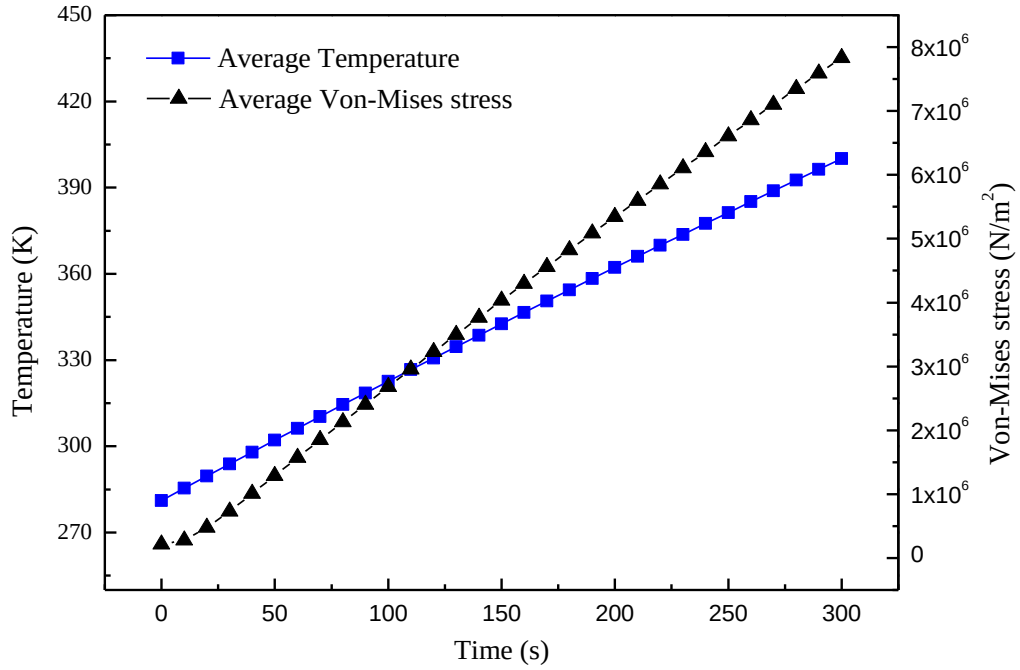

Figure 27. Average temperature and Von-Mises stress over time.

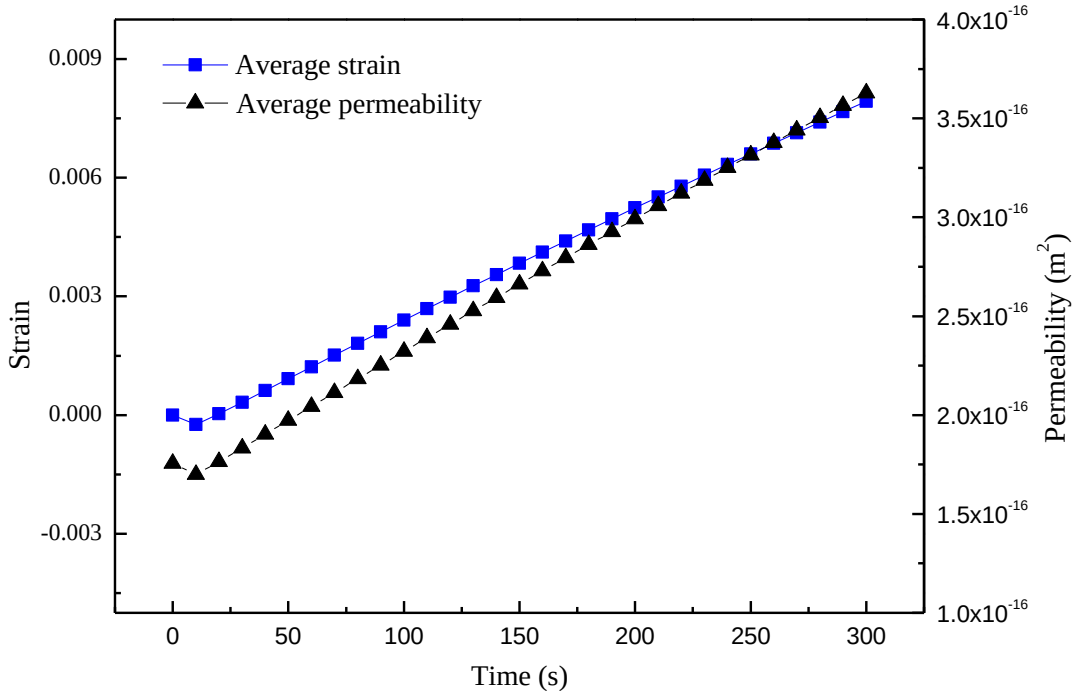

Figure 28. Average strain and permeability over time.

4.5 Conclusions

Previous work has simulated the microwave heating effects of coal samples under various circumstances. Lin [81], for example, studied the influencing factors of microwave frequency, power, coal permittivity and coal size on microwave

heating with a coupled electromagnetic and heat transfer model. However, these models only considered microwave's heating effect of the coal sample, while no further investigation of its effect on coal seam permeability was undertaken.

In this paper, a coupled electromagnetic, thermal and mechanical model was established with COMSOL Multiphysics. The temperature, Von-Mises stress and strain distribution of coal sample are simulated and their time-dependent relations are obtained. Based on the relationship between strain and permeability from articles, the average permeability was calculated. It was found the average permeability increase significantly under microwave radiation, which increased from 1.65×10^{-16} m^2 to 3.63×10^{-16} under 2.45 GHz and 500 W microwave radiation in 300 s.

These findings fill the gap in studying microwave's effect on coal seam permeability enhancement and could be very helpful when applying microwave on-site to improve coal seam permeability. However, further studies are still required due to the limitations of this paper. Moisture's effect should also be taken into consideration in the future works.

5 Chapter 5

A numerical model for coalbed methane reservoir enhancement using microwave heating

This chapter has submitted to The Australian Mine Ventilation Conference 2019. It was written by Jinxin Huang and revised by Prof Guang Xu, Mr. Ping Chang and Prof Guozhong Hu.

Please cite this paper as: Huang, J., Xu, G., Chang, P., & Hu, G. (2019). A numerical model for coalbed methane reservoir enhancement using microwave heating. *Conference Proceedings - The Australian Mine Ventilation Conference 2019*.

Few studies have investigated microwave's heating effect on coal reservoir. In this chapter, a modified electromagnetic, thermal and mechanical model for coal reservoir was proposed. This model was compared with original models for microwave heating of coal. Based on the simulation results, the effect of microwave power on reservoir heating effect and the effect of treatment time on reservoir permeability development were made clear.

5.1 Abstract

Microwave heating is a promising technology to substitute hydraulic fracturing in coalbed methane (CBM) stimulation. The microwave assisted enhancement is realized through generating thermal fractures in coal under nonuniform microwave heating. And the moisture contents were removed during this process, which facilitate the desorption, diffusion and permeation of CBM. Microwave heating has the advantages of no water consuming, widely applicable, environmental and economical friendly. Even though the effects of microwave heating on coal samples were experimented and simulated comprehensively, few studies has been conducted to its effect on coalbed methane reservoir. To address this, a coupled electromagnetic, thermal and mechanical model was established in this paper to study the microwave heating effect on coal seam. This model was compared with the previous model in detail. The electric field, thermal field, stress and permeability distribution were then simulated using the established model. The results showed that microwave fracturing makes significant contribution to the permeability evolution. Moreover, the effect of microwave power and treatment time on heating performance were also investigated. The simulation results suggest larger microwave power is more suitable for reservoir treatment. It was also found microwave heating is capable to increase the permeability of coal seam within small range in very short time. However, it takes much longer time to enhance the deeper coal seam.

5.2 Introduction

Coalbed methane is a clean energy with 229 trillion m3 reserves worldwide and thus draw attention due to its huge economic potential [127]. Meanwhile, it is also a potential safety hazard that may result in gas outburst and gas explosion [128].

Therefore, exploitation of CBM together with coal mining is both necessary and meaningful.

However, the permeability of many coal reservoirs is extremely low, which makes it hard to drain the gas. Many methods have been applied to enhance coal seam permeability, such as hydraulic fracturing [4], CO2/N2 injection [129], electrochemical treatment [14] and so on. Nevertheless, these methods are either restricted by in-situ conditions or not environmentally friendly. The alternative stimulation methods are in badly demand. Recently, microwave heating was proposed to enhance coal seam permeability because of the following advantages [52, 130]. First of all, microwave heating does not require any water or chemical reagent, which is totally environmentally friendly [57]. Secondly, microwave is effective in fracturing with numerous industrial applications. Finally, microwave is easy to generate and doesn't require transportation or storage.

Lots of numerical models have been proposed to simulate microwave heating on coal [73, 83, 87]. However, most of these models studied microwave heating effect of small coal samples in microwave oven. Few experiments or numerical simulations have been conducted to study the microwave heating effect on coal reservoir. As the penetration depth of microwave is limited, in-situ application of microwave heating is quite different with laboratory experiments.

The objective of this paper is to investigate the microwave heating effect on coal reservoir. To address this, a coupled electromagnetic, thermal and mechanical model was established with COMSOL Multiphysics. The difference between this model and previous proposed models was discussed in detail. The electric field, thermal field, stress and permeability distribution were then simulated using the established model. Based on the simulation results, the effect of microwave power on reservoir heating effect and the effect of treatment time on reservoir permeability development were made clear.

5.3 Model Description

5.3.1 Assumptions

In order to save simulation time and to simplify the problem, the following assumptions are made based on the previous studies [35, 83, 115]:

1. The coal seam is homogeneous and isotropic at the beginning.
2. Heat capacity, coefficient of thermal expansion of coal is independent of temperature.
3. Dielectric constant of coal remain constant before reaching 450 K.
4. The coal seam is assumed as linear elastic material.
5. No chemical reaction happen during microwave heating.

5.3.2 Geometry and Meshing

A 2D model is built for coal reservoir. In order to investigate the effect of microwave power on heating effect of coal reservoir. The reservoir was divided into two equal regions (Region 1 and Region 2), each region is 5 m long and 5 m wide. A microwave port, which is filled with air, is set in the middle of each region bottom. The output power of port 1 and port 2 are 1 kW and 5 kW respectively.

User-controlled mesh was applied to all the domain. As shown in Figure 29, there are 3328 elements in the entire geometry with average element quality of 0.9271. As the meshes for coal reservoir have very high quality, the simulation results are thus reliable and accurate.

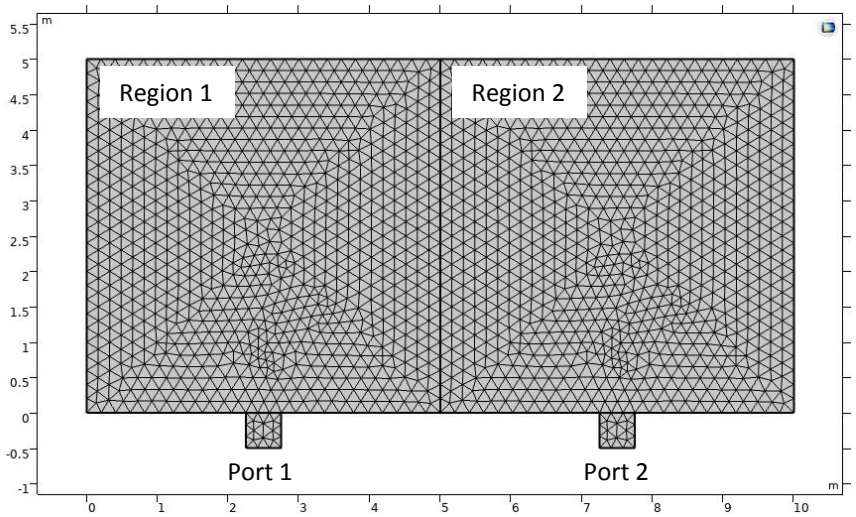

Figure 29. Geometry and mesh of coal reservoir model

5.3.3 Governing Equations

In this model, Maxwell's equation is used to describe electromagnetic propagation, which is given as:

$$\nabla \times \mu_r^{-1}(\nabla \times E) - k'^2\left(\varepsilon_r - \frac{j\sigma}{\omega\varepsilon_0}\right)E = 0 \tag{20}$$

where μ_r is relative permeability; E represents the electric field intensity; ε_r is relative permittivity; σ denotes the electrical conductivity; ω represents the angular frequency; ε_0 is the permittivity of free space (8.85×10^{-12} F/m) and k' is the wave number in the vacuum.

Heat transfer is solved in coal domain, using Fourier's law of heat conduction coupled with microwave heat.

$$d_z\rho C_p\frac{\partial T}{\partial t} + d_z\rho C_p\boldsymbol{u}\cdot\nabla T + \nabla\cdot\boldsymbol{q} = d_z Q_{ted} \tag{21}$$

where ρ is the density of coal; C_p represents the specific heat capacity; T is the temperature; Q_{ted} is microwave heat and q is heat flux, which is expressed as:

$$\mathbf{q} = -d_z \mathrm{k}\nabla\mathrm{T} \tag{22}$$

where k is the thermal conductivity (W/(m2·K)).

The coal is assumed as linear elastic material in this model. The governing equation for linear elastic motion is defined as:

$$\nabla\cdot\mathrm{S} + \mathbf{F}_v = 0 \tag{23}$$

where $\mathbf{F}_v$ is the external force and S represents strain, given as:

Stress ε is defined as:

$$\varepsilon = \frac{1}{2}(\nabla\boldsymbol{u} + \nabla\boldsymbol{u}^T) \tag{24}$$

where $\boldsymbol{u}$ is displacement vector.

It was reported the relation between permeability and volumetric strain of coal is approximately linear [122] and the permeability is thus defined as:

$$\eta = \eta_0 + \lambda\mathrm{S} \tag{25}$$

According to the experiment results, $\eta_0 = 1.756\times10^{-16}$ and coefficient $\lambda = 2.361\times10^{-14}$.

5.3.4 Parameter Determination and Initial Conditions

In order to investigate electromagnetic, thermal and stress field of coal seam under microwave irradiation, physical properties of coal were predefined following the experimental data from literature, as shown in Table 11 [35, 83, 115]. The initial conditions are shown in Table 12.

Table 11. Physical properties of coal

Name	Description	Expression
ε	Relative permittivity	2-0.2i
σ	Electrical conductivity	0.02 [S/m]
k	Thermal conductivity	0.478 [W/(m · K)]
ρ	Density	1300 [kg/m^3]
C_p	Heat capacity at constant pressure	4187 [J/(kg · K)]
E	Yong's modulus	2713 [Mpa]
ν	Poisson's ratio	0.339

Table 12. Initial conditions and microwave setting

Name	Description	Expression
T_0	Initial temperature of the coal sample and air	293.15 [K]
E_0	Initial electric field intensity in all domain	0
f	Microwave frequency	2.45 [GHz]
P_1	Microwave power of port 1	1 [kW]
P_2	Microwave power of port 2	5 [kW]

5.4 Results and Discussion

5.4.1 Computation Sequence

The electric field distribution was first calculated in the frequency domain. Heat transfer in solid and solid mechanics were then simulated using time-dependent solver. The coupled electric, thermal and mechanical model for coal reservoir were simulate for 200 days, simulation results were recorded every 1 day.

Take the simulation results after 10 days for example, the electric field distribution (see Figure 30) was first calculated. It is obvious that even though larger output power lead to higher electric field intensity, these two ports have similar electric field distribution pattern. It is worth to notice that the penetration depths is about 0.2 m in this case, which means microwave attenuate quickly within the short distance of coal seam. It suggest that microwave heating only effect on the surface of coal seam at first, the heat gradually transmits to the inner part as time goes on. The thermal field distribution after 10 days is shown in Figure 31. Based on the thermal field, the stress and permeability distribution were calculated and depicted as Figure 32 and Figure 33. The stress and permeability distribution suggest that microwave heating can be effective to coal seam enhancement for as far as 1.5 m after 10 days. The permeability of coal seam almost doubled within 1 m×1 m area.

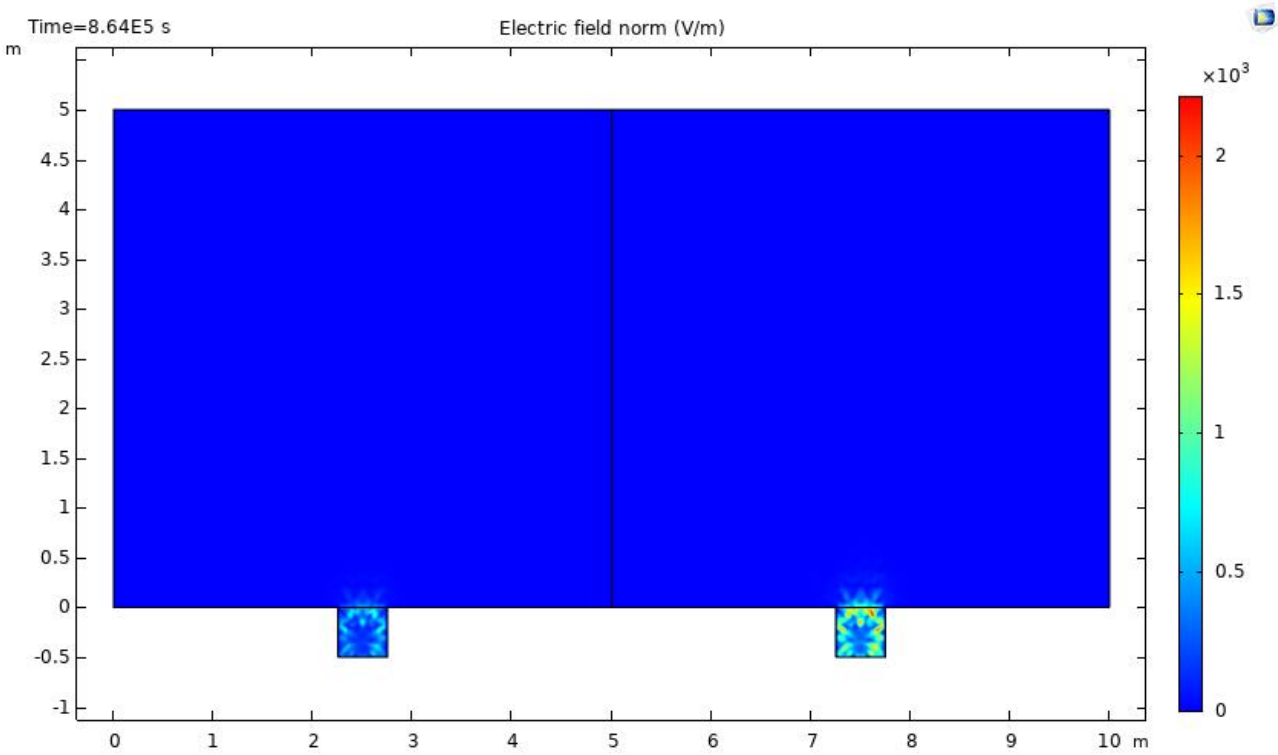

Figure 30. Electric field distribution after 10 days

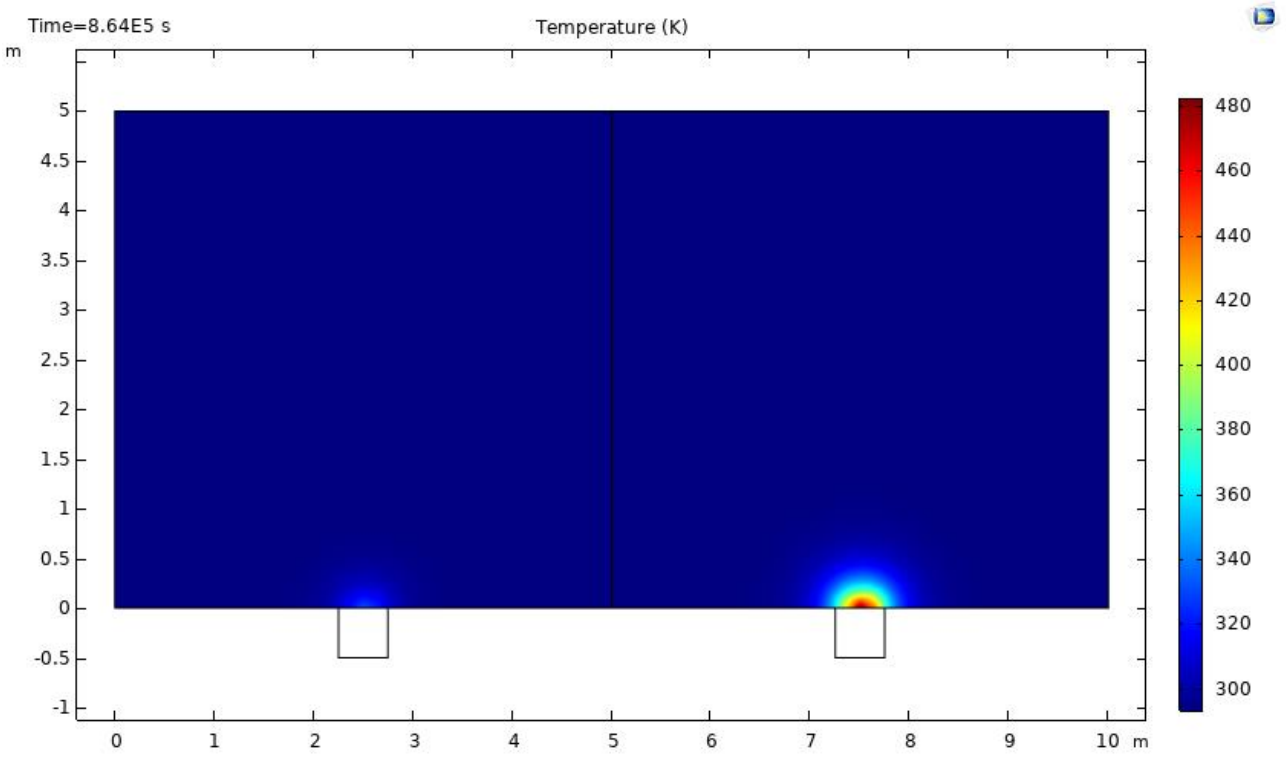

Figure 31. Thermal field distribution after 10 days

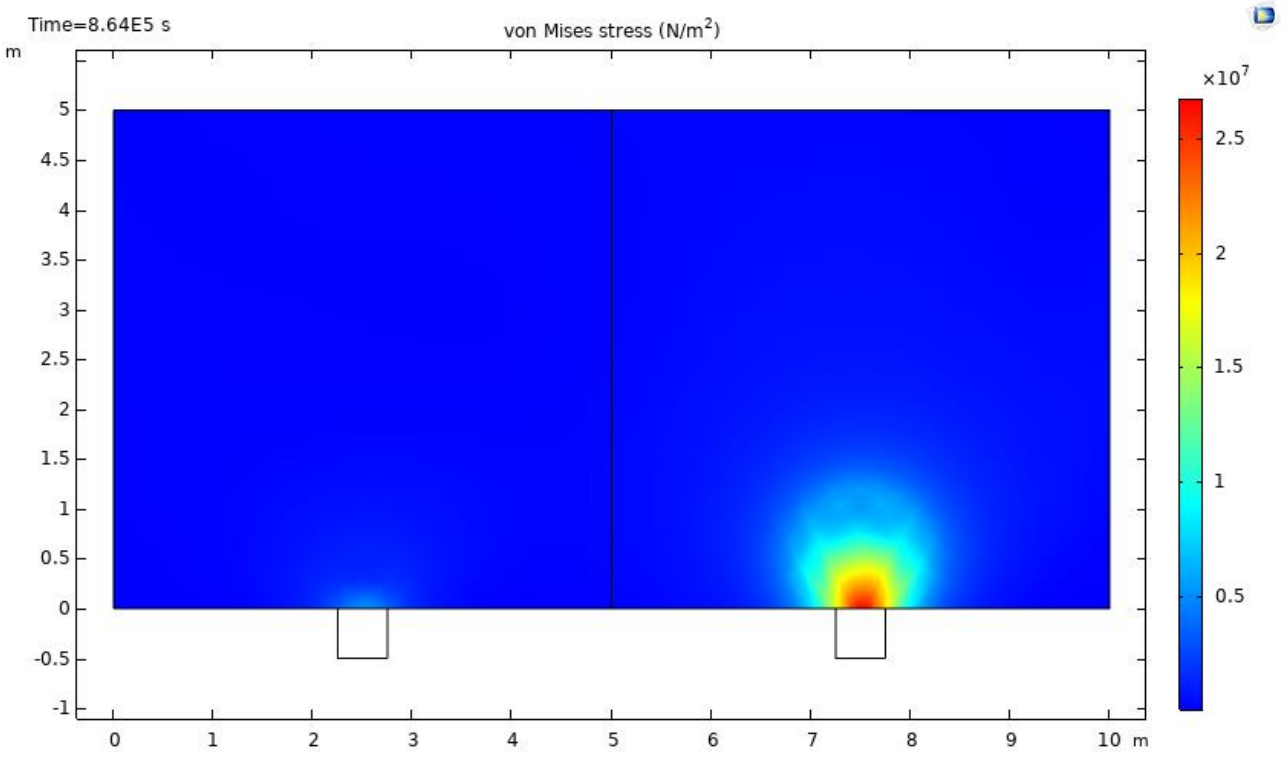

Figure 32. Stress distribution after 10 days

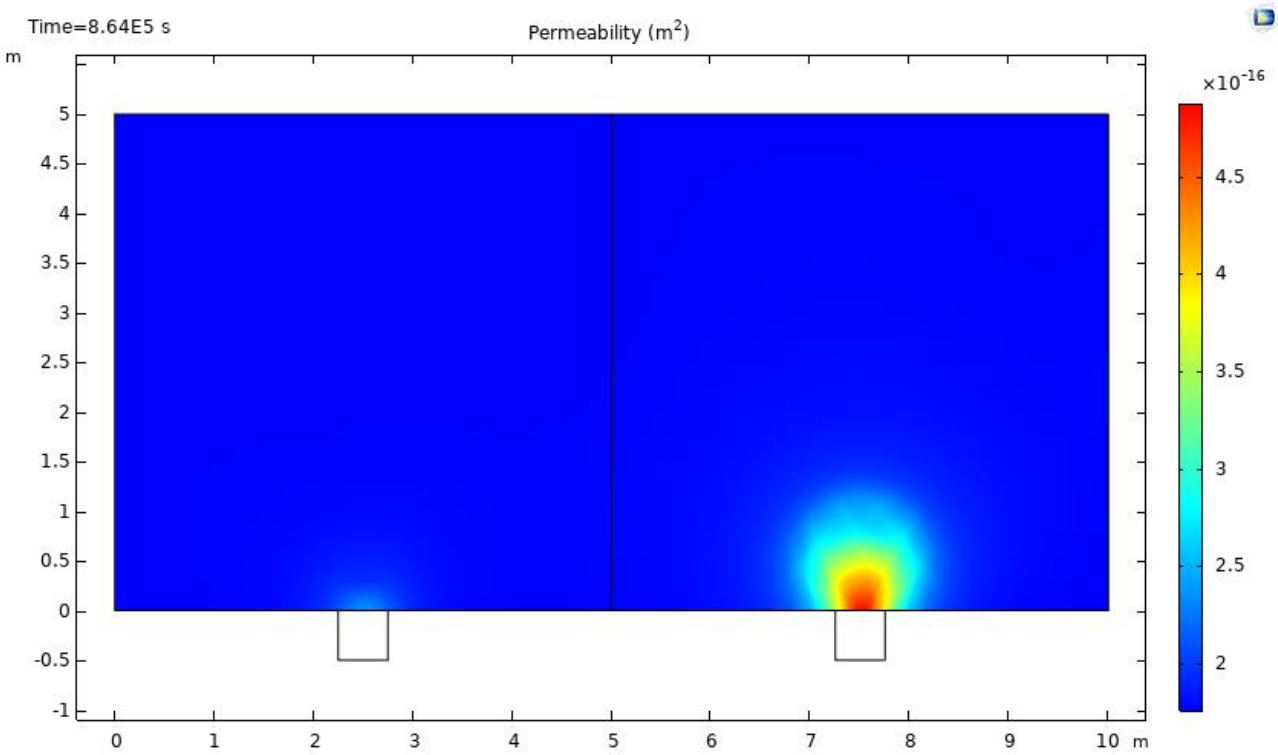

Figure 33. Permeability distribution after 10 days

5.4.2 Comparison of Original and Modified Models

It was reported that lower microwave power should be chosen for coal reservoir heating to avoid overheat [83]. In these models, the dielectric constant of coal reservoir was assumed to be constant throughout the heating process. As penetration depth of microwave is very limited, microwave heating is only effective in the area that close to the port. Instead of heating by microwave, the inner part is heated through heat transfer. With the increase of temperature of surface coal, the heat gradually transfers to the inner part. Therefore, large thermal gradient is required to achieve large heating area, and overheat occurs for the surface coal consequently.

However, this simulation method overlooks the fact that moisture evaporates during heating process while coal's loss factor depends on its saturation significantly. It was reported that bulk material of coal has negligible loss factor (less than 0.25) compared to that of water (as large as 12 at 25 °C and 2.45 GHz) [29, 124].The actual situation of microwave heating is very complicated as the saturation condition and coal permittivity, which determines the ability to absorb microwave energy, changes over time. As moisture content is not considered in this manuscript, coal

seam is assumed to be completely dry when reaching 450 K to simplify the model and save computational cost. In this modified model, coal permittivity is 2-0.2j when temperature is less than 450K and is set as 1 when temperature reaching 450 K.

Obviously, there is no difference between the simulation results of original and modified models at the beginning. However, the surface coal in modified model becomes almost transparent to microwave when its temperature reaches 450 K, while the surface coal in original model continues to absorb microwave energy. The temperature distribution of region 2 after 100 days and 200 days using original and modified models were shown in Figure 34 and Figure 35 respectively. In order to compare the temperature distribution using two models, the temperature variation along the central axis is recorded and depicted as Figure 36. As shown in Figure 36, the simulated coal temperature of near port area increases to over 600 K after 100 days and continues to rise afterwards when using the original model. As for the modified model, the temperature of near port area remained stable after reaching 450 K and microwave start to take effects on the deeper coal seams. The original model assumes coal permittivity remain the same after microwave heating, and the deeper coal seam is heated by heat transfer. On the contrary, the modified model believes that the coal becomes almost transparent to microwave after the removal of moisture, and the deeper coal seam is then heated by microwave irradiation.

The simulation results also suggest the thermal gradient using original model is significantly larger than that using modified model. Overheat of near port area becomes the major issue for original model. As the assumption for modified model is more accordant with the actual situation, the simulation results of modified model is more reasonable.

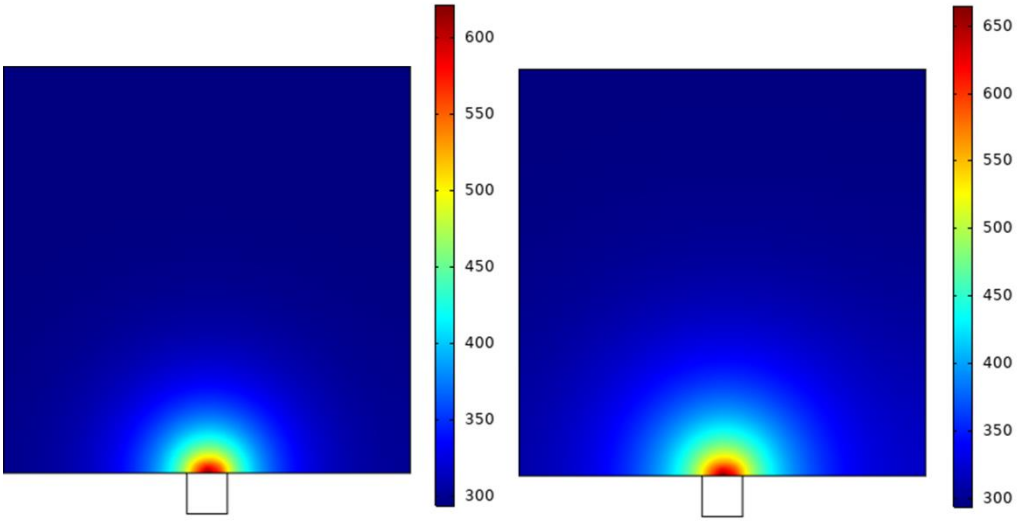

Figure 34. Temperature distribution of region 2 after 100 days and 200 days using original model

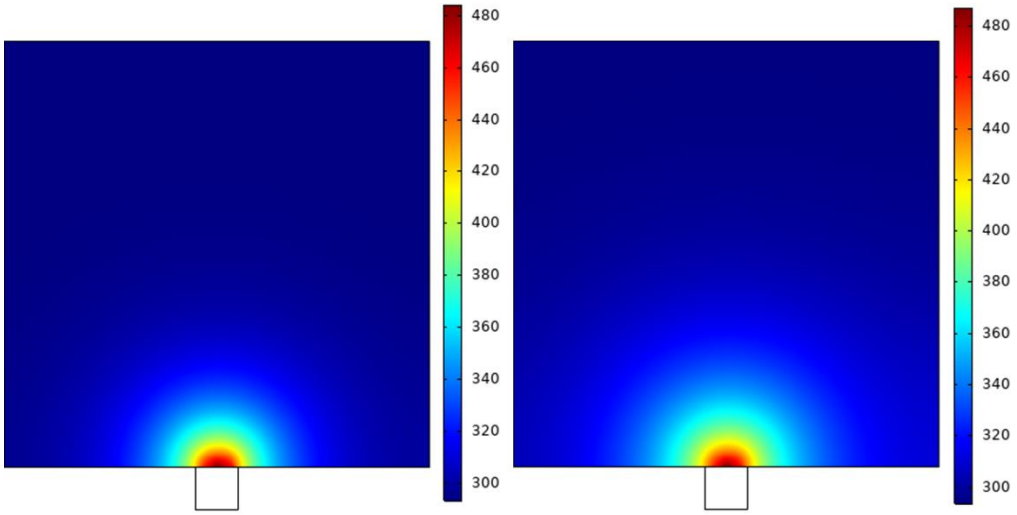

Figure 35. Temperature distribution of region 2 after 100 days and 200 days using modified model

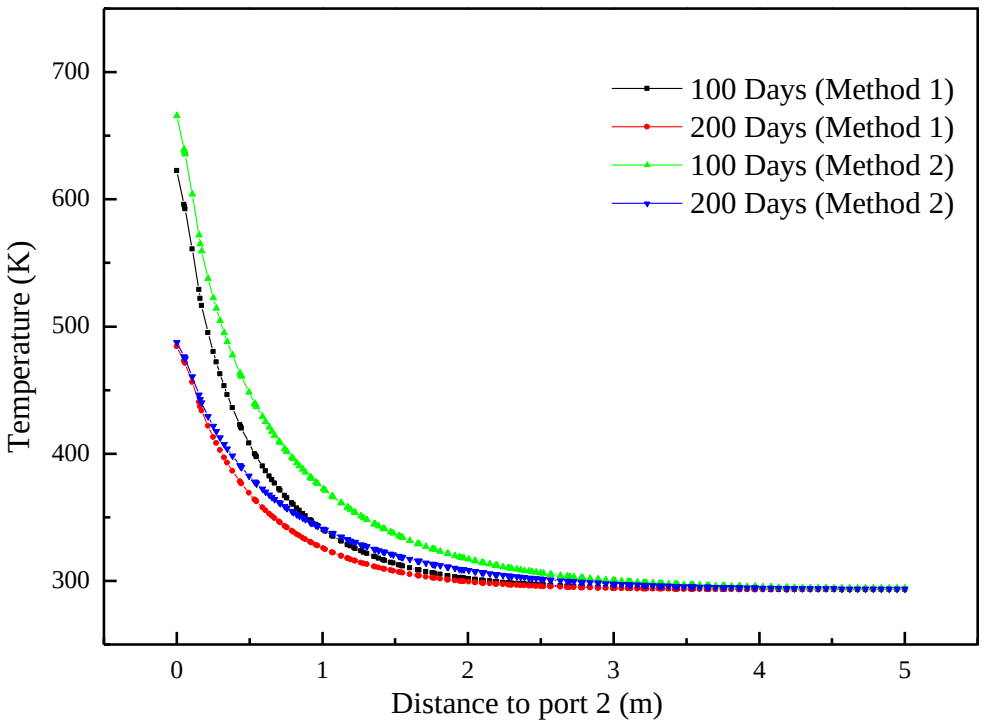

Figure 36. Temperature variation along the central axis after 100 days and 200 days using original and modified models

5.4.3 Effect of Microwave Power

Through previous discussion, it can be concluded that modified model is more reliable in reservoir stimulation. In this section, the modified model was used to investigate the effect of microwave power on heating effect of coal reservoir.

As shown in Figure 30, Figure 31, Figure 32 and Figure 33, the coal reservoir treated with microwave power of 5 kW has significant larger temperature, thermal stress and permeability comparing to that treated with microwave power of 1 kW. In order to quantify the effect of microwave power, the average temperature variation of each region over time were calculated and depicted as Figure 37. As shown in Figure 37, the average temperature increase almost linealy with time under certain microwave power. The average temperature of region 1 over time is fitted as $y = 0.04x + 290.69$ with R2 of 0.993, while the average temperature of region 2 over time is fitted as $y = 0.1x + 295.61$ with R2 of 0.999. It is obvious that larger microwave power leads to better microwave heating effect. However, increased microwave energy does not necessarily all turns into heat. The microwave power of Region 2 is five times as large as Region 1, while the heating rate of Region 2 is only 2.5 times larger than that of Region 1.

According to the fitted curves, it takes 10 days to increase the temperature of 5 m × 5 m area by 1℃ using 5 kW. And it takes 25 days to achieve the same effect using 1 kW. As heating efficiency is of great importance to reservoir stimulation, larger microwave power seems to be more suitable for reservoir treatment.

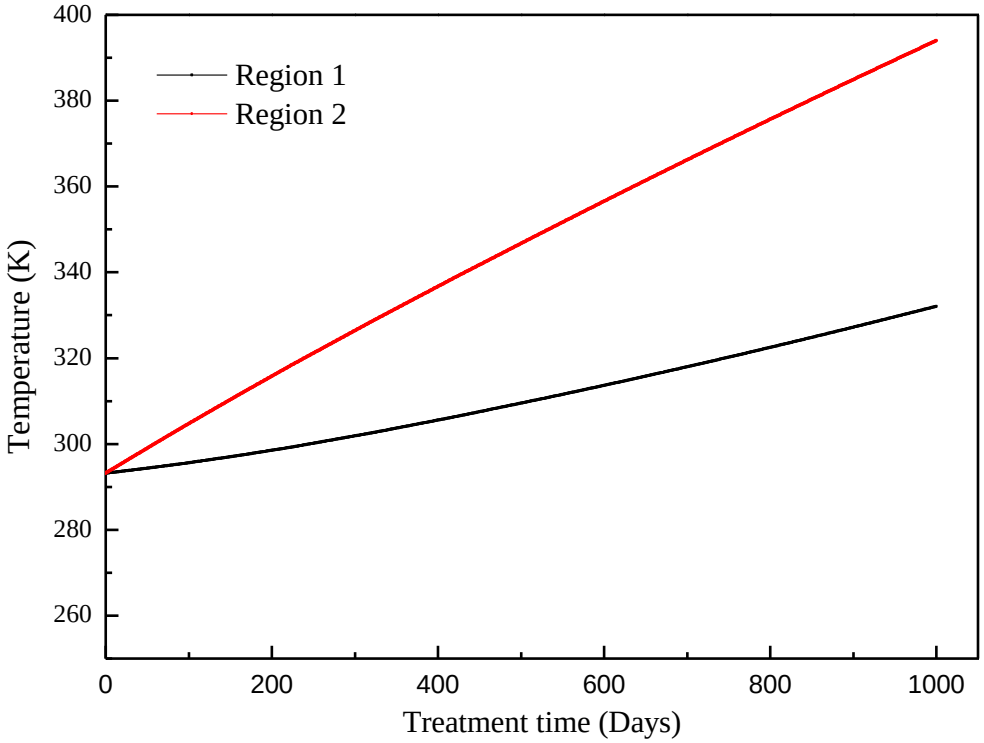

Figure 37. Average temperature of region 1 and region 2 over time

5.4.4 Permeability Development Over Time

In this section, the modified model was used to simulate the permeability development along the central axis of Region 2. As shown in Figure 38, the permeability increases with irradiation time in all the positions. Microwave has very limited effect on coal permeability after 1 day. Then, the permeability of coal seam within 2 m shows significant increase after 10 days. Even though the permeability continues to increase afterwards, its variation is not as evident as that in the first 10 days. It is also worth to mention that the permeability of near port area (specifically within 0.25 m) remain relatively stable after 10 days. Although microwave gradually effect on deeper coal seams as time goes on, it takes over 50 days and over 100 days to take effect on the coal seam deeper than 3 m and 4 m respectively.

Therefore, microwave heating is capable to increase the permeability of coal seam within small range in very short time. However, it takes much longer time to

enhance the permeability of deeper coal seam. Therefore, it's better to use microwave heating for about 10 days to achieve great enhancing effect within short time for coalbed methane pre-drainage. As for coalbed methane reservoir or shale gas reservoirs, microwave assisted recovery is feasible to operate throughout the production process.

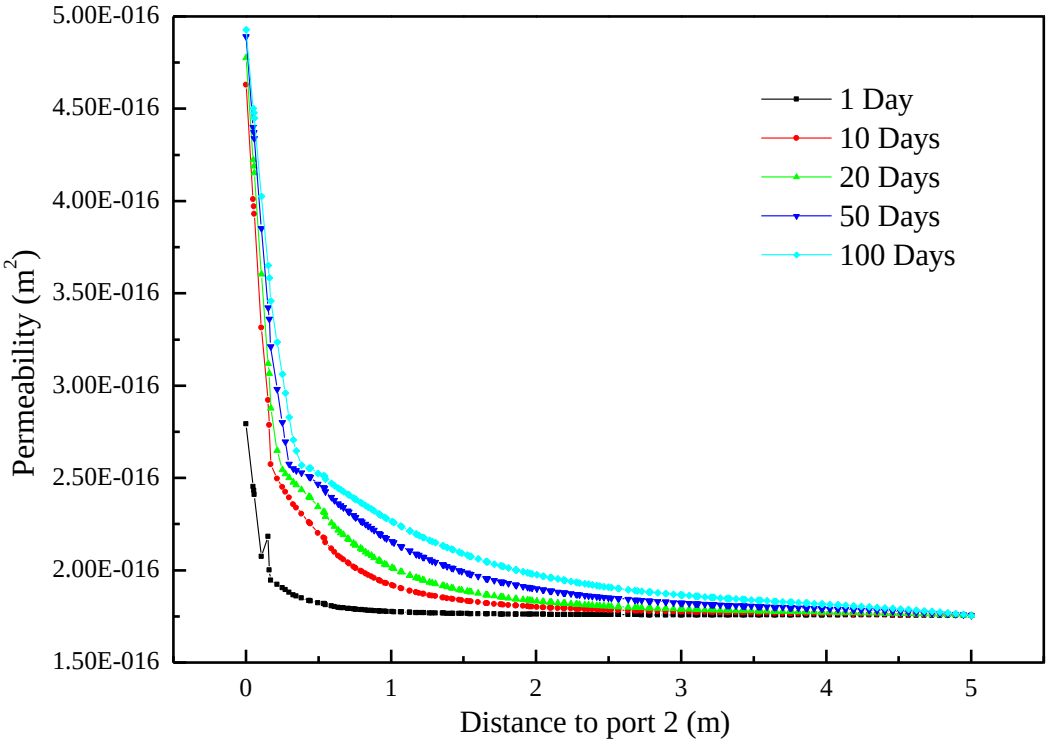

Figure 38. Permeability development along the central axis over time

5.5 Conclusions

Previous studies have investigated the microwave heating effects on coal samples, while few research simulated the microwave heating effect on coal reservoir. As the penetration depth of microwave is limited in coal, field application of microwave heating is quite different with laboratory experiments.

To address this, a coupled electromagnetic, thermal and mechanical model was established for coal reservoir. The difference between this model and the previous proposed models was discussed in detail. Using the established model, the electric field, thermal field, stress and permeability distribution were then simulated. It was found heating rate under 5 kW microwave power is 2.5 times larger than that under 1 kW. In order to achieve great heating efficiency for reservoir stimulation, larger microwave power is more suitable for reservoir treatment. It was also found

microwave heating significantly increase the permeability of coal seam in very short time. However, the effective range is relative small at the beginning and it takes very long time to enhance the deeper coal seam. Even though this proposed numerical model is closer to reality comparing to the previous model, field experiments need to be conducted in the further studies to calibrate and validate this proposed model.

6 Chapter 6

The development of microstructure of coal by microwave irradiation stimulation

This chapter was published on Journal of Natural Gas Science and Engineering. It was written by Jinxin Huang and revised by Prof Guozhong Hu, Prof Guang Xu, Prof Baisheng Nie and Prof Jialin Xu.

Please cite this paper as:

Huang, J., Hu, G., Xu, G., Nie, B., Yang, N., & Xu, J. (2019). The development of microstructure of coal by microwave irradiation stimulation. *Journal of Natural Gas Science and Engineering, 66, 86-95.*

https://doi.org/10.1016/j.jngse.2019.03.016

Chapter 6 to chapter 8 are laboratory experiments in studying the fissure development and heating effect under microwave irradiation. Few previous studies have investigated moisture's effect on microwave fracturing of coal. In this chapter, NMR and SEM were conducted to obtain the microstructure of coal before and after microwave treatment. Influencing factors including moisture content, microwave power and treatment time for microwave fracturing were made clear through investigating the pore development of coal samples with different saturations under various microwave powers and treatment times.

6.1 Abstract

Due to the benefit of environmentally friendly, widely applicable and economical, microwave fracturing has been proposed as an alternative approach to stimulate coalbed methane reservoirs. Different microwave parameters (microwave power and treatment time) and saturation conditions of coal have great effect on the microwave heating effect, which further results in different microwave fracturing effects. In this study, repeated nuclear magnetic resonance experiments and quantitative analysis were performed to investigate the effects of microwave power, irradiation time and saturation condition on microstructure development of coal. Three indicators including macropore and fissure proportion variation (MFPV), variation rate of water porosity (VRWP) and moisture loss were proposed to evaluate microwave's effect on pore structure. It was found that the pore size, water porosity and moisture loss increase with rising microwave power and irradiation time. Microwave's effect on coal sample with saturations ranged from 0% to 100% was first studied in this paper. The results show that microwave irradiation has great effect on pore structure of coal samples when water saturation is less than 25% and becomes insignificant when the water saturation is larger than 50%. Surface topography measurements and SEM experiments were also performed before and after microwave treatment to observe the microstructure development. New fissures and cracks were observed on the surface of samples and the surface become smooth with less accumulated particles after microwave irradiation.

Keywords: coal microstructure; microwave irradiation; microwave fracturing; coalbed methane recovery

6.2 Introduction

Due to the increasing energy demands, coalbed methane (CBM) was recognized as an alternative clean energy source in recent years [131, 132]. Meanwhile, it is also a safety hazard resulting in gas explosion or gas outburst accidents, which still occur every now and then in spite of mechanical progress [133,

134]. The main reasons are: on one hand, the increasing production rate leads to more gas released to underground environment; on the other hand, the coal permeability decreases with the increasing mining depth, which makes it hard to extract the gas [35]. Therefore, to ensure the safety production of coal mines, to reduce greenhouse effect and to improve the energy utilization efficiency, CBM need to be extracted prior to underground mining activities [35]. In order to increase gas extraction rate, many stimulating methods are developed in enhancing coal seam permeability, including hydraulic fracturing, CO_2 enhanced coalbed methane (ECBM), heat injection, liquid nitrogen fracturing and so on [2, 80, 135, 136]. However, these methods have the shortcomings such as: hydraulic fracturing contaminates surface water and ground water [137, 138], which has been banned in some countries and regions [139]. Heat injection is restricted by geological conditions and low power conversion efficiency [115]. ECBM is only suitable for the coal seams with high pre-existing permeability [12]. Therefore, an effective substitute way to stimulate is in a badly demand.

Recently, microwave fracturing has been proposed to address this problem. The mechanism of microwave fracturing is the moisture and minerals adsorb most of the microwave energy under microwave irradiation, the temperature distribution of coal body is therefore non-uniform and thermal fractures are thus formed [55, 140, 141]. During this process, moisture that prevent the desorption, diffusion and permeation of CBM is evaporated, and the void volume in the coal increases significantly as the moisture removed from coal body [142]. Beyond that, the accompanying steam flow also helps expand the pores and fissures [143, 144]. Under the combined effects mentioned above, coal seam permeability increases under microwave radiation. It should be noted that the microwave fracturing technology can be also applied in shale and oil sand reservoir to assist traditional methods [35, 145-147]. As microwave fracturing is a promising technology with the advantages of economical, widely applicable and no water usage and contamination, it attracts extensive attention worldwide in recent years.

Experiments have been carried out to test microwave's effect on rock breakage. Variations in thermal and ultrasonic properties of gabbro under microwave irradiation were investigated [148]. It was found both intergranular and transgranular cracks appear at power of 1500 W and 2000 W. The P-wave velocity results suggest severe damage has been induced in specimens even though there is no obvious fissures on the surface [148]. Effect of microwave irradiation on coal petrophysical properties were studied [39, 40, 59, 62, 88, 149]. Hong et al. [112] evaluated the effect of microwave irradiation on the fractal dimension of coal samples. It was found the permeability increases while the fractal dimensions of coal samples decrease after microwave treatment. Liu et al. [62] investigated pore structure of lignite through N_2 adsorption/desorption experiments at 77 K, whose results suggest that the average pore diameter and total pore volume increase after microwave treatment.

However, these studies are mainly focused on the microwave power and irradiation time's effects on coal structure, while few studies have discussed the influence of saturation conditions [32]. Furthermore, no such experiment results can be found for coal sample with saturations larger than 15%. As this aspect is critical before on-site application, additional experiments should be carried out to investigate the effective range of saturation conditions for microwave fracturing. Beyond that, these studies tried to obtain the effect of microwave irradiation on coal petrophysical properties with only one sample for each experiment condition. As coal samples have large individual differences, these experiment results are questionable. In order to achieve tenable experiment results, experiments should be repeated for multiple samples under the same experiment condition and quantitative analysis is required to conclude the quantitative effects of microwave power, irradiation time and saturation condition on microstructure of coal.

The aim of this paper is to investigate the effects of microwave radiation on the microstructure of coal samples with different saturations under different microwave powers and microwave irradiation (MI) times in detail. NMR and SEM were introduced to compare coal microstructure before and after microwave treatment. Repeated NMR experiments were conducted for three coal cores under each microwave setting and saturation condition to avoid the randomness of results. Quantitative analysis is then carried out to conclude the quantitative effect of microwave power, irradiation time and saturation condition on microstructure development of coal. This study also fills the research gap in studying microwave's effect on coal with high saturations. Therefore, these experiment results could be very useful to on-site application and the following studies.

6.3 Experiments

6.3.1 Coal Sample Preparation

The coal samples in this study were taken from Zhangminggou coal mine in Shanxi province of China. They were drilled into cylindrical cores with 50 mm diameter and 50 mm height for testing. The proximate analysis of these coal samples is provided by Jiangsu Geology Minerals Design & Research Institute, whose result is shown in Table 13.

To prepare the coal sample with specific water saturation, all the coal cores were fully saturated and then dried for a certain time. The fully saturation was realized by vacuum saturation for 24 hours at room temperature and the drying process was conducted in vacuum drying oven at 50℃. Several coal cores were used for pre-experiments to obtain the approximate drying time needed to achieve certain water saturations. It was found that it takes 1 hour, 5.5 hours and 16.5 hours respectively in the vacuum drying oven at 50℃ to achieve coal cores with approximately 75%, 50% and 25% water saturations.

Table 13. Proximate analysis of coal samples

Proximate analysis (%)			
M_{ad}	A_d	V_{daf}	FC_d
8.7	6.73	35.79	59.89

M_{ad} and A_d refer to moisture and ash yield on an air dried basis, respectively; V_{daf} and FC_d denote the volatile matter and fixed carbon content on a dry ash-free basis, respectively.

6.3.2 Experimental Process

The experiments in this paper include using NMR and SEM to investigate microwave irradiation's influence on the microstructure of coal sample. The experimental procedure of NMR (blue arrows) and SEM test (yellow arrows) were shown in Figure 39. To investigate the initial microstructure of coal samples, NMR T_2 measurements were performed for the totally dried and saturated conditions of all the coal cores before microwave treatment (step 3 and step 5). These coal cores were then processed into different moisture conditions (step 6) and treated with microwave oven under various irradiation settings (step 7): 12 saturated coal cores with water saturation of 50% were treated with microwave power ranging from 800 W to 2000 W for 5 minutes to investigate microwave power's effect on pore structure; 11 coal cores with water saturation of 50% were treated with 2000 W microwave for 3 to 6 minutes respectively to study the effect of MI time on pore structure; 11 coal cores with different water saturations (from 0% to 100%) were treated with 2000 W microwave for 5 minutes to observe the MI's effect on coal samples with different water saturations. Finally, all the coal cores were fully saturated again (step 8) and NMR tests were performed for these saturated coal cores (step 9). As for the SEM experiments, coal slices were collected from raw coal sample (step 1). The surface micro-topographies of coal slices were measured before (step 2) and after (step 4) microwave treatment of 2000 W and 3 minutes, whose results were compared to analyse the microstructure change under microwave irradiation.

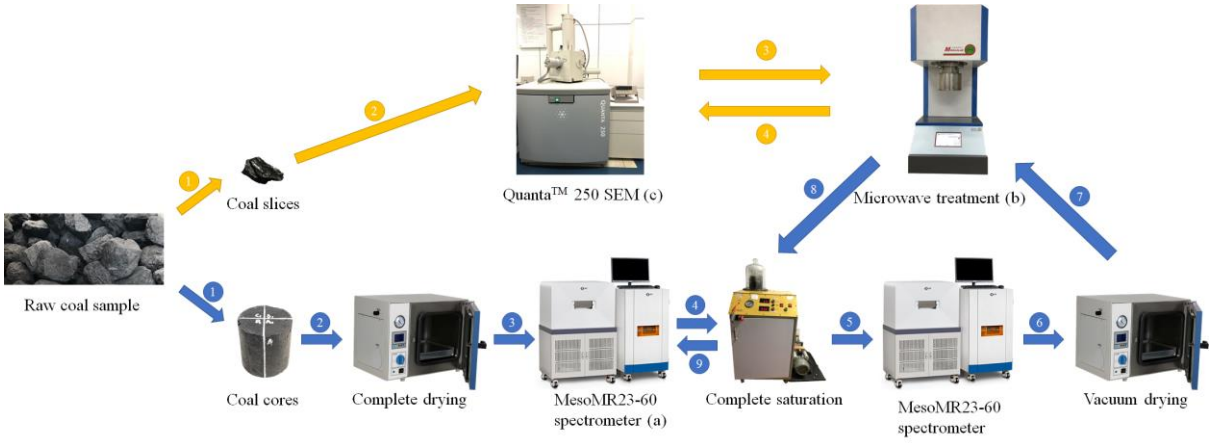

Figure 39. Procedure of NMR experiment

6.3.3 NMR Test Principle

Nuclear magnetic resonance (NMR) is a physical phenomenon that the spin nuclei absorb external radio frequency field energy in strong magnetic field. T_2 spectrum is obtained from detecting the NMR signals of water within the pore and fissures [63]. For pore fluids in the coal body, T_2 times are influenced by three possible relaxation mechanisms: bulk relaxation (T_{2B}), surface relaxation (T_{2S}) and diffusion in the magnetic field gradients (T_{2D}) [150]:

$$\frac{1}{T_2} = \frac{1}{T_{2B}} + \frac{1}{T_{2S}} + \frac{1}{T_{2D}} \tag{26}$$

Bulk relaxation (T_{2B}) is the fluid's intrinsic relaxation property, which is determined by the viscosity (η) and chemical composition of the fluid [151]. For the fluid with small viscosity, such as water, the bulk relaxation can be neglected.

Surface relaxation (T_{2S}) occurs at the grain surface of coal, which is given as [151]:

$$\frac{1}{T_{2S}} = \rho_2 (\frac{S}{V})_{pore} \tag{27}$$

where ρ_2 $[\mu m/ms]$ is T_2 surface relaxivity, $(\frac{S}{V})_{pore}$ $[m^{-1}]$ denotes the ratio of pore surface to fluid volume.

Diffusion induced relaxation (T_{2D}) is significant when fluids are in a large gradient magnetic field and subjected to CPMG with long echo spacing time. For coal sample saturated with water, the influence of T_{2D} on T_2 spectrum is negligible [112].

Therefore, transversal relaxation T_2 can be expressed as [152]:

$$\frac{1}{T_2} \approx \frac{1}{T_{2S}} = \rho_2 \left(\frac{S}{V}\right)_{pore} = F_s * \rho_2 / r_c \quad (28)$$

where F_s is the pore geometry morphologic, with $F_s = 2$ for tubular pores and $F_s = 3$ for spherical pores.

As F_s and ρ_2 are both constant, equation (28) can be transformed to:

$$r_c = \mathrm{C} * T_2 \quad (29)$$

where C is a constant related to pore structure. Therefore, pore radius is proportional to transversal relaxation T_2.

According to previous study, $T_2 < 10\ ms$ is equivalent to micropores, T_2 lies between 10 and 100 *ms* corresponds to mesopores, and $T_2 > 100\ ms$ represent macropores for coal samples [32].

6.3.4 Experimental Equipment

The NMR experiments were operated with MesoMR23-60 spectrometer produced by Suzhou Niumag analytical instrument corporation, as shown in Figure 39 (a). The specific parameter settings of the instrument are listed in Table 14. As shown in Table 14, SEQ denotes pulse sequence, which is Carr-Purcell-Meiboom-Gill (CPMG) in this case. SF is the main resonance frequency, while O_1 is the frequency offset that need to be adjusted according to the temperature. SW is the receiver bandwidth as well as sampling rate. P_1 and P_2 represent pulse width of 90° and 180° radio-frequency respectively. TD is sampling number. TW refers to the waiting time that signal completely restored to the balanced state. TE is the echo spacing and NECH is the number of echoes.

Table 14. Parameters of NMR experiments

Parameter	Value	Parameter	Value
SEQ	CPMG	P_2	26 us
SF	23MHz	TD	100020
O_1	403856.51 Hz	TW	2000.000 ms
SW	250 kHz	TE	0.1 ms
P_1	13.00 us	NECH	4000

A microwave irradiation system with continuously adjustable powers ranging from 0 to 2000 W was used in this study, as shown in Figure 39 (b). This system

consists of a microwave transmitter, a wave guide, four antennas, a cooling fan and a control system.

The SEM tests in this study were conducted via Quanta^{TM} 250 manufactured by FEI Company, as shown in Figure 39 (c). This system has three vacuum modes: high vacuum, low vacuum (<1.3 mbar), and ESEM (<40 mbar). Its magnification is up to 1,000,000 times.

6.4 Results and Discussions

6.4.1 Initial Microstructure of Coal Samples

To investigate the initial characteristics of coal cores' microstructure, the coal cores under both fully dried and saturated state were tested with low-field NMR. The results suggest that almost all the samples have similar NMR spectrums, with only one obvious peak for dried samples and two peaks for saturated samples, as shown in

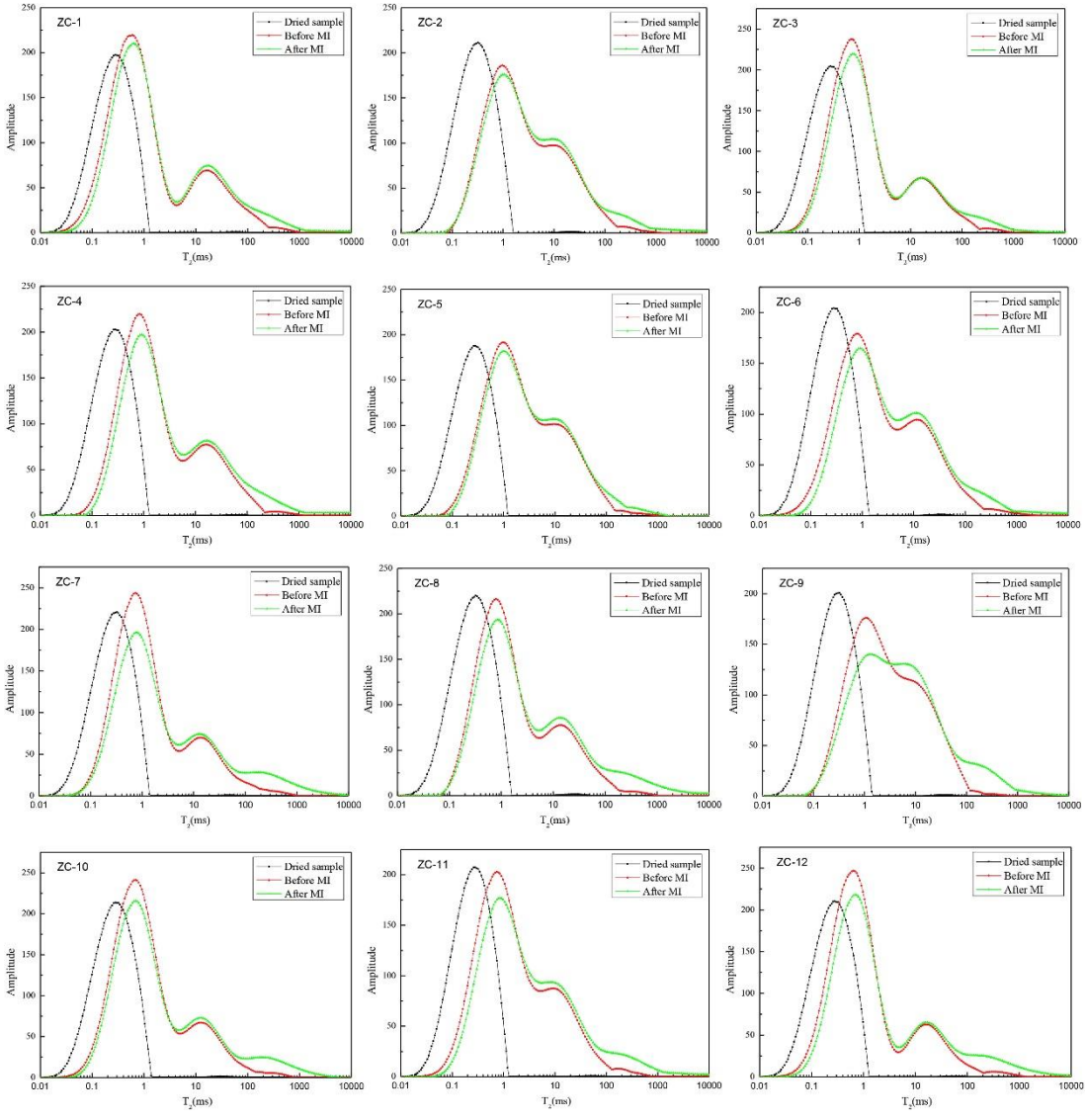

Figure 41.. A typical analyse result is shown in Figure 40. The water exists in coal sample can be divided into irreducible water and free water. There are two models in explaining the occurrence of irreducible water. The first one called the small pore bound-water model assumes that movable water resides only in large pores, while the irreducible water resides in small pores only [151]. This theory was widely applied in estimating the bulk volume of irreducible water (BVI) [32, 151]. The second model called the membrane bound-water model insists that irreducible water exists in large pores as well [151]. After long term studies and verifications, it was found the second model is more reliable [88].

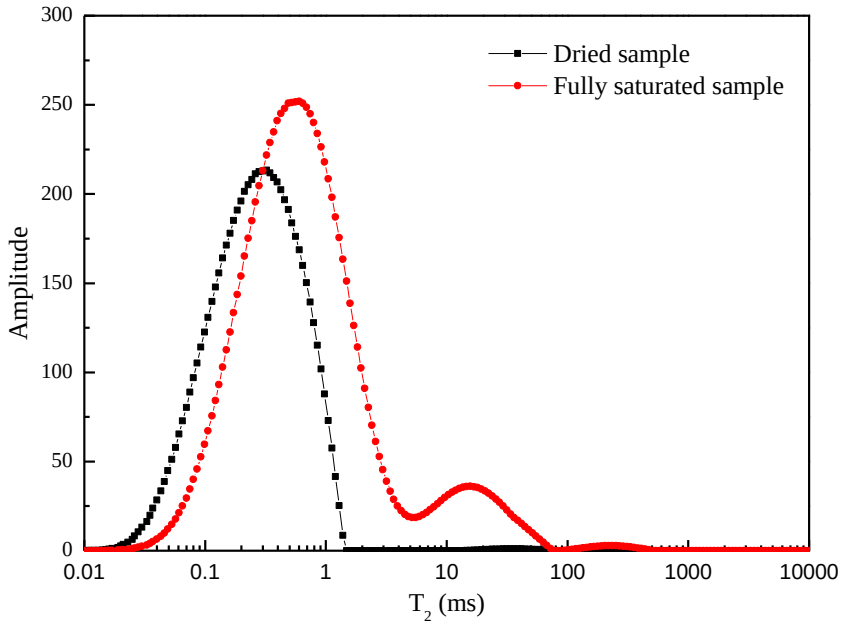

Figure 40. T_2 spectrum of original dried and saturated sample ZC-18

The validity of the membrane bound water model is supported by the NMR experiments results, thus the widely used cutoff-BVI based on the small pore bound-water model is not proper to evaluate the porosity. The pore structure was obtained from NMR test through detecting the bound water and saturated water within the coal sample. As revealed in Figure 40, the black curve is the NMR spectrum of completely dried coal sample, which reflects the bound water trapped within the sample. The red curve is the NMR spectrum of completely saturated sample. It represents coal sample's initial pore distribution: micropores account for most of the portion (as much as 92.66%), mesopores take up 6.91% and macropores are negligible (0.43%). It seems counter-intuitive that the dried sample has more micropores whose T_2 ranged from 0.01 to 0.28. This phenomenon can be found for all the coal samples at certain T_2 range, as shown in

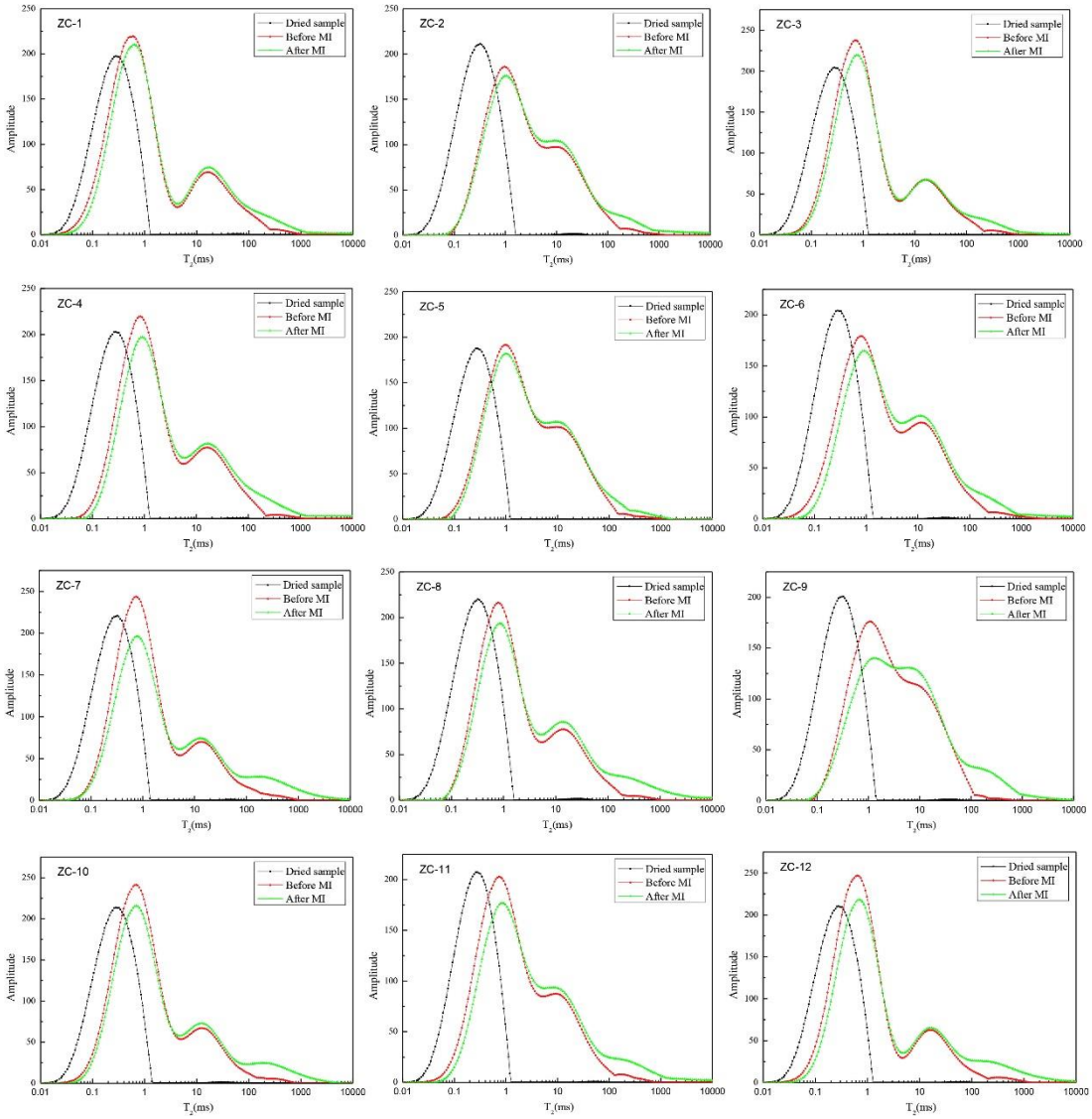

Figure 41., Figure 44 and

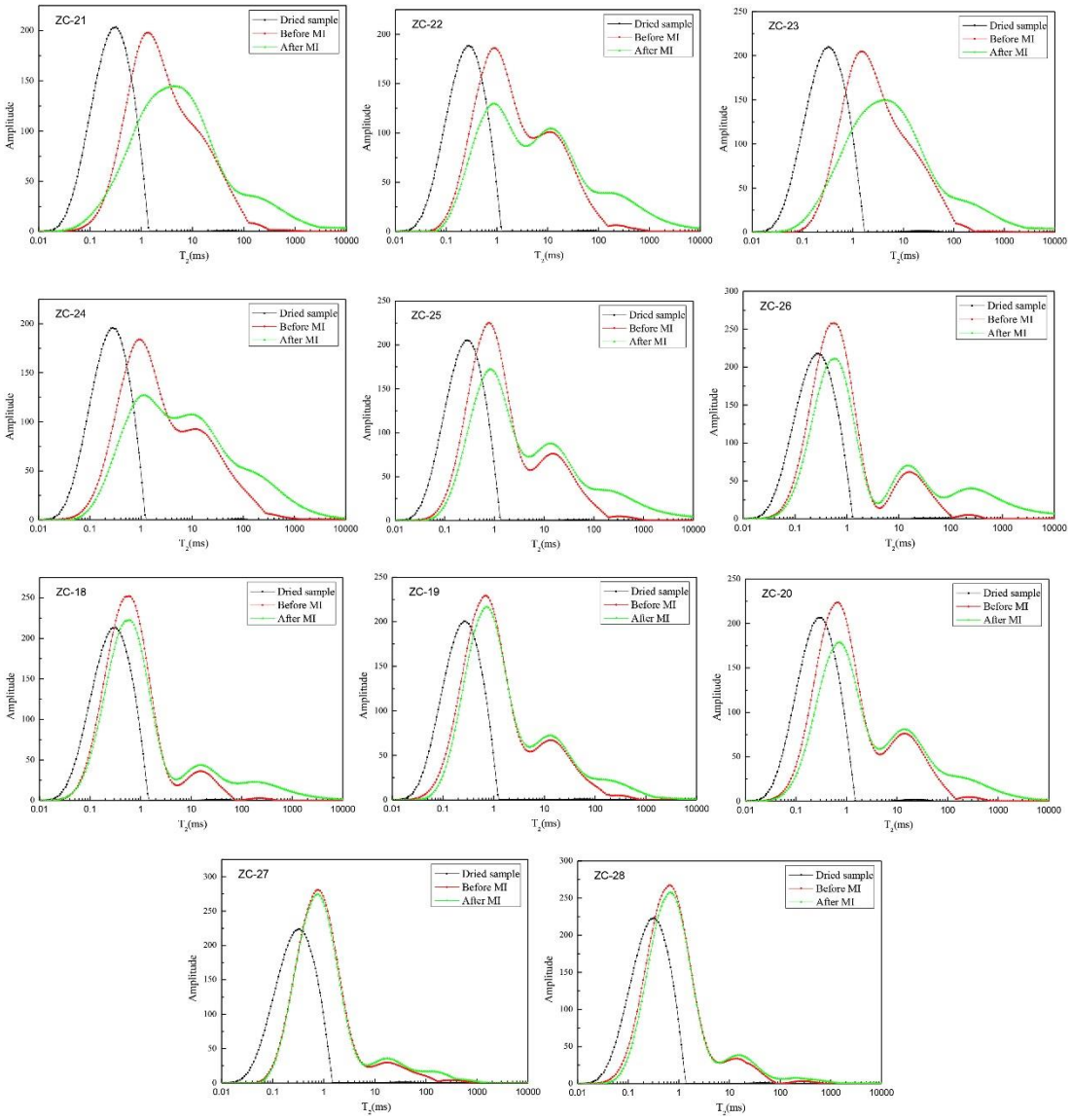

Figure 47. As the initial bound water still exists and the initial empty micropore cavity is filled with water after saturation, the detected micropores of saturated samples should be larger than that of dried ones. According to the model, we believe that bound water also existed in larger pores, which was regarded as micropore in the NMR test for dried samples. When the dry sample is saturated, those larger pores were filled with water and thus no longer regarded as micropores. Therefore, T_2 spectrum of sample ZC-18 as well as all other coal samples support the membrane bound-water model. Thus, the small pore bound-water model is not suitable for this case, and the NMR logging method called cutoff BVI that based on this model does not applicable in this study. To address this, three indicators were introduced to evaluate microwave's effect on the pore structure. They are: macropore and fissure proportion variation, variation rate of water porosity and moisture loss.

As macropores and fissures are the main pathways for the gas, their proportion should be focused and taken as an important indicator for the pore

structure. The proportion of macropore and fissure can be calculated with the following equation:

$$\mathrm{r} = \frac{\int_{100}^{10000} A(T_i)dT}{\int_{0.01}^{10000} A(T_i)dT} \tag{30}$$

Where *A* is the amplitude and *T* represents relaxation time in T_2 spectrum.

To quantify the effect of microwave on pore structure, the variation of macropore and fissure proportion (VMFP) is defined as the difference between the macropore and fissure proportion after MI (r_2) and that before MI (r_1), given as：

$$\Delta\mathrm{r} = r_2 - r_1 \tag{31}$$

Water porosity is another indicator for pore structure of coal as larger water porosity means more space to store water, which suggest the fissure system is more developed. In this study, the water porosity of all the samples before (φ_1) and after (φ_2) MI were calculated using gravimetric methods. The variation rate of water porosity (VRWP) is defined as:

$$\Delta\varphi = \frac{\varphi_2 - \varphi_1}{\varphi_1} \tag{32}$$

Beyond that, the mass loss during MI was regarded as moisture loss, given by:

$$\Delta\mathrm{M} = M_b - M_a \tag{33}$$

where M_b refers the weight of coal sample before MI, while M_a is the weight of coal sample after MI.

6.4.2 Effect of Microwave Power

In order to investigate microwave power's effect on pore structure of coal, 12 coal cores with saturation of 50% were treated with microwave according to Table 15 for 5 minutes. Their T_2 spectrums before and after MI are compared as Figure 41.

As shown in Figure 41, the number of micropores decreased after MI, while the number of mesopores and macropores increased. It suggests that pore structure expand under MI and some smaller pores connect with each other and form larger pores. This phenomenon becomes much more obvious with the increase of microwave power. The T_2 spectrums of coal samples generally have 2 or 3 peaks in this study. It was reported that the pore connectivity is reflected by the connection among peaks [88]. The T_2 spectrums shown in Figure 41 suggest all the samples have connective multi-pores system. It is obvious that the shape of T_2 spectrums basically remain unchanged after MI. However, the first peak (micropores) drops

while the second peak (mesopores) and the connection part between them rise after MI. Spectrum of sample ZC-9 suggests that the two peaks may finally merge into one peak after absorbing enough microwave energy.

It also should be noticed that there is significant increase in macropores and fissures for the coal samples under microwave irradiation with power of 1600 W and 2000 W. The proportion of macropore and fissure for all the coal samples before and after MI were presented in Table 15. The relation between VMFP and microwave power were depicted in Figure 42. As revealed in Figure 42, the VMFP shows an overall increasing trend with rising microwave power. However, the VMFP doesn't increase linearly with rising microwave power. It was anticipated that larger microwave power will certainly leads to greater VMFP. However, Figure 42 suggests that microwave with power of 1600 W has better effect on coal than that of 2000 W. This may be resulted by the significant individual difference between coal samples. A possible explanation is some of the coal cores contain more metallic elements, which increase coal samples' ability in absorbing microwave energy. The VRWP and moisture loss were also calculated and presented in Figure 43. They have the similar trend with VMFP with the increase of microwave power. Even though the averaged VRWP and moisture loss of samples under 1600 W are also higher than that under 2000 W, the VRWP of samples under 2000 W are greater than that under 1600 W except for ZC-7.

Due to the heterogeneity of coal sample, even the same microwave power has much difference in the effects on different coal samples. For instance, VMFP of ZC-4 (4.854%) is more than twice of that of ZC-5 (2.157%). Even though no statistical regularity between microwave power and pore structure was obtained with limited data, it was found that microwave with power larger than 1600 W is effective in fracturing. It also can be concluded that the microwave fracturing effect on coal is largely depend on its initial properties. Therefore, the experiments with only one sample under each microwave conditions are still doubtful. More researches on microwave power's effect on coal structure is required in the future.

Table 15. Calculated macropore and fissure proportion before and after 5 mins MI

No.	MI power (W)	r_1	r_2	Δr
ZC-1	800	2.876032	6.231132	3.36
ZC-2	800	2.3168	6.27166	3.95
ZC-3	800	2.220007	5.577985	3.36
ZC-4	1200	2.328959	7.18298	4.85
ZC-5	1200	1.630238	3.787116	2.16
ZC-6	1200	2.963956	6.763755	3.80
ZC-7	1600	2.220782	9.497935	7.28
ZC-8	1600	2.031018	8.740805	6.71

ZC-9	1600	0.86715	8.269283	7.40
ZC-10	2000	1.528294	7.522473	5.99
ZC-11	2000	1.516832	6.889697	5.37
ZC-12	2000	2.020875	8.637563	6.62

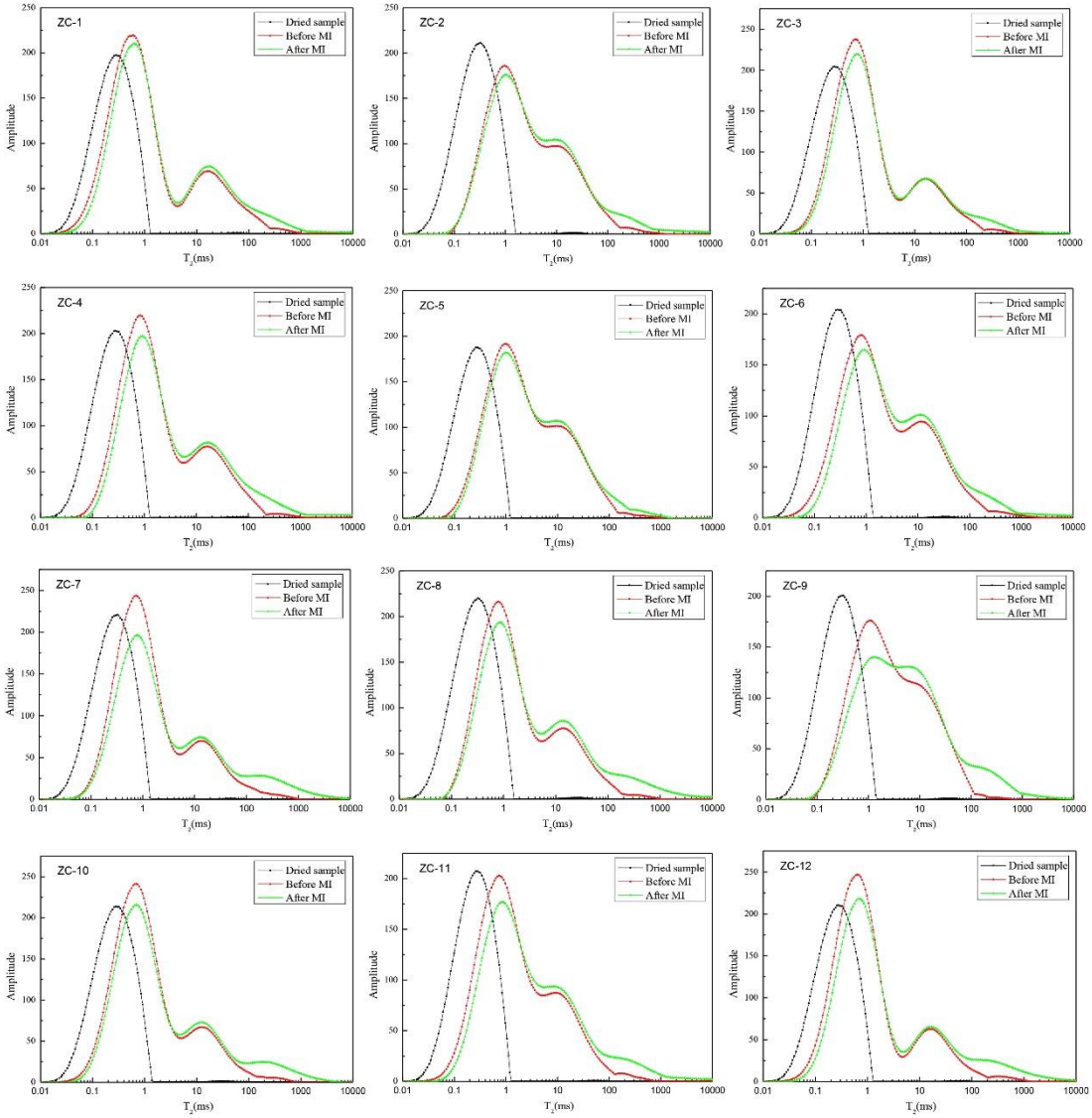

Figure 41. T_2 spectrums of coal samples under different microwave powers

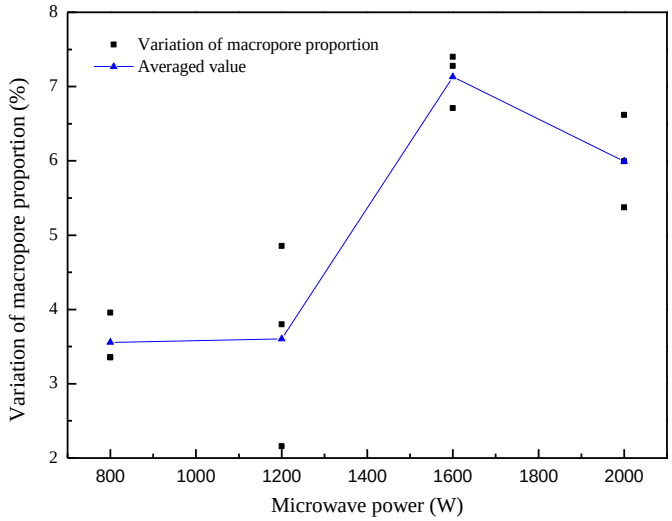

Figure 42. Effect of microwave power on VMFP

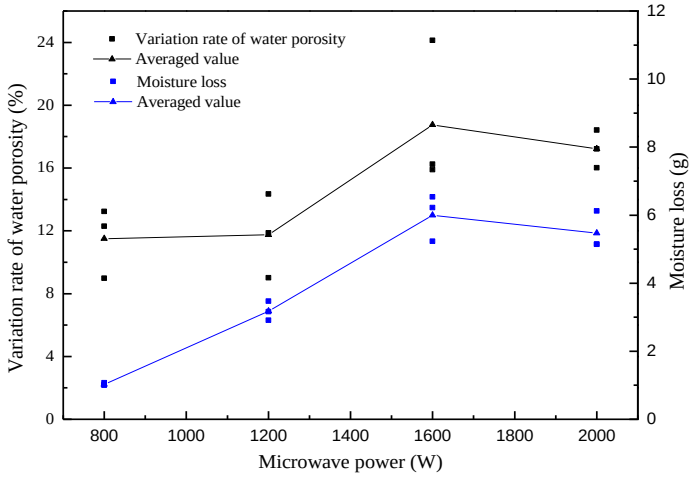

Figure 43. Effect of microwave power on VRWP and moisture loss

6.4.3 Effect of Microwave Time

To find out the effect of MI time on pore structure of coal, 11 coal samples with water saturation of 50% were treated with 2000 W microwave for different times, as shown in Table 16. Their T_2 spectrums before and after MI are shown in Figure 44.

As shown in Figure 44, T_2 spectrums suggest that microwave's effect increases steadily over time. The difference of T_2 spectrums before and after MI is relatively small when MI time is short. For instance, the T_2 spectrums of ZC-13, ZC-16 and ZC-17 had very little change after MI. With the extension of time, the number of micropores decreased sharply, while the number of macropores and fissures increased significantly. VMFP of the above coal samples were another prove, as presented in Table 16. The relation between VMFP and MI time were depicted in Figure 45. It can be seen that, even though there are outliers, the VMFP shows upward trend with the increase of MI time. Curve fitting was performed to obtain the correlation between VMFP and MI time, which is $y = 1.3271x - 1.2157$

with R-square of 0.834. It can be seen from the fitting curve that VMFP increases linearly with MI time.

The change of VRWP and moisture loss over MI time follow the same trend with that of VMFP, as depicted in Figure 46. Both VRWP and moisture loss show increasing trend over time. Through comparing Figure 45 and Figure 46, it's not hard to find that moisture loss increase steadily with the extension of MI time, while the data of VMFP and VRWP have much bigger fluctuation. That is to say, the microwave drying effect is predictable when applying microwave on site. On the contrary, the microwave fracturing effect is largely depending on the coal property.

Table 16. Calculated macropore and fissure proportion before and after 2000 W MI

No.	MI time (min)	r_1	r_2	Δr
ZC-13	3	1.48	3.59	2.11
ZC-14	3	1.14	5.24	4.10
ZC-15	4	1.65	6.54	4.89
ZC-16	4	1.98	4.28	2.30
ZC-17	4	2.98	5.67	2.69
ZC-10	5	1.53	7.52	5.99
ZC-11	5	1.52	6.89	5.37
ZC-12	5	2.02	8.64	6.62
ZC-18	6	0.43	7.87	7.44
ZC-19	6	1.62	6.17	4.55
ZC-20	6	1.12	9.02	7.91

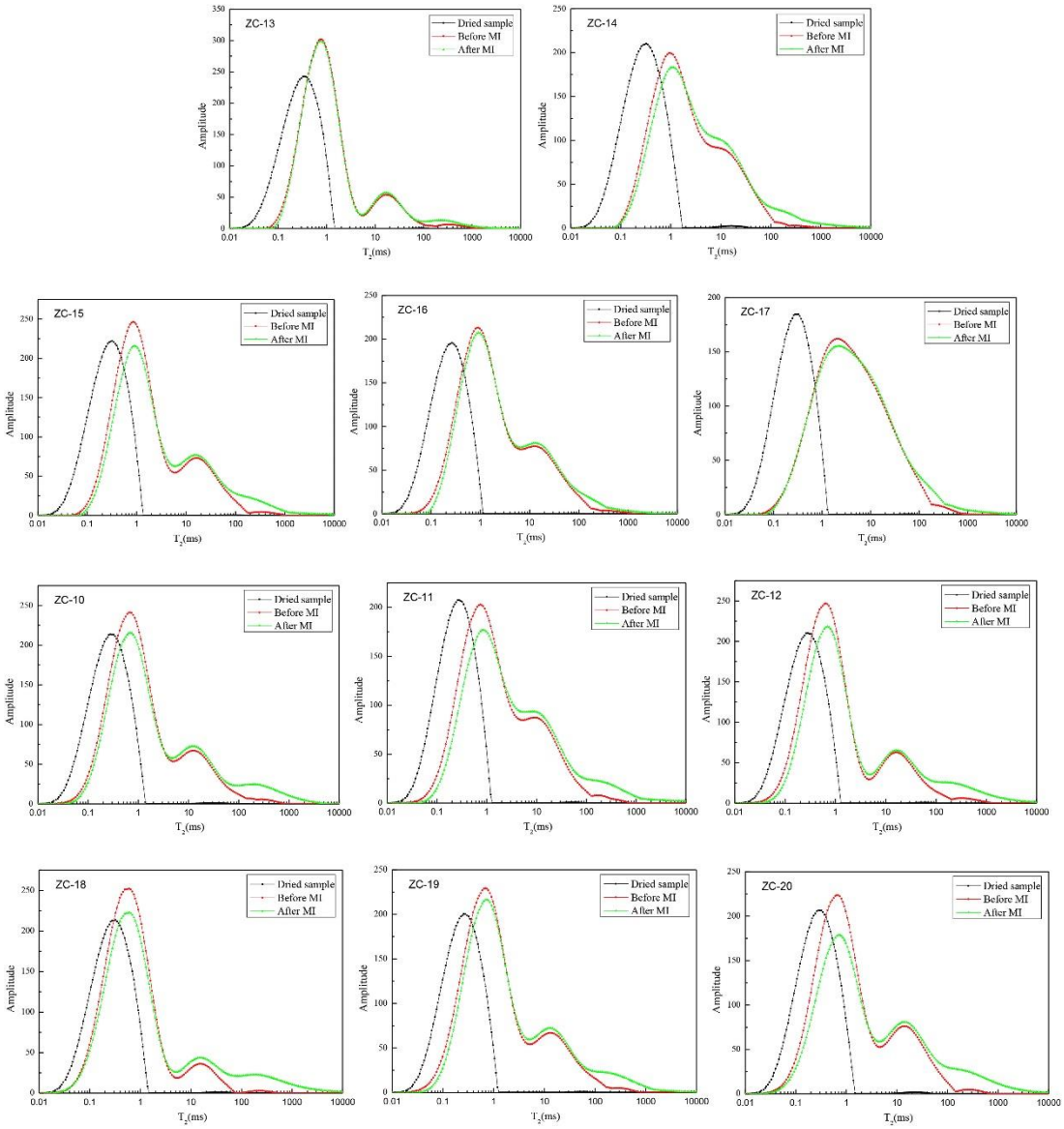

Figure 44. T_2 spectrums of coal samples under different treatment times

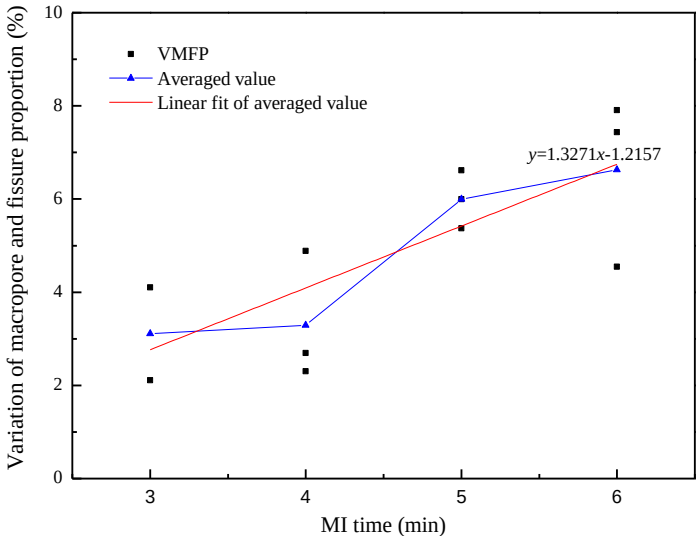

Figure 45. Effect of MI time on VMFP

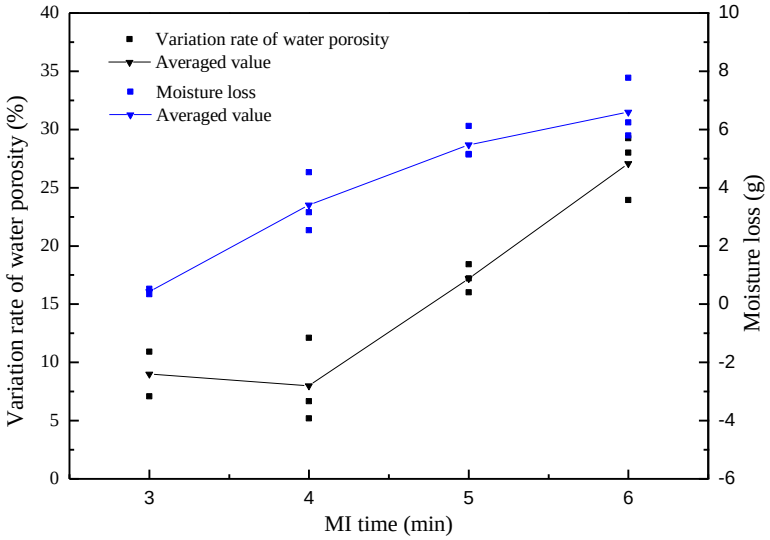

Figure 46. Effect of MI time on VRWP and moisture loss

6.4.4 Effect of Water Saturation

Moisture has both positive and negative effects on microwave fracturing. On one hand, moisture significantly increases the dielectric constant of the coal sample, which increases coal sample's ability in absorbing microwave energy. On the other hand, microwave energy is firstly absorbed by the moisture within the coal sample, which takes the energy away as it evaporates. Moisture also prevents the coal sample from brittle fracture, which restricts the microwave fracturing effect to a certain content. To investigate the effect of MI on coal samples with different water saturations, 11 coal samples with different water saturations were treated with 2000 W microwave for 5 minutes, as shown in Table 17. Their T_2 spectrums before and after MI are shown in Figure 47.

As revealed in Figure 47, the T_2 spectrums suggest microwave has much better effect on the coal cores with low water saturations. The shapes of T_2 spectrums have tremendous change for the coal cores with lower water saturations (0% and 25%), all of which form a new peak within $100 < T_2 < 1000$. For the unimodal spectrums before MI, such as ZC-21 and ZC-23, the peak migrated towards larger T_2 value and the peak amplitude declined sharply after MI. For the bimodal spectrums before MI (including ZC-22, ZC-24, ZC-25 and ZC-26), the first peak decreased dramatically while the second peak had certain growth. T_2 spectrum of ZC-22 and ZC-24 suggest these two peaks will eventually merge into one peak. The above-

mentioned phenomenon can also be spotted on samples with about 50% water saturation, but not very obvious. As for the samples with high saturations (75% and 100%), the T_2 spectrums before and after MI nearly overlap with each other, which indicates MI has little effect for coal samples with higher water saturations.

VMFP was also calculated for these coal cores to quantify the effect of water saturation, as shown in Figure 48. It also suggests that microwave has better effect on coal cores with low water saturations. The VMFP increased more than 10 percent for the coal cores with saturations of 0% and 25%. It then deceased sharply with the increase of water saturation. When the water saturation is larger than 75%, MI's influence on VMFP is minimal (less than 2.5 percent). Beyond that, coal cores with water saturations of 25% and 50% have the largest VRWP and moisture loss, as shown in Figure 49. VRWP shows the same trend with VMFP (decreasing sharply) when the saturation is larger than 50%. For the fully saturated sample, VRWP and VMFP are minimal while the moisture loss rate is high. It is worth to mention that there is still moisture loss for the totally dried samples. The lost moisture is the bound water within coal samples. The removal of bound water within short time proves microwave to be very effective in drying.

In conclusion, a certain amount of water is helpful to microwave fracturing. For the samples with high water saturations, microwave only shows drying effect, while its effect on pore structure is negligible. Therefore, for the fully saturated reservoir, it is predictable that the microwave fracturing at the first stage is not evident. The microwave stimulation will become more effective over time as the water is gradually removed from the coal seam.

Table 17. Calculated macropore and fissure proportion before and after MI (6 mins, 2 kW)

No.	Drying time (h)	r_1	r_2	Δr
ZC-21	36	1.45	10.95	9.50
ZC-22	36	1.78	14.17	12.38
ZC-23	36	1.11	10.88	9.78
ZC-24	16.5	3.67	14.58	10.91
ZC-25	16.5	1.91	12.37	10.46
ZC-26	16.5	0.77	14.96	14.18
ZC-18	5.5	0.43	7.87	7.44
ZC-19	5.5	1.62	6.17	4.55
ZC-20	5.5	1.12	9.02	7.91
ZC-27	1	1.14	3.23	2.09
ZC-28	0	0.55	2.27	1.71

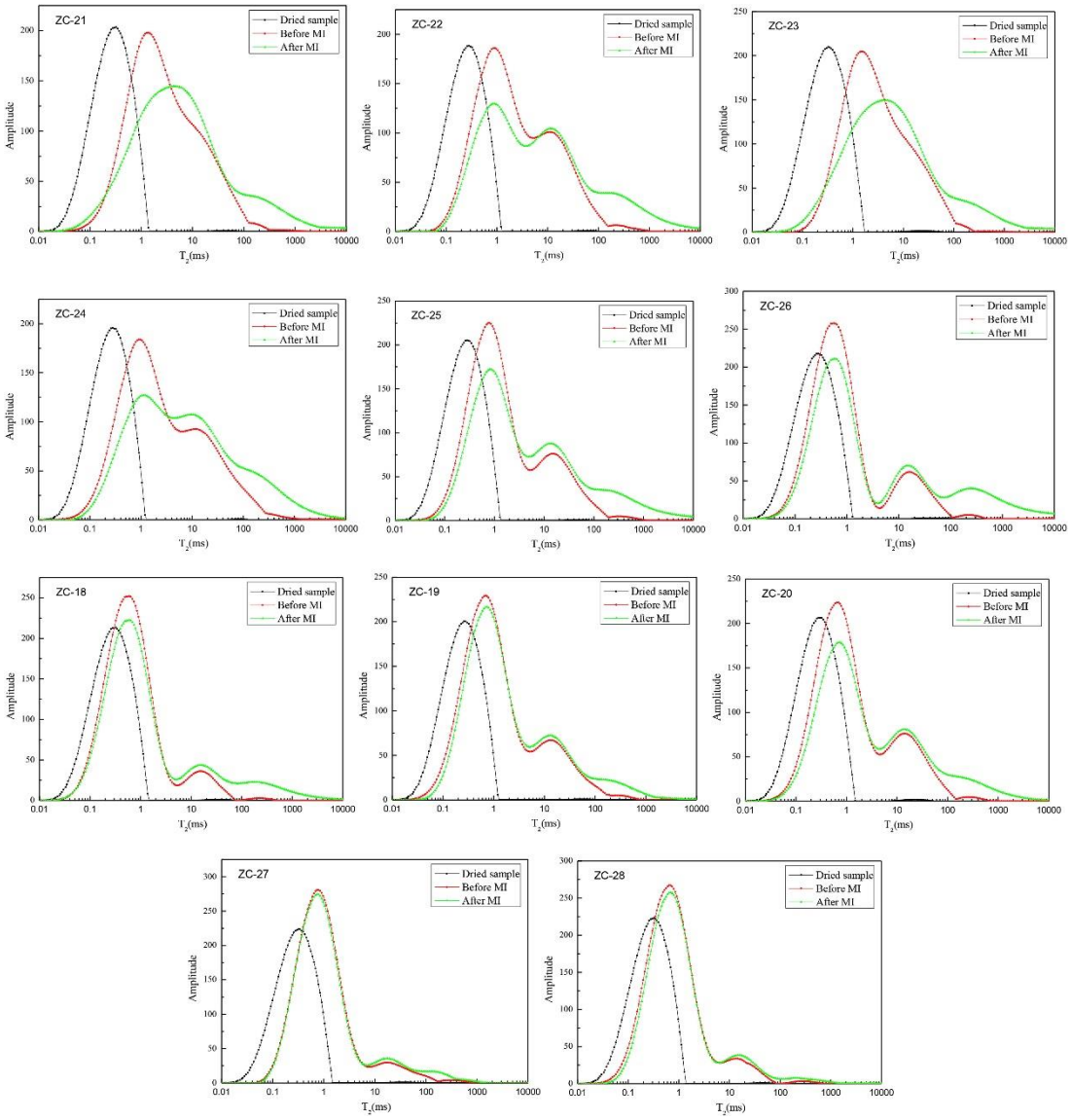

Figure 47. T_2 spectrum of coal samples with different water saturations

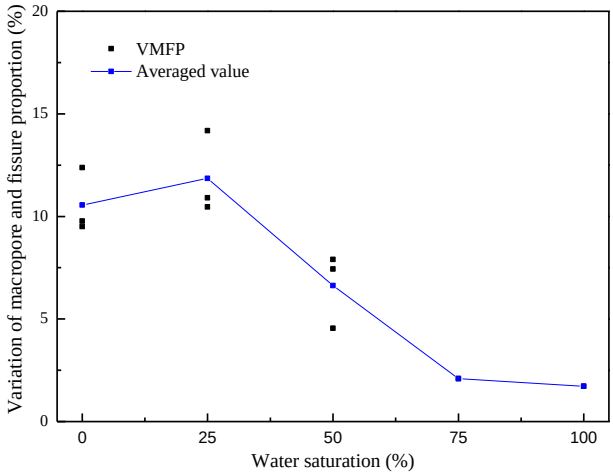

Figure 48. Effect of water saturation on VMFP

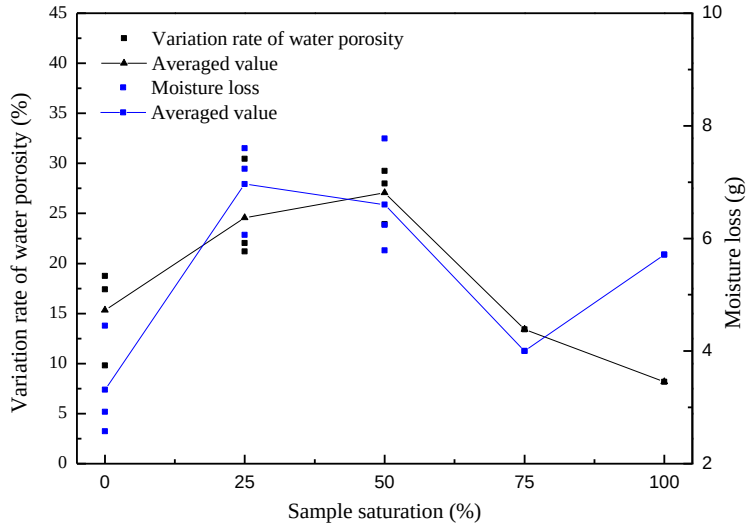

Figure 49. Effect of water saturation on VRWP and moisture loss

6.4.5 Surface Fissure Growth

The surface fissures of coal sample before and after MI are shown in Figure 50. It was found the original vertical fissures expanded for most of the samples, while no evident difference was spotted for the rest samples. As for the horizontal fissures, the situation is more complicated. For some samples, the original horizontal fissures expanded but not as evident as its vertical fissures. For some other samples, the original horizontal fissures even became less evident after MI, as shown in Figure 50. As all the coal samples were drilled along the direction of face cleat, it can be concluded that the thermal expansion of coal sample is along the horizontal direction (direction of butt cleats). That's to say, the vertical fissures (face cleats) expand under MI while whether the horizontal fissures (butt cleats) expand or shrink is uncertain.

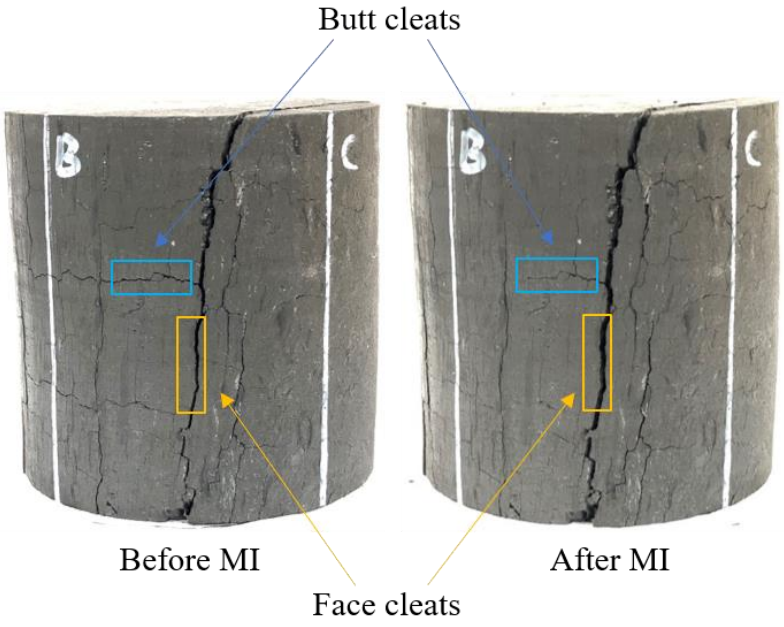

Figure 50. High resolution photos of coal core before and after MI (at 2000 W for 5 mins)

To study the micro-fracture development on the surface of coal samples after MI, the surface micro topographies were taken before and after MI using SEM. For raw samples, visible fissures can be hardly seen, as shown in

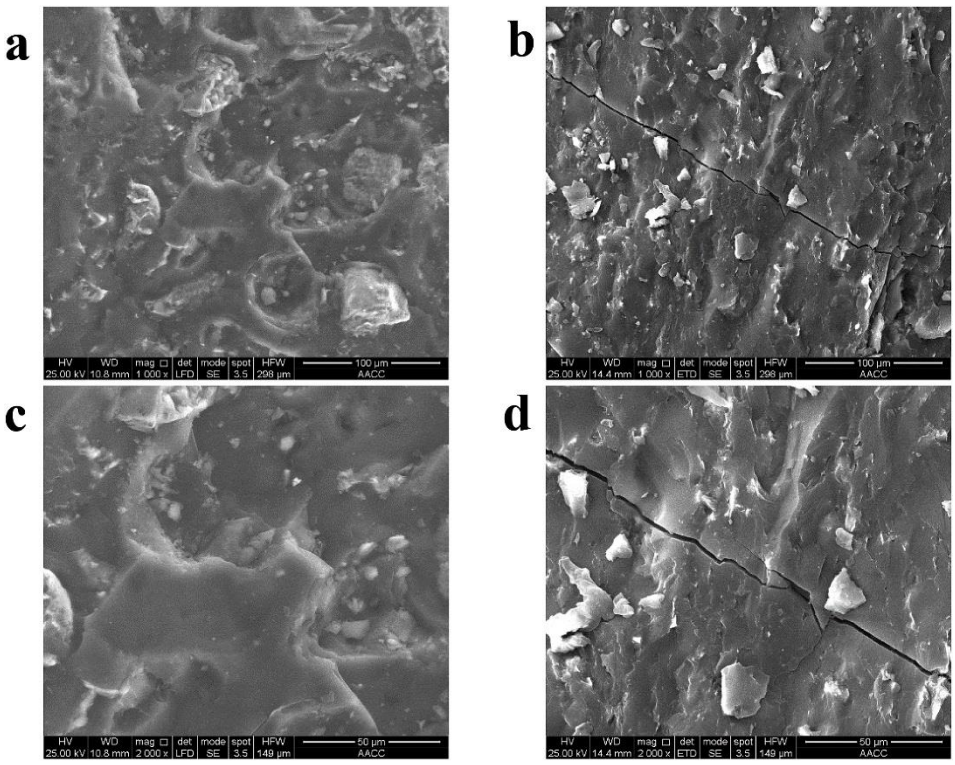

Figure 51. Many small particles and voids were observed on the surface, which contribute to the number of fine pore network [62]. As for the microwave treated coal samples, fissures and cracks appear on the surface of samples, while the surface becomes smooth with less accumulated particles. This phenomenon suggests the small particles decompose under MI, which results in the decrease of fine pore networks and the development of fracture system.

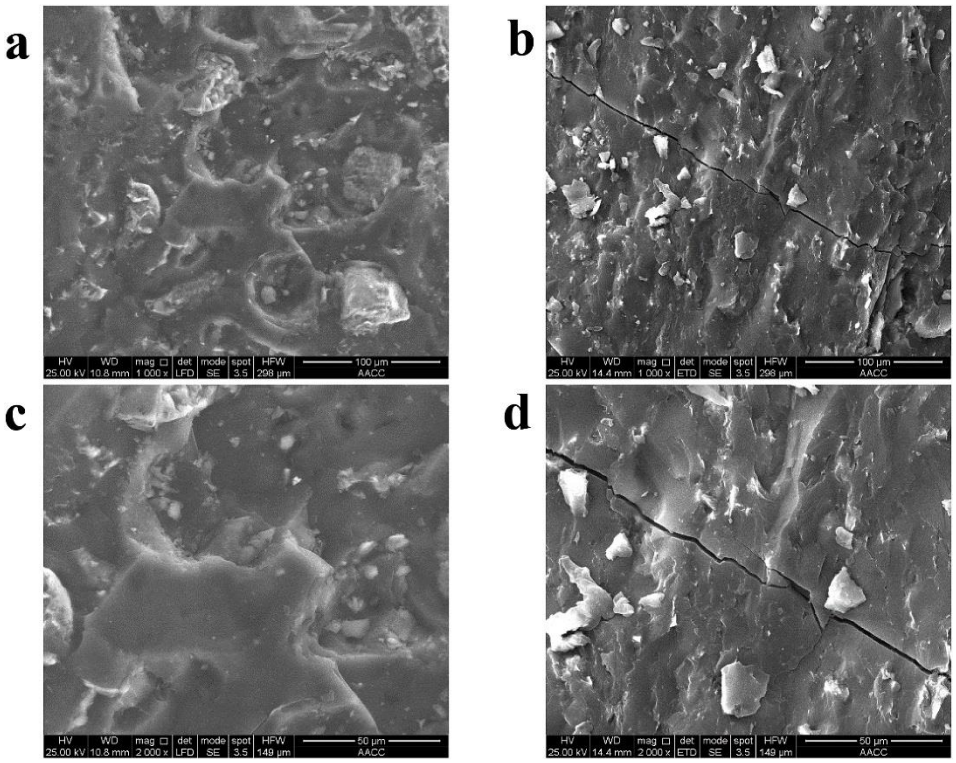

Figure 51. SEM images of coal sample before (a,c) and after (b,d) MI (at 2000 W for 3 mins)

6.5 Conclusions

In this study, NMR was introduced to investigate the effects of microwave radiation on the petrophysical properties of coal samples under different microwave powers, MI times and saturation conditions. Microwave's effect on pore structure was evaluated with three indicators: macropore and fissure proportion variation (MFPV), variation rate of water porosity (VRWP) and moisture loss. It was found the pore size, water porosity and moisture loss increase with rising microwave power and irradiation time. Moreover, moisture has both positive and negative effects on microwave fracturing. It was found the microwave fracturing effect increases with rising water saturation within certain range. Microwave fracturing should have the best performance when water saturation is between 25% and 50%. As for the highly saturated samples, microwave only has drying effect, while its effect on pore structure is minimal. Beyond that, high resolution photos were taken to study the evolution of fissure under MI. SEM were also introduced to compare the surface properties of samples before and after microwave treatment. All the experiment results suggest that microwave leads to the occurrence of new fissures and the expansion of existed fissures.

The experiment results filled the research gap in studying microwave's effect on coal structure with various water saturations from 0% to 100%. Moreover, the repeated experiments of microwave's effect on coal samples under different microwave powers and times are also more persuasive comparing to the previous

studies. Even though these experiment results made clear the microwave's effect under various circumstances, further field experiments are required before any on-site application.

6.6 Acknowledgements

This work was supported by the National Natural Science Foundation of China (Grant No. 51774279), the Petrochemical Joint Funds of National Natural Science Foundation of China and China National Petroleum Corporation (Grant No. U1762105) and Fundamental Research Funds for the Central Universities (Grant No. 2015XKZD04).

7 Chapter 7

Moisture content's effect on fracture development in coal under microwave irradiation

This chapter was presented on the 17th North American Mine Ventilation Symposium, Montreal, Canada. It was written by Jinxin Huang and revised by Prof Guang Xu and Mr Ping Chang.

Please cite this paper as:

Huang, J., Xu, G., & Chang, P. (2019) Moisture content's effect on fracture development in coal under microwave irradiation. *Proceedings of the 17th North American Mine Ventilation Symposium*.

As a continuous study of chapter 6, this chapter focused on the water saturation's effect on fissure development of coal under microwave irradiation. High resolution images were taken for the coal cores with various water saturations (0%, 25%, 50%, 75% and 100%) before and after microwave treatment. Image processing was applied to calculate and analyse the surface fissure areas before and after MI.

7.1 Abstract

As hydraulic fracturing is forbidden in some countries due to its accompanying environmental pollutions, microwave fracturing was proposed as a substitute technology to enhance coal seam permeability. Its mechanism includes: on the one hand, thermal stress caused by non-uniform microwave heating leads to fracture development in coal body, which increases coal seam permeability for gas; on the other hand, moisture within the coal body that hinders gas desorption and diffusion is removed during this process. To study the effect of moisture content on fracture development under microwave irradiation, high resolution photographs were taken before and after microwave treatment. These photographs were then binarized and skeletonized. Based on the processed photographs, the total area were calculated using ImageJ. The results showed that coal samples with 0% and 25% water saturation have more variation in fracture development as compared to that of samples with 50%, 75% and 100% water saturation. This study can be very useful in gas drainage and gas control in coal mines.

7.2 Introduction

Coalbed methane (CBM) is a clean energy source as well as a natural hazard to underground mining [153, 154]. One of the main goals of mine ventilation is diluting methane and removing underground contaminants [128]. Coalbed methane (CBM) has to be extracted prior and during underground mining to avoid methane outburst and explosion accidents. However, with the increase of mining depth, the coal permeability decreases significantly, which makes it hard to extract the methane [35]. To enhance the coal seam permeability, many CBM recovery methods have been applied on-site, such as hydraulic fracturing and enhanced coalbed methane (ECBM). However, hydraulic fracturing is restricted due to environmental concerns

and ECBM is only suitable for the coal seam with relative large permeability [12, 35, 115].

Recently, microwave fracturing was proposed as an optional enhancing technique because of the following advantages. First of all, it does not require the use of water or any chemical reagent, which is totally environmentally friendly [57]. Secondly, microwave fracturing is widely applicable as a non-contact fracturing method. Beyond that, microwave can be turned on or off instantly, which makes it easily controlled [58]. Finally, microwave is economical and easy to generate. Because of these advantages, microwave fracturing has attracted great attentions [52, 130]. Many experiments have been conducted to investigate the microwave's effect on physical properties of coal by using P-wave velocity test [40], NMR [32, 40, 88, 112], SEM [59, 62], X-ray CT scanner [40], gas adsorption and diffusion test [59, 62], and indirect gas penetrability test [59]. The NMR, X-ray CT and SEM tests suggested pore size distribution, total pore volume and the pore connectivity of coal samples increase under MI [32, 40, 59, 62, 88, 112]. It was also found coal sample's adsorption capacity decreases, while its diffusion capacity increases after MI [59]. However, few studies investigated the effect of coal's water saturation on microwave fracturing. Before applying microwave fracturing on-site, it is important to find out the most effective saturation condition of coal for microwave fracturing.

The aim of this work is to investigate the effect of saturation of coal on microwave fracturing. High resolution images were taken for the coal cores with various saturations (0%, 25%, 50%, 75% and 100%) before MI. These coal samples were then treated with 2 kW microwave for 6 mins and were taken images again. The surface fissures of images before and after MI were extracted with ImageJ. Finally, the total surface fissure areas were calculated and analysed, whose results were used to analyse the effect of saturation on microwave fracturing. As microwave fracturing is a promising technology for coalbed enhancement and gas drainage, this study can be very helpful in these areas as well.

7.3 Methods

7.3.1 Coal Samples

The coal samples used in this study were sampled from Zhangminggou coal mine in Shaanxi province of China. They were then processed into cylindrical coal cores with 50 mm diameter and 50 mm height. The proximate analysis has been conducted for the coal samples, whose result is given in Table 18.

Table 18. Proximate analysis of coal samples

Proximate analysis (%)			
M_{ad}	A_d	V_{daf}	FC_d
8. 7	6. 73	35. 79	59. 89

7.3.2 Experimental Procedure

The experimental procedure is shown in Figure 52. To investigate the effect of moisture content on microwave fracturing effect, 5 coal samples were processed to saturation of 0%, 25%, 50%, 75%, and 100%, respectively. High resolution photos were taken for these coal samples from various angles. These coal samples were weighted and then treated with 2 kW microwave for 6 mins. After that, they were weighed again and high resolution photos were taken in the same positions. Finally, the fissure images before and after MI were compared and analysed.

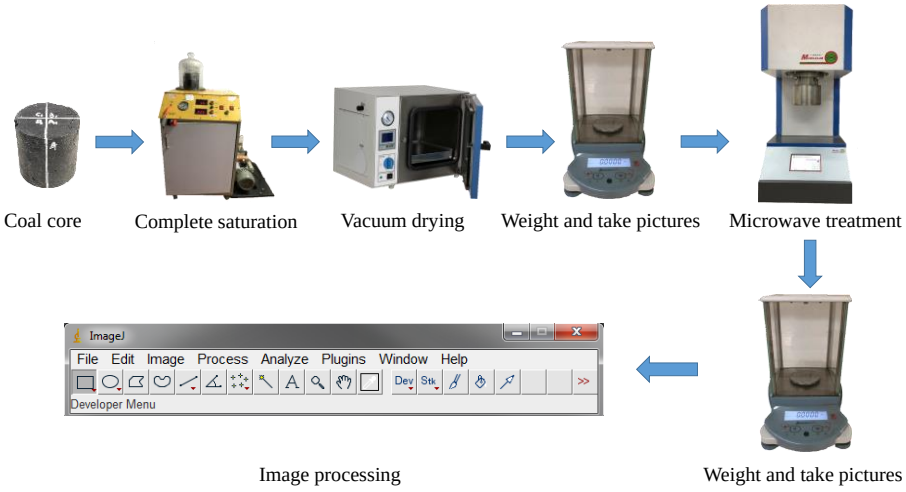

Figure 52. Experimental procedure

7.3.3 Image Processing

Sample 1 was selected as the reprehensive, whose image was processed as displayed in Figure 53. For the image processing, the original image was first converted into 8-bit image by ImageJ, a public domain image processing software developed by the U. S. National Institutes of Health [155]. Sharpen tool was then applied to the image to enhance the contrast and accentuate noise. After that, through adjusting the Min/Max values in threshold tool, the fissure system was selected and extracted as displayed in Figure 53 (d, e). Then, we eliminated the shape that less than 0. 1 mm^2 and obtained the outlines of the rest. Finally, the area of each shape in Figure 53 (f) was calculated and the total area and average size were obtained based on the results.

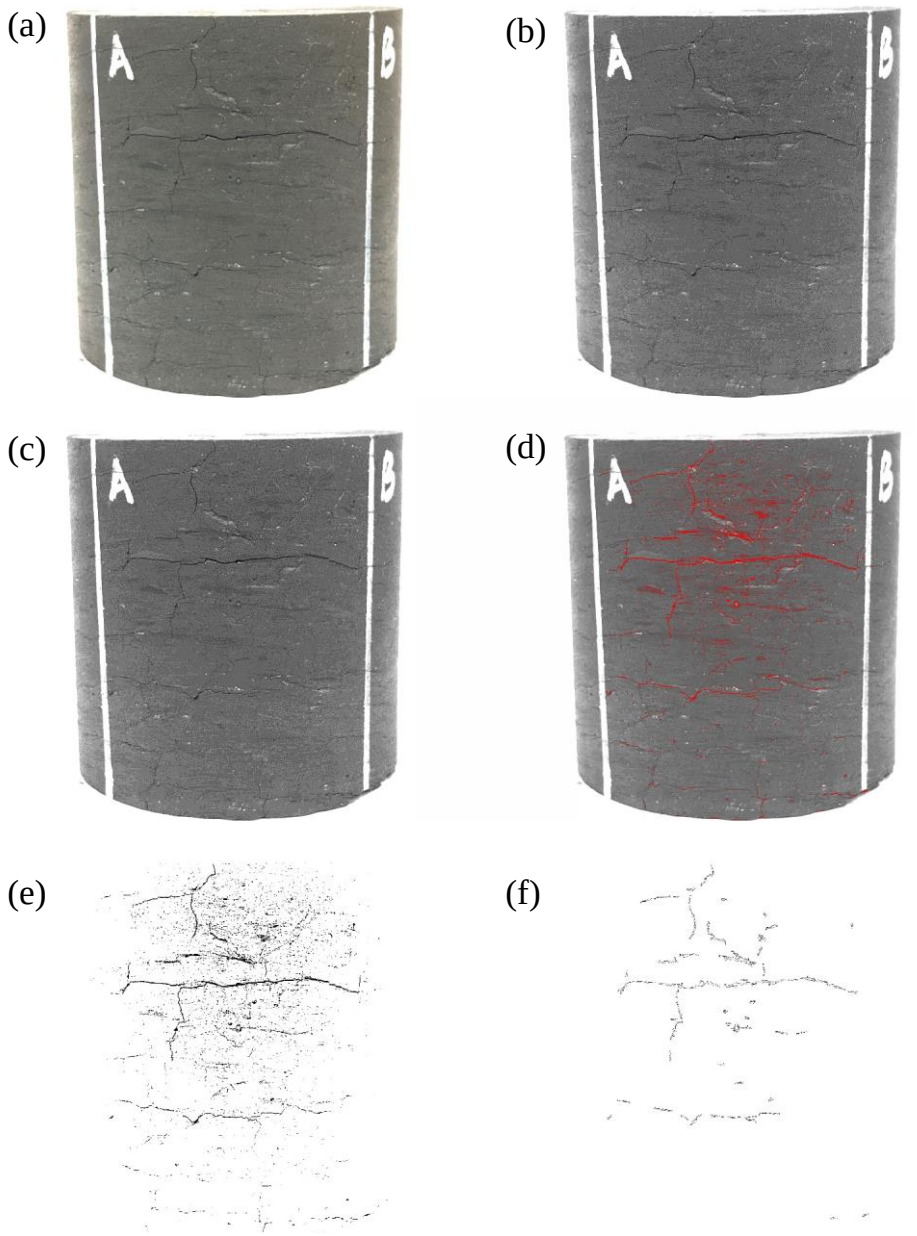

Figure 53. Image processing procedure of NO.1 coal core (a) original image (b) 8-bit image (c) sharpened image (d) selected fissures (e) extracted fissures (f) outline of filtered fissures

7.4 Results and Discussions

5 coal cores with saturation of 0% (Sample 1), 25% (Sample 2), 50% (Sample 3), 75% (Sample 4), 100% (Sample 5) were treated with 2 kW microwave for 6 mins. High resolution images were taken before and after MI, which were processed following the procedure mentioned in section 7.3.3. The extracted fissures are shown in Figure 55. The texture directions of sample 1 and 2 are horizontal and vertical, respectively. As shown in Figure 54 (a, b, c, d), most of the expansion

happens at the fissures that extend along the texture direction. For sample 1, the main horizontal fissure at upper part expands significantly, while some vertical fissures disappear after MI. For sample 2, some of the horizontal fissures in the central part become less evident, while most of the vertical fissures have a certain expansion after MI. It is worth to notice that there are new fractures formed at the right bottom of the sample, which do not follow the pre-exist fissure direction. As depicted in Figure 54 (e, f, g, h), no obvious fissure expansion can be observed for the coal sample with 50% and 75% saturation.

In order to quantify the microwave fracturing effect, the fissures with area larger than 0.1 mm^2 in Figure 55 have been selected, whose number, total area and averaged area were calculated and depicted in Table 19 and Figure 55.

As shown in Figure 55, the total area before MI shows an overall decreasing trend with the increase of water saturation. For the coal sample with 100% saturation, the surface fissures can be hardly observed. It can be concluded that the moisture content blocks the fissures and makes it less evident. Therefore, the fissure expansion under MI was contributed by both the moisture removal and thermal expansion of the coal body. It was calculated that the weight loss of sample 4 (75%) and 5 (100%) are 4.01g and 5.71g, and their saturation after MI are 28. 03% and 36. 98%, respectively. Considering the total fissure area of sample 4 and 5 after MI is 15.63 and 10.15, respectively, which is close to that of the sample 2 before MI, it can be concluded that the moisture removal contributes to the most part of the fissure expansion under MI for the coal sample with large saturation.

Beyond that, the coal sample with 25% water saturation has the largest total area difference before and after MI, followed by 0%, 100%, 75% and 50%. Moisture and minerals have much higher dielectric constant comparing to that of coal matrix, which means the moisture within coal body absorbs most of the microwave energy [42, 43]. Therefore, when coal sample is saturated with water, the coal sample will be uniformed heated under MI, during which the evaporation of moisture takes lots of energy away from coal sample. On the contrary, 25% moisture content means the moisture is distributed unevenly within the coal sample 2. The parts with moisture are selective heated under MI, and fissures are formed at the interface due to thermal expansion. As for the totally dried sample 1, its ability to absorb microwave energy

is much lower than the water saturated samples. However, even though the weight of sample 1 remains stabled in vacuum drying oven, the fact that the weight of sample 1 decreased 2.92 g after MI suggests microwave is particularly effective in drying and there is still bound water within the vacuum dried samples. Therefore, the bound water and minerals ensure effective microwave fracturing for dried coal samples, which leads to increase of 11. 09 mm^2 in fissure area.

According to the experiment results, the microwave fracturing can be divided into three stages for fully saturated coal: In the first stage, the coal that immersed in water is uniformed heated. Water absorbs microwave energy and evaporate, during which the water that blocks the fissure is removed from coal. Microwave's effect is mainly reflected on the water removal, whose fracturing effect is very limited in this stage. In the second stage, there is some water left in coal. Due to selective heating, the coal is ununiformed heated, which results in ununiformed thermal expansion and thus leads to the expansion of original fissures and formation of new fissures. Microwave fracturing has the best performance in this stage. In the last stage, there is little water left in coal. The coal's ability of absorbing microwave power is limited as it only depends on the small part of minerals within coal body. Therefore, even though the coal is heated ununiformed, the microwave fracturing effect is restricted in this stage.

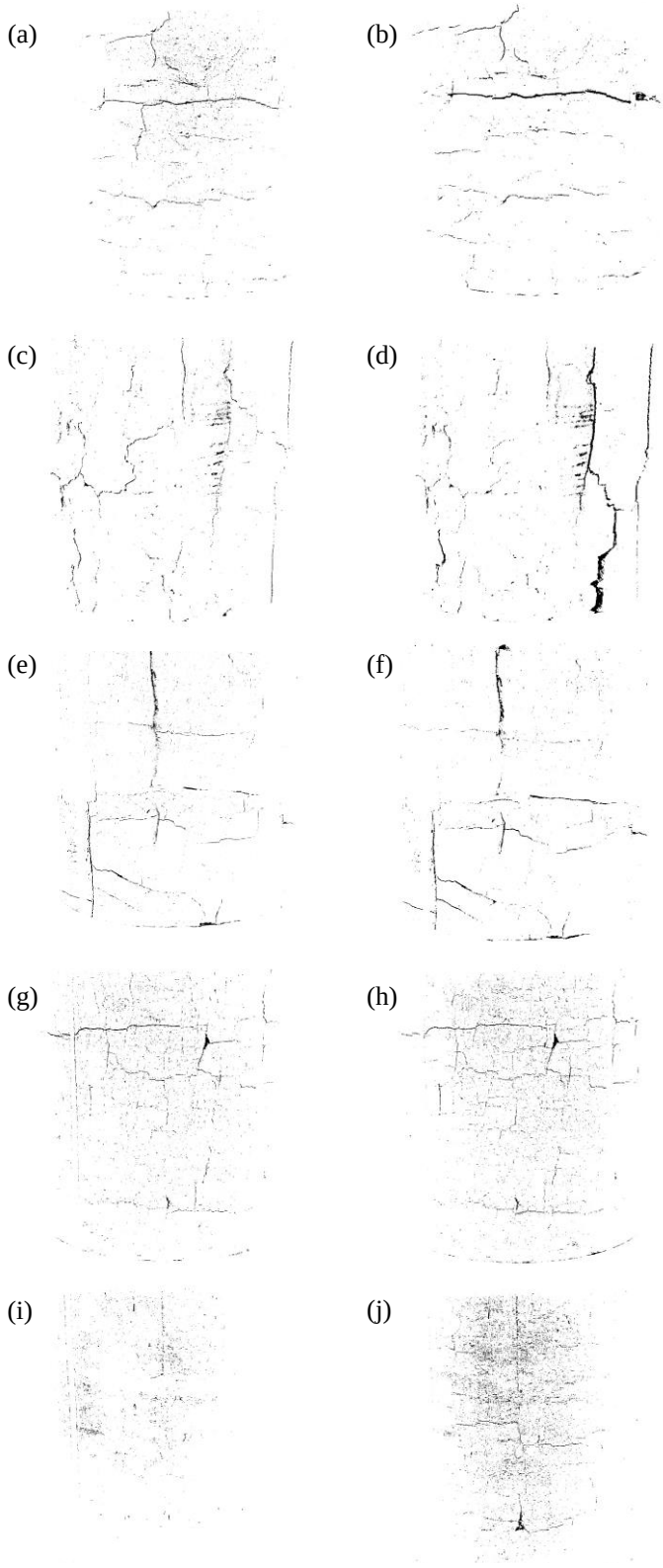

Figure 54. Extracted fissures of coal cores before (a, c, e, g, i) and after (b, d, f, h, j) MI under saturation of 0% (a, b), 25% (c, d), 50% (e, f), 75% (g, h), 100% (i, j)

Table 19. Parameter of coal cores before and after MI

Sample No.	Water saturation (%)	Dry weight (g)	Before MI			After MI		
			Fissure number	Average size (mm^2)	Weight (g)	Fissure number	Average size (mm^2)	Weight (g)
1	0	109. 73	59	0. 315	109. 73	56	0. 530	106. 81
2	25	114. 89	63	0. 219	116. 26	62	0. 731	110. 20
3	50	124. 40	37	0. 364	128. 35	43	0. 438	120. 58
4	75	128. 50	23	0. 361	135. 21	52	0. 301	131. 20
5	100	131. 35	7	0. 137	140. 41	56	0. 181	134. 70

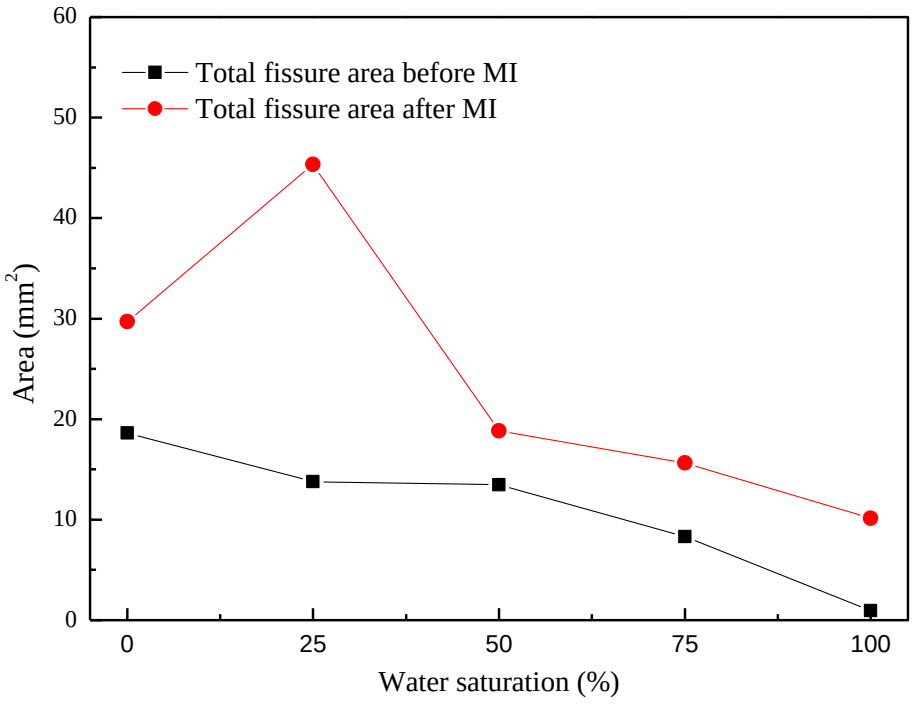

Figure 55. Total fissure area before and after MI under various saturation conditions

7.5 Conclusions

Diluting coalbed methane is one of the main goals for mine ventilation. To effectively extract the coalbed methane, microwave fracturing was proposed to enhance the coal seam permeability. Previous studies have investigated the effect of microwave power and irradiation time on the fracturing effect, while moisture's effect is still not clear. To investigate the effect of saturation of coal on microwave fracturing effect, image processing have been applied to coal samples with different water saturations before and after MI. The total fissure areas before MI show a decreasing trend with the increase of water saturation, which suggest that the moisture content blocks the fissures and makes it less evident. It was also found the coal sample with 25% water saturation has the largest total area difference after MI, followed by 0%, 100%, 75% and 50%. It can be concluded that for the coal sample with high water saturation, microwave's effect is mainly reflected on the water removal, whose fracturing effect is very limited. On the contrary, the coal sample with low water saturation has the best microwave fracturing performance. Due to selective heating, the coal is ununiformed heated, which results in an ununiformed thermal expansion and thus lead to the expansion of original fissures and formation of new fissures.

8 Chapter 8

Effective microwave heating of coal with various properties for thermally enhanced gas recovery

This chapter is under reviewed by Fuel. It was written by Jinxin Huang and revised by Prof Guang Xu and Prof Guozhong Hu. Mr Nan Yang and Mr Jieqi Zhu assisted in laboratory experiments.

Please cite this paper as:

Xu, G., Huang, J., Hu, G., Yang, N., & Zhu, J. (2019). Effective microwave heating of coal with various properties for thermally enhanced gas recovery. *Fuel*.

Chapter 8 focused on the influencing factors for effective microwave heating of coal. Infrared thermal images were taken for coal samples before and after MI to study the effect of dielectric property and saturation of coal samples, microwave power and irradiation time on microwave heating effects.

8.1 Abstract

Microwave heating is a promising technology in coal processing and coalbed methane enhancement. It is vital to investigate the influencing factors to ensure the optimal heating effect and the best energy efficiency. To address this, different types and saturation conditions of coal samples were treated with various microwave powers and irradiation times. Thermocouple and infrared thermal image system were used to measure the temperature of coal samples during and after microwave treatment. Through analysing the temperature, the effects of dielectric property and saturation conditions of coal, microwave power and treatment time on microwave heating were investigated. It was found the heating rate of coal samples increases with the loss factor at the initial heating period. The heating rate will then change as the composition changes under microwave irradiation. It was also found that coal samples with low saturation conditions have a much better microwave heating effects. This is because high moisture content not only impedes microwave heating but also facilitates uniformed heating,which impedes the formation of thermal fractures. Additionally, the experiment results suggest the average temperature increases with microwave power and irradiation time. However, when the microwave power increases to a certain extent, further increase of power is not as effective as extending the microwave irradiation time.

Keywords: microwave heating; coalbed methane recovery; dielectric property; saturation condition

8.2 Introduction

Coalbed methane (CBM) was recognized as a cheap and clean energy source in recent years. However, it may also result in major mine disasters such as gas explosion or gas outburst accidents [133, 156]. Therefore, CBM need to be pre-drained before mining activities to ensure the safety production of coal mines, as well as to increase the energy utilization efficiency [35, 115, 157].

Coalbed methane (CBM) has four occurrence states in coal seam: adsorbed within micropores, trapped in coal matrix, dissolved in moisture and as free gas in fractures [158]. The majority of CBM, which attached onto the micropore surface, exists in absorbed state [1]. Therefore, the main goal of increasing gas extraction rate is to facilitate gas desorption. As temperature is critical to the gas adsorption and desorption in coal seam, experiments has been conducted to study the effect of temperature on gas adsorption and desorption [159]. It was found the methane adsorption capacity decreases by 0.12 m^3/ton every 1 ℃-increase within 20-65 ℃ at 5 Mpa [38]. As the gas desorption from coal is an endothermic process, high temperature promote the gas transits from adsorbed state into free state [159, 160]. Based on these experiment results, thermally enhanced gas recovery (TEGR) has been proposed to improve gas extraction efficiency [18]. Traditional TEGR includes using geothermal resources and heat injection. Through increasing the temperature of coal seam with various methods, more gas is desorbed and drained from coal seam under the same pressure. Meanwhile, TEGR of coal lead to the evaporation of volatile matter, the pore volume and permeability increases consequently [161]. TEGR does not require the use of water, thus reducing the water usage and the possibility of ground water contamination. However, geothermal resources are not easily accessible and heat injection has low power conversion efficiency and high cost. More importantly, heat is hard to apply to the deeper coal seams for these methods. To address this, microwave heating, a noncontact fracturing method, is proposed as an ideal TEGR technology. It is not only economical as it is easy to generate without transportation and storage cost, but also applicable to various geographic conditions [148].

The mechanism of microwave fracturing mainly includes: selective heating, moisture removal and steam flow. As we know, the microwave energy absorption ability is determined by the material's dielectric property. Comparing to the carbonaceous matter with negligible dielectric loss factor, moisture and minerals within the coal body are the two major content that absorb the microwave energy [55, 140]. Due to such a selective heating effect, the temperature distribution of coal is non-uniform and thermal fractures are thus formed after microwave irradiation [140, 141]. Meanwhile, heating causes moisture evaporation, which not only frees the dissolved gas in it, but also increase the void volume in the coal [162]. Because of these characteristic, microwave has been widely applied in coal processing, including drying [23, 163], coking [24], pyrolysis [27, 28, 164], flotation [26], increasing grindability [29, 141], and sulphur removal [165].

It was reported the microwave heating behaviour is highly sensitive to the dielectric property [166], saturation of samples [32], microwave power [167] and treatment time [168]. Numerical simulations have been conducted to simulate the effect of these factors on microwave heating [35, 80, 81, 169]. However, almost all the previous experiments focused on microwave's effect on coal physical and petrographic characteristics instead of the microwave heating effect [40, 59, 62, 112, 170]. Moreover, few experiments were conducted to verify these simulation results. As heating effect is one of the most important indicators in microwave processing and fracturing, investigation of the influence factors is vital to the industrial microwave application to enhance coalbed permeability on-site.

To fill the research gap, experiments were carried out to study the influence factors for effective microwave heating, including dielectric property and saturation of coal samples, microwave power and irradiation time. Firstly, three different coal samples (SX, CQ, AH) were treated under the same microwave condition, whose temperatures were recorded over time. Combining with the proximate analysis and complex permittivity measurement of these samples, the effect of dielectric property on microwave heating effect was discussed in detail. Then, coal samples with various saturations were treated under different microwave conditions. After that, infrared thermal image system was used to measure the surface temperature of coal samples after microwave irradiation (MI). Finally, the effect of microwave power, MI time and saturation condition of coal samples were discussed in detail through analysing the average and standard deviation of surface temperature. This paper provided detailed experiment data concerning coal permittivity and temperature under MI, which can be helpful in verifying and calibrating numerical model in microwave heating. The work is also instructive in optimizing microwave parameter for microwave assisted coalbed methane enhancement and industrial coal processing.

8.3 Experimental

8.3.1 Sample Preparation

8.3.1.1 Coal Powders

The experimental samples were taken from Shanxi, Chongqing and Anhui province. They were crushed, pulverized and screened after taking to the ground. Pulverized coal with particle size between 0.154 and 0.180 mm were selected for experiment. The proximate analysis of these coal samples are shown in Tab.1.

Table 20. Proximate analysis of coal samples

Coal samples	Proximate analysis (%)			
	M_{ad}	A_d	V_{daf}	FC_d
Shanxi (SX)	8.70	6.73	35.79	59.89
Chongqing (CQ)	1.16	12.79	20.32	69.49
Anhui (AH)	0.80	10.83	36.94	56.23

where M_{ad} is moisture content, A_d is ash content, V_{daf}, is volatile matter, FC_d, is fixed carbon content.

8.3.1.2 Coal briquette specimens

In order to measure the dielectric property of coal samples with vector network analyser, coal powders have to be processed into hollow cylinder. The mould used in this study is shown in Figure 56. The pressing of coal particles forms voids within the small coal briquette specimens, which is filled with air and can lead to large measurement error. In order to fill the gaps between coal particles, coal samples were mixed with dissolved paraffin at a volume ratio of 4:3 and compressed into a toroidal shape with length of 7 ± 0.2 mm, 3.04 mm inner diameter and 2.0 mm thickness [171]. Two such coal briquette specimens were made for each coal type for repetitive measurement.

Figure 56. Mold for small coal briquette specimens

8.3.1.3 Coal cores

Coal samples taken from Shanxi province mentioned in 2.1.1 were drilled into large coal cores with 50 mm diameter and 50 mm height. These coal cores were then processed to water saturation of 0%, 25%, 50%, 75% and 100% for experiments.

8.3.2 Experimental Procedure

The experiment procedure is shown in Figure 57. To study the dielectric properties' effect on microwave heating, 18 g pulverized coal powder from various sampling spots was put into the same beaker and treated with microwave power of 2.0 kW for 4 minutes. The coal samples were pressed to make sure the top surface is horizontal and smooth. The thermocouple embedded in microwave oven was used to record the temperature at the bottom centre of coal samples. These pulverized coal sample were also processed into small briquette specimens (as mentioned in section 2.1.2), whose complex permittivity were then measured with Agilent E5071C vector network analyser.

In order to investigate the correlationship between microwave time and temperature of coal body, a large coal core SX-0 was repeatedly treated with microwave for a certain time (see Table 21). During the interval, this sample was taken out of the microwave oven for infrared thermal images and was put back to the microwave oven immediately. As shown in Figure 58, this coal core was deliberately break into two pieces before MI to measure the temperature of the section. The fracture face of two pieces totally match with each other and thus the separation has little influence on the coal structure as a whole.

To investigate the microwave heating effect under various microwave powers and saturation conditions, 8 coal cores (from SX-1 to SX-8) were treated with various microwave power and other 5 coal cores (from SX-9 to SX-13) were processed to the same saturation before microwave treatment, as shown in Table 21. The surface temperature of these samples were measured with infrared thermography and the averaged surface temperature were calculated using IRS RDIRs analytic software.

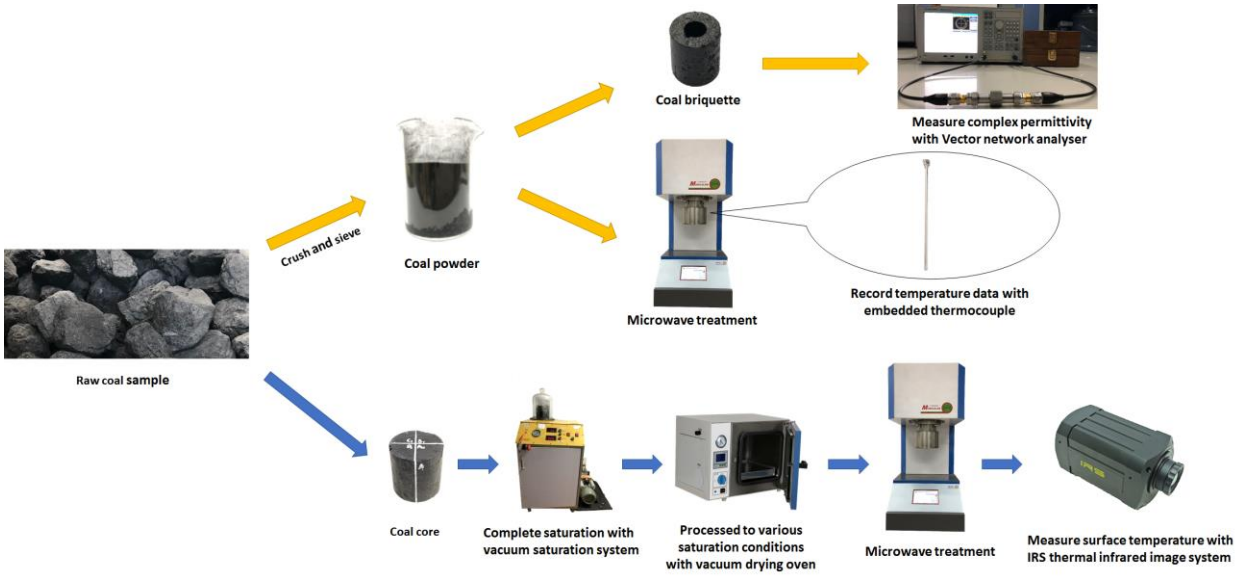

Figure 57. Experimental procedure

Table 21. Experiment conditions for coal cores

Sample No.	Water saturation (%)	Microwave power (W)	Irradiation time (mins)
SX-0	50	2000	1, 2.5, 4.5, 6.5, 8.5, 10.5
SX-1	50	800	5
SX-2	50	800	5
SX-3	50	1200	5
SX-4	50	1200	5
SX-5	50	1600	5
SX-6	50	1600	5
SX-7	50	2000	5
SX-8	50	2000	5
SX-9	0	2000	6
SX-10	25	2000	6
SX-11	50	2000	6
SX-12	75	2000	6
SX-13	100	2000	6

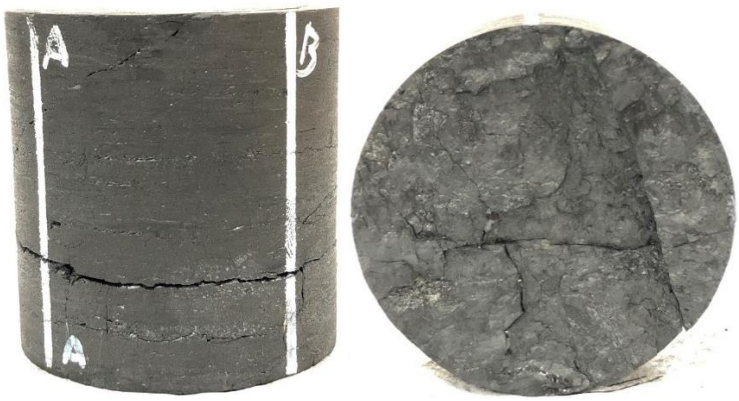

Figure 58. Surface and section image of SX-0

8.3.3 Complex Permittivity Measurement

The complex permittivity of coal samples are measured with an Agilent E5071C vector network analyser. First of all, the test system was set up by connecting the vector network analyser, coaxial cable, the connection part and a coaxial air line, as shown in Figure 59. Secondly, the test software was started and parameters were set, including frequency range, size of coaxial air line and size of sample to be tested. Then, the test system was calibrated with the Agilent 85031B calibration kit. Finally, the complex permittivity of prepared coal briquette specimens (ε) was measured, whose results were saved and exported.

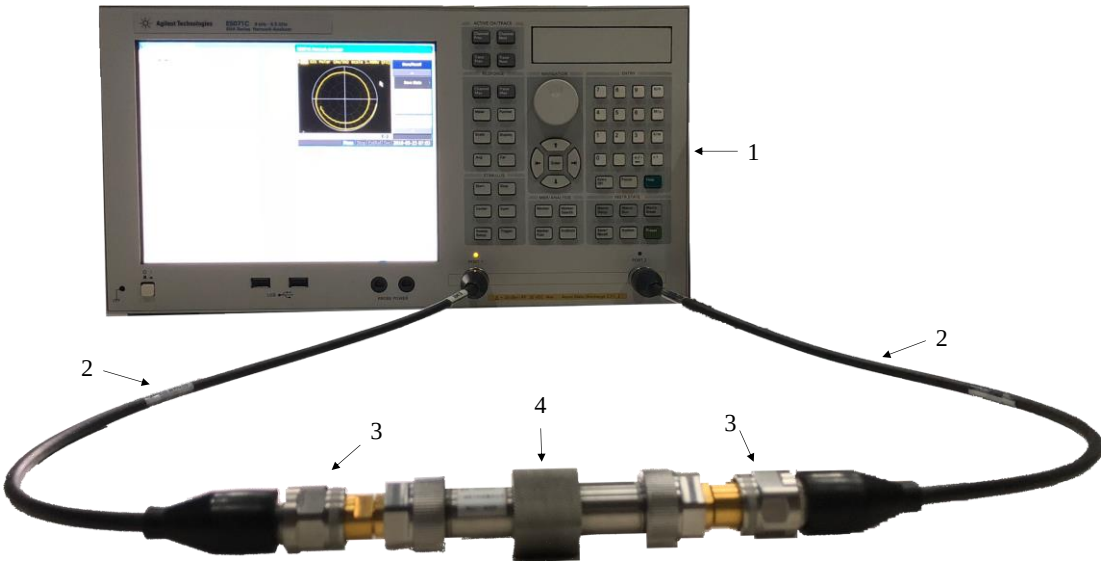

Figure 59. Agilent E5071C vector network analyzer assembly. 1. Vector network analyser, 2. Coaxial cable, 3. Transition joint, 4. Coaxial air line.

The small coal briquettes are assumed to be uniformly mixed with coal and paraffin, and the mixed dielectric is assumed to be isotropic, symmetric and

homogeneous [172]. According to Logarithm principle of Lichtenecker, complex permittivity of the mixed sample ε^* can be expressed as [173]:

$$\ln\varepsilon^* = v_c \ln\varepsilon_c^* + v_p \ln\varepsilon_p^* \quad (34)$$

where ε_c^* and ε_p^* refer to the complex permittivity of coal and paraffin respectively, v_c and v_p refer to the volume fraction of the coal and paraffin respectively, in this case $v_c = {}^4/_7$ and $v_p = {}^3/_7$.

The complex permittivity ε^* is given as:

$$\varepsilon^* = \varepsilon' - i\varepsilon'' \quad (35)$$

where ε' is real permittivity representing the capacity to store electromagnetic energy, and ε'' is imaginary permittivity reflecting the dissipation of stored energy into heat [32].

8.3.4 Microwave Irradiation

The microwave oven used in this study consists of a microwave transmitter, a wave guide, a thermocouple, cooling system and a control panel. Its microwave power is continuously adjustable ranging from 0 to 2.0 kW and its microwave frequency is 2450 MHz. The temperature of the object that contact with the thermocouple inside the oven was recorded, which can be monitored and exported through the control panel.

8.3.5 Thermal Infrared Imagery (TII)

The surface temperature of the coal cores was measured with an IRS-S65 infrared thermal image system. These infrared thermal images were then processed with the IRS RDIRs analytic software. As shown in Figure 60 (a), a rectangular box was drawn around the boundary of the coal sample. The temperature distribution matrix with 280 rows and 246 columns was then obtained based on the data within the rectangular box. The same procedure was repeated for the back side and the section of the coal sample (Figure 60 (b)).

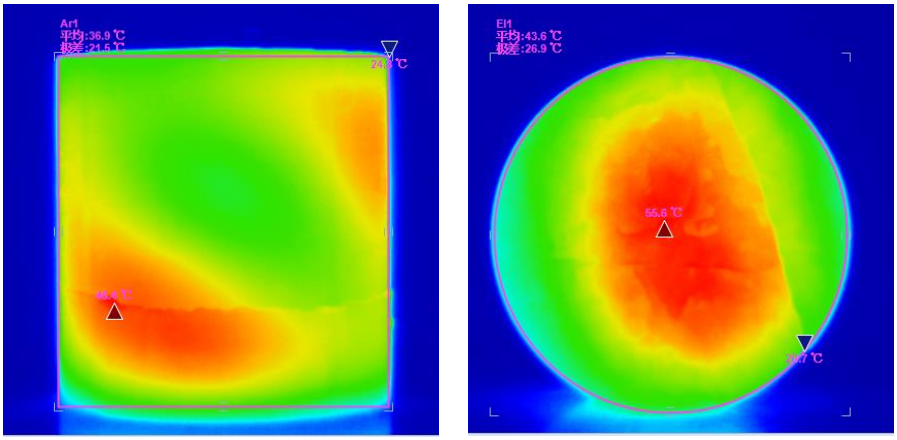

Figure 60. Infrared thermal images of the surface (a) and section (b) of SX-0

8.4 Results and Discussions

8.4.1 Effect of Dielectric Properties

The measurement results of coal permittivity were displayed in Figure 61. It is obvious that the results of specimens from the same sampling spot are very close to each other, which prove the results to be accurate. The complex permittivity at 2450 MHz is recorded, and the corresponding permittivity (ε_c' and ε_c'') are then calculated with Equation (34), as shown in Table 22.

Table 22. Complex permittivity of samples

	ε'	ε''	ε_c'	ε_c''
SX I	3.7657	0.1907	5.604704	0.963378
SX II	3.7520	0.1967	5.569069	1.017046
CQ I	3.2094	0.0827	4.237058	0.223263
CQ II	3.2534	0.0817	4.339236	0.21856
AH I	3.0404	0.0541	3.854353	0.106238
AH II	3.0163	0.0503	3.801046	0.093525

The temperature variation of three samples under MI were recorded and depicted in Figure 62. It was found the microwave heating rate at the beginning is

closely correlated with the dielectric property of coal sample. The coal sample with larger loss factor has a much higher heating rate.

Although the heating rate of all the samples showed a decreasing trend over time, the temperature variation of different coal samples differs a lot. For instance, the temperature variation of SX can be divided into two stages. In the first stage, the temperature quickly increased to 340 ℃ in 100 s. Then, it almost remained the same in the next 140 s, during which yellow smoke with pungent smell was observed. On the contrary, there is no such limit for CQ. Although CQ's heating rate is less than SX at the beginning, its temperature surpasses that of SX after 189 s and still keep increasing after 4 minutes.

The difference in the temperature variation pattern between various samples is resulted by their compositions. As carbonaceous matter can hardly absorb microwave energy, most of the microwave energy is absorbed by the moisture and minerals within the coal body. Under microwave irradiation, the physical and chemical reactions including moisture evaporation and pyrolysis change the compositions significantly. The complex permittivity of coal sample, which determines the ability to absorb microwave power, changes correspondently under microwave irradiation. Beyond that, most of these physical and chemical reactions are endothermic and their reaction rates increase with temperature, which makes the heating rate decrease over time. The proximate analysis shows that SX's M_{ad} is as much as 8.7%, followed by CQ (1.16%) and AH (0.8%). High moisture content contributes to the large loss factor of SX, which lead to its high heating rate at the beginning. However, as the moisture evaporates during MI, the heating rate drop sharply and reduce to near zero after 2 minutes. As for CQ, minerals within A_d (12.79%) contribute to a great part of the complex permittivity except for the M_{ad} (1.16%). Thus, moisture evaporation doesn't have much influence on the heating rate of CQ. In conclusion, moisture and mineral content determine the loss factor and the microwave heating rate. The heating rate will drop sharply for the sample with large saturation as the moisture evaporates during microwave heating.

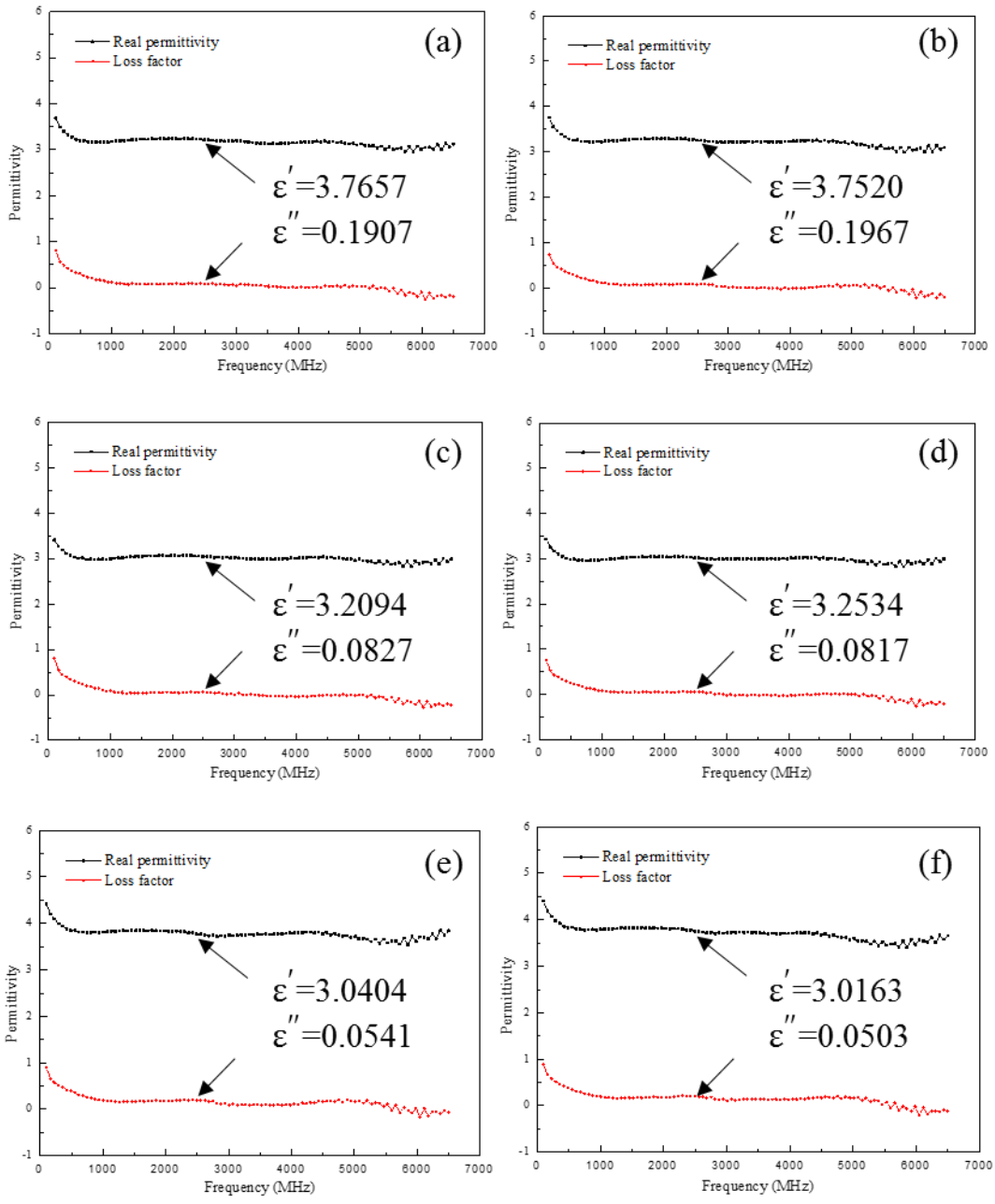

Figure 61. Permittivity of SX (a, b), CQ (c, d) and AH (e, f)

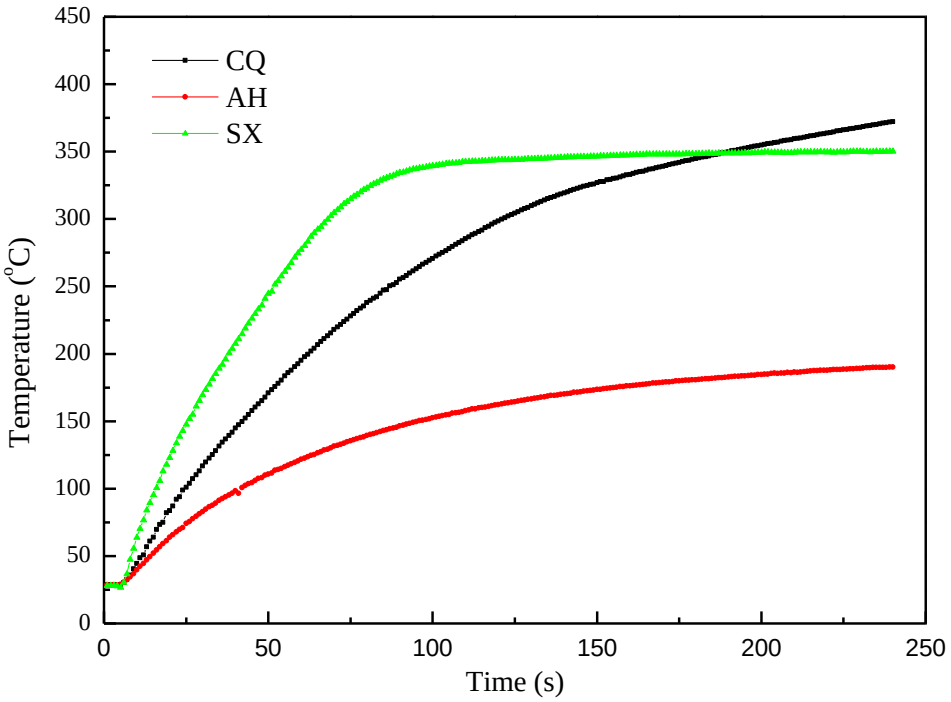

Figure 62. Temperature of various coal samples over time under 2 kW MI

8.4.2 Effect of Treatment Time

The infrared thermal images of the front side (in Figure 63) and the section (in Figure 64) were taken for SX-0 repeatedly after MI. It was found that thermal field distribution changes significantly over time. The hot spot lies at the left bottom of the coal sample at first and the temperature gradually becomes evenly distributed after 4.5 minutes. Finally, the hot spot appears around the fracture at the centre bottom of the coal sample after 8.5 minutes.

Based on these infrared thermal images, the average temperature of the whole surface and the section were calculated and displayed in Figure 65. It is obvious that the section temperature is much higher than the surface temperature after the same MI time. This is because microwave oven is a small closed cavity, where microwave bounces and emerges at the centre. And the centre part of the coal sample thus has much larger electric intensity, which consequently results in higher temperature comparing to the surface. However, when applying microwave on-sited, the microwave attenuates as it penetrating the coal seam. Thus, the electric field intensity as well as microwave heating effect decrease with the distance to the microwave port. Beyond that, it was found the average temperature increases almost linearly with time. The linear fitting equation of surface temperature and section

temperature over time are $y = 7.326x + 32.95$ and $y = 8.543x + 39.80$ respectively.

As the mass of load is more than 10 times of the SX coal sample in Section 3.1, the rising rate of temperature is much smaller consequently. It can be speculated that the temperature variation of SX-0 also has two stages. Because of the large load mass, the temperature variation still remains in the first stage after 10.5 minutes microwave irradiation. And the rising rate of temperature should slow down at a certain point and remained stable as time goes on.

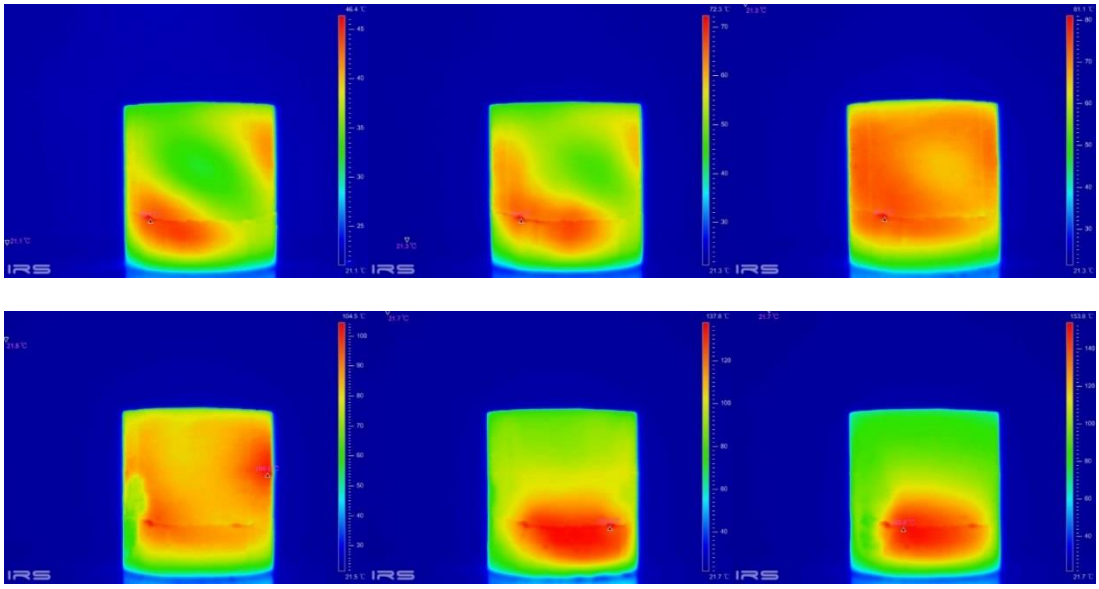

Figure 63. Infrared thermal images of the front side at (a) 1 min, (b) 2.5 mins, (c) 4.5 mins, (d) 6.5 mins, (e) 8.5 mins, (f) 10.5 mins

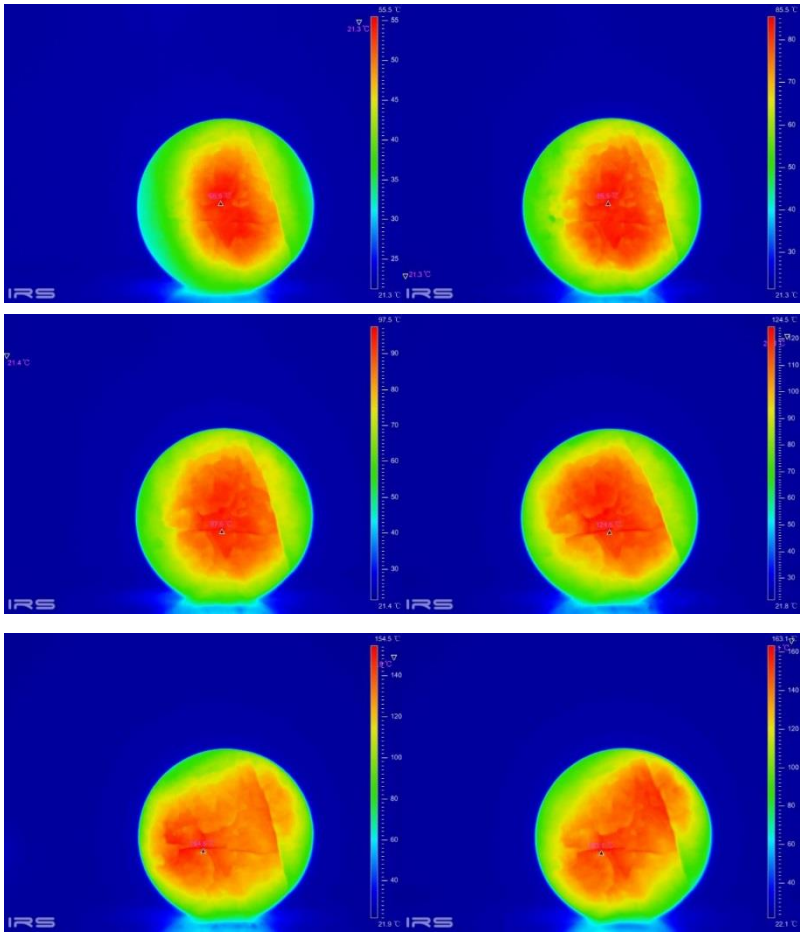

Figure 64. Infrared thermal images of the section at (a) 1 min, (b) 2.5 mins, (c) 4.5 mins, (d) 6.5 mins, (e) 8.5 mins, (f) 10.5 mins

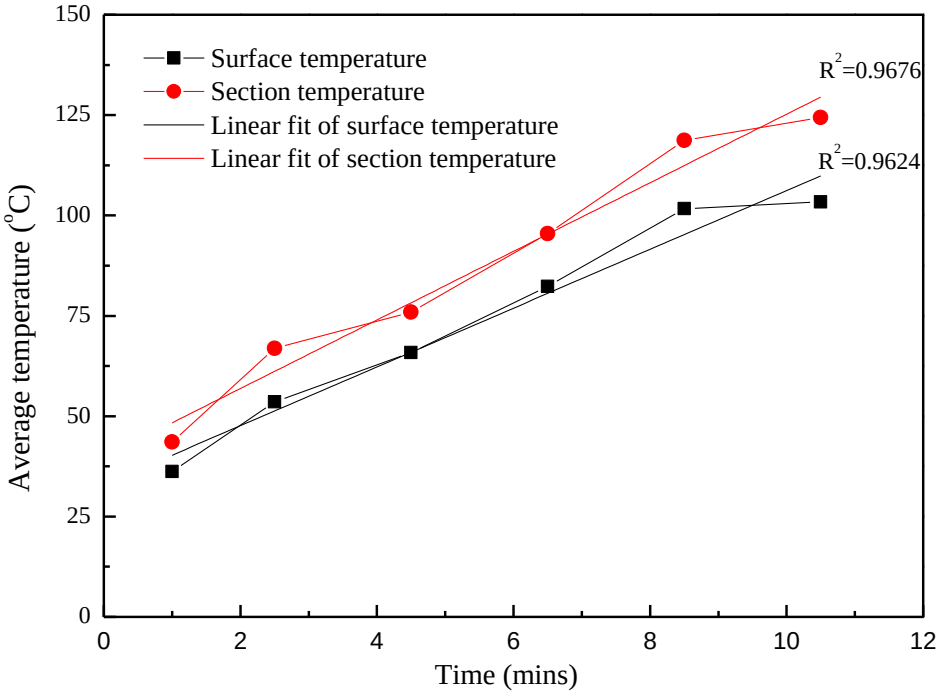

Figure 65. Average temperature of coal samples over time under 2 kW MI

8.4.3 Effect of Microwave Power

The average temperature and standard deviation of temperature of coal cores (SX-1 to SX-8) after MI are displayed in Figure 67. As shown inFigure 67, the temperature of samples treated with 800W microwave power (SX-1 and SX-2) increases to 51.8℃ after 5 minutes of microwave irradiation. All the other coal samples (SX-3 to SX-8) have a much larger temperature after the same period of MH. However, although the average temperature increases with microwave power, the temperature increase is very limited (from 77.6 to 82.8℃) when the power increases from 1200W to 2000W. It can be speculated from the temperature trend that further increase of power will have even less influence on the average temperature. The small difference between samples treated under the same experiment condition also suggests the results are reliable. It can be concluded that low power microwave has little heating effect and is thus not suitable for microwave heating. However, when the microwave power increase to a certain extent, further increase of power is not as effective as extending the MI time.

Furthermore, the standard deviation of temperature should also be considered in microwave heating. Larger standard deviation of temperature means the coal sample is more unevenly heated, and thus has better microwave fracturing effect. As shown Figure 66, the average standard deviation of temperature increases with microwave power, which is in accordance with the simulation results [35]. However, microwave power's effect on standard deviation of temperature is insignificant, with less than 0.005 ℃/K incease in the standard deviation of temperature.

In conclusion, choosing an appropriate microwave power is of great importance for microwave heating. The laboratory experiments show that microwave power of 1200 W and 1600 W are much better than 800 W and 2000 W considering both the microwave heating effect and energy efficiency. However, it still requires further investigation to find an appropriate microwave power for field application.

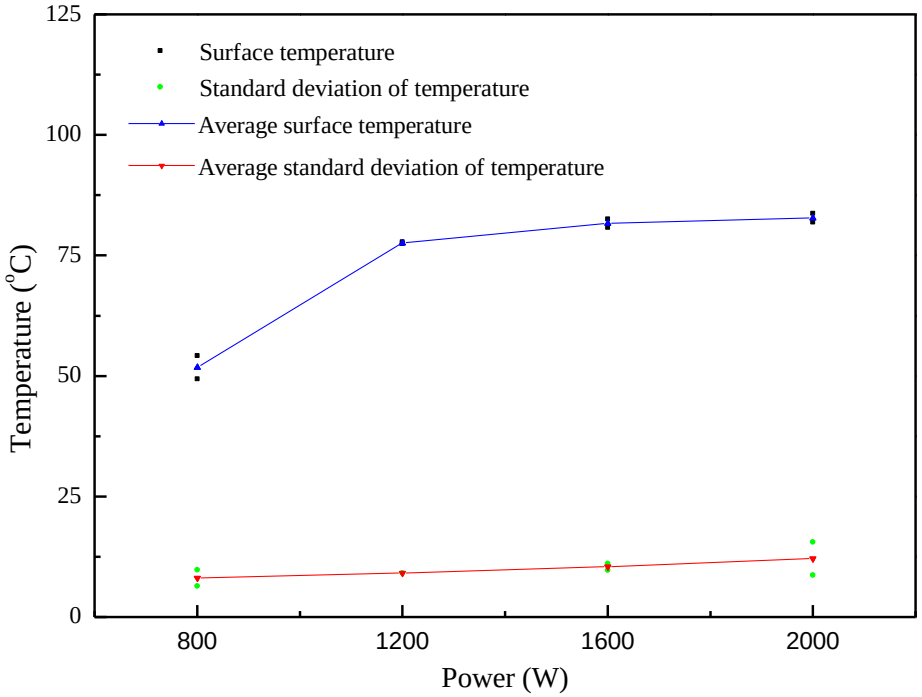

Figure 66. Average temperature and standard deviation of coal samples after 5 mins MI with various power

8.4.4 Effect of Moisture Content

The average temperature and standard deviation of temperature of coal cores (SX-9 to SX-13) after MI are displayed in Figure 67. It was found that the coal samples with low saturation have much better microwave heating effect. Therefore, the moisture within the coal body does more harm than good in microwave heating. As shown in Figure 67, for the samples with saturations less than 50%, their average temperatures exceed 100℃ after 6 minutes MI. As for the coal samples with high saturations (75% to 100%), the average temperature is around 75℃. As mentioned before, the coal matrix itself can hardly absorb microwave energy, while most of the microwave energy is absorbed by the moisture and minerals within the coal body. However, the experiment results show that the temperature of coal sample with 0% saturation is only slightly less than that with 25% saturation, while much larger than the rest samples. It suggests that the minerals and bound water within the dried sample have strong capacity in absorbing microwave energy. It also can be concluded that even though the moisture content contributes in absorbing more microwave energy for coal body, this benefit is compromised by the energy waste in heating and evaporation of water for the samples with high saturation conditions.

Beyond that, the standard deviations of temperature suggest moisture content facilitates the uniform heating of coal sample. For the coal samples with high saturation, most of the coal is saturated with water. The thermal field of coal sample thus distributed relatively evenly as moisture absorbs most of the microwave energy. With the decrease of saturation, the moisture within the coal body becomes more and more unevenly distributed, which further leads to the uneven thermal field distribution. When the saturation drops to 0, the standard deviation of temperature peaks at 39.45℃, as much as 5.4 times of that when fully saturated. As stated before, a larger temperature difference leads to better microwave fracturing effect. It can be concluded that microwave heating and fracturing are more effective for coal with low saturation conditions. This finding agrees well with the previous researches, which suggest microwave heating/fracturing effect increases with moisture content at low saturation conditions and then decrease sharply with further increase of saturations [32, 35, 56].

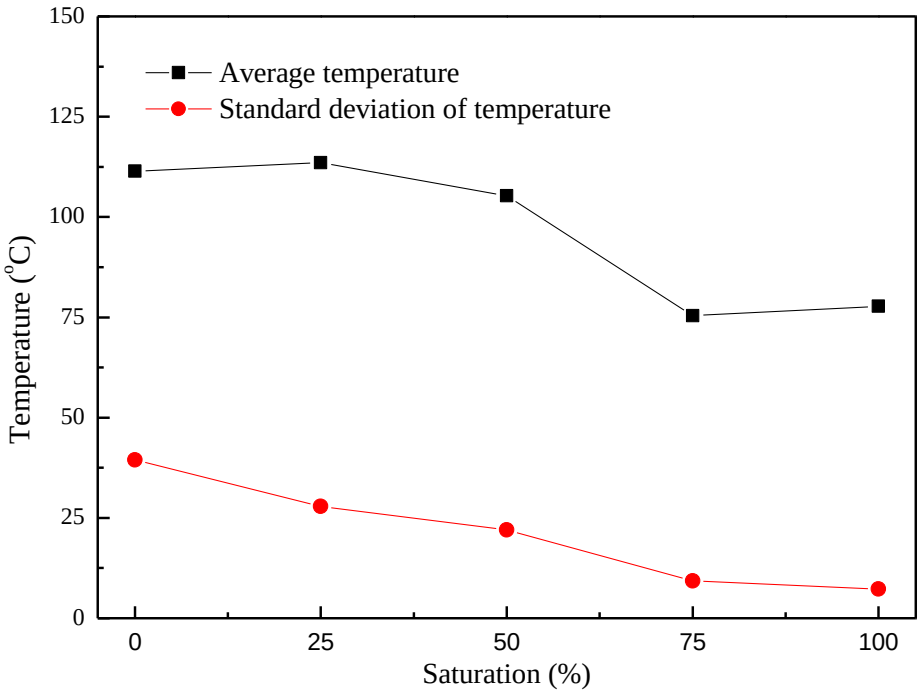

Figure 67. Average temperature and standard deviation of coal samples with various saturation under 2000 W MI for 6 mins

8.5 Conclusions

In this study, the influencing factors for microwave heating, including dielectric property and saturation condition of coal samples, microwave power and

treatment time were studied in detail. It was found the microwave heating rate increases initially with the increase of coal sample's original loss factor. During microwave irradiation, the composition changes lead to the change of loss factor, which reduces the heating rate to various degrees. It was also found the moisture within coal reduces microwave heating efficiency. High water saturations lead to uniformed heating of coal, which seriously impedes the microwave fracturing effect. Moreover, the results show the average temperature increase with microwave power and irradiation time. However, when the microwave power increases to a certain extent, further increase of power is not as effective as extending the MI time. For field application, microwave fracturing is more suitable for the coal seams with low saturation and relative large loss factor. And extending irradiation time instead of increasing microwave power seems to be a better choice to achieve great microwave heating effect and high energy efficiency.

Most of the previous studies focused on the evolution of coal petrophysical properties under MI, while few experiments have been conducted to investigate microwave's heating effect on coal. The experiments in this paper filled the research gap in investigating the influencing factors for microwave heating of coal. The experiment results discussed the relation between coal permittivity and microwave heating effect in detail, which can be very useful in verifying and calibrating existed numerical models. Even though the findings are valuable in optimizing microwave parameters for coalbed permeability enhancement, further field experiments should be carried out before on-site applications.

9 Chapter 9

Conclusions and Future Works

9.1 Conclusions

This thesis consists of a literature review, three numerical simulations and three experimental studies in studying microwave irradiation's effect on coal petrophysical property. This thesis presents a comprehensive and in-depth study in microwave-assist coal seam enhancement and could be very helpful to the potential field applications.

Chapter 2 reviewed hundreds of literature in studying coal permeability enhancement using microwave heating/fracturing. The mechanism and advantages of microwave heating/fracturing were explained in detail. Both experimental studies and numerical simulation in studying MI's effect on coal were summarized and reviewed, following by the discussion about the influencing factors on microwave fracturing effects. Finally, the outstanding challenges for on-site application of microwave heating were presented, and the conceptual design of an on-site microwave heating system was proposed.

Chapter 3 established a coupled electromagnetic, heat and mass transfer model for microwave heating of coal. It was found microwave heating is extremely sensitive to microwave frequency, which has a great impact on the electric field and thermal distributions. It was also found larger microwave power increases the maximum temperature difference, which facilitates fissure development within coal samples. The simulation result suggested that moisture capacity has great influence on microwave heating. Under the microwave settings of 1 KW at 2.45 GHz, the best heating effect occurs for coal samples with 5% specific moisture capacity.

Chapter 4 and chapter 5 proposed a coupled electromagnetic, thermal and mechanical model in studying microwave's effect on coal permeability in laboratory scale and field scale. Both simulation results suggest microwave is effective in coal seam permeability enhancement.

Chapter 6 and chapter 7 are experimental studies in the variation of coal's petrophysical properties under MI. Both of these studies mainly focused on the moisture's effect on pore development of coal under MI. The experiment results suggest moisture content has both positive and negative effect on microwave fracturing. On the one hand, it increases coal's dielectric constant, which results in

better microwave heating effect. On the other hand, moisture blocks the passage for gas flow and therefore significantly decrease the gas permeability. Moreover, large moisture content results in uniform heating of coal, which mitigates the thermal stress and strain within the coal body. It can be concluded microwave has the best fracturing effect for coal with low water saturation.

Chapter 8 is an experimental study in the influencing factors for microwave heating effect of coal. Influencing factors including dielectric property and saturation condition of coals, microwave power and irradiation time were discussed in detail. It was found the microwave heating rate at the beginning is closely related to the coal's original loss factor. The heating rate of all the samples has certain decrease due to the mineral decomposition and water evaporation. The experiment results illustrate even though the average temperature increases with microwave power and treatment time, further increase of power is not as effective as extending the MI time when the microwave power increases to a certain extent.

9.2 Highlights of the studies

The researches in this thesis made great progress in both numerical simulations and experimental experiment in studying microwave irradiation's effect on coal petrophysical property. Key highlights are summarized as below:

- Studies related to microwave heating/fracturing of coal are carefully reviewed and summarized.
- A coupled electromagnetic, heat and mass transfer model for microwave heating of coal is established, which is the first proposed model that consider moisture vaporization in simulating microwave heating of coal.
- A coupled electric, heat transfer and mechanics model is established for both coal sample and coal reservoir. Microwave's heating effect and the accompanying thermal stress's effect on permeability are made clear.
- The influencing factors for microwave heating/fracturing of coal are made clear, including microwave power, irradiation time, dielectric property and saturation of coal. It is worth to mention that no previous study has investigated microwave heating of coal under both low and high saturation conditions before.
- Various experimental methods are adopted in this study, including NMR, SEM, MH, TII, dielectric constant measurement and image processing.

9.3 Limittions and Future Works

Even though this work has made a great contribution in both numerical and experimental studies of microwave-assist coal permeability enhancement, there are still some limitations to be solved by future works.

For instance, although chapter 3 firstly considered the effect of coal sample's moisture in microwave heating model, it was assumed the moisture conductivity and mass transfer coefficient remains constant during microwave heating. To better reflect actual situations and to improve the model accuracy, laboratory experiments need to be done to obtain the variation of moisture conductivity and mass transfer coefficient during MI. Beyond that, coal should be defined as initial non-homogeneity material to study the thermal stress and fissure development in coal samples under MI.

In chapter 5, a modified numerical model was proposed for microwave treatment of coalbed methane reservoir. Theoretically, this model is closer to reality comparing to previous reservoir models. However, it still requires to be verified by field data. The main research shortage in microwave-assisted coal seam enhancement is lack of field experiment. Currently, no field application is reported, and little on-site experiment data is available for reference. As encouraging laboratory experimental results cannot ensure good performance on-site, further experiments are still required to apply microwave heating on coal seam at the field scale. Numerical models for coal reservoirs need to be modified or verified based on the field test.

References

1. W. Gunter, et al., *Deep coalbed methane in Alberta, Canada: a fuel resource with the potential of zero greenhouse gas emissions.* Energy Conversion and Management, 1997. **38**: p. S217-S222.
2. C.M. White, et al., *Sequestration of carbon dioxide in coal with enhanced coalbed methane recovery a review.* Energy & Fuels, 2005. **19**(3): p. 659-724.
3. I. Gray, *Reservoir engineering in coal seams: Part 1-The physical process of gas storage and movement in coal seams.* SPE Reservoir Engineering, 1987. **2**(01): p. 28-34.
4. J. Xu, C. Zhai, and L. Qin, *Mechanism and application of pulse hydraulic fracturing in improving drainage of coalbed methane.* Journal of Natural Gas Science and Engineering, 2017. **40**: p. 79-90.
5. C. Shen, et al., *Induced drill-spray during hydraulic slotting of a coal seam and its influence on gas extraction.* International Journal of Mining Science and Technology, 2012. **22**(6): p. 785-791.
6. F. Yan, et al., *A novel ECBM extraction technology based on the integration of hydraulic slotting and hydraulic fracturing.* Journal of Natural Gas Science and Engineering, 2015. **22**: p. 571-579.
7. Y. Lei, et al., *Contrast test of different permeability improvement technologies for gas-rich low-permeability coal seams.* Journal of Natural Gas Science and Engineering, 2016. **33**: p. 1282-1290.
8. J. Sanchidrián, L. López, and P. Segarra, *The influence of some blasting techniques on the probability of ignition of firedamp by permissible explosives.* Journal of hazardous materials, 2008. **155**(3): p. 580-589.
9. C. Clark, et al., *Hydraulic fracturing and shale gas production: technology, impacts, and policy.* Argonne National Laboratory, 2012.
10. A. Busch and Y. Gensterblum, *CBM and CO2-ECBM related sorption processes in coal: a review.* International Journal of Coal Geology, 2011. **87**(2): p. 49-71.
11. A. Kronimus, et al., *A preliminary evaluation of the CO2 storage potential in unminable coal seams of the Münster Cretaceous Basin, Germany.* International Journal of Greenhouse Gas Control, 2008. **2**(3): p. 329-341.
12. A.M.M. Bustin, et al., *Learnings from a failed nitrogen enhanced coalbed methane pilot: Piceance Basin, Colorado.* International Journal of Coal Geology, 2016. **165**: p. 64-75.
13. C. Zhai, et al., *Pore structure in coal: pore evolution after cryogenic freezing with cyclic liquid nitrogen injection and its implication on coalbed methane extraction.* Energy & Fuels, 2016. **30**(7): p. 6009-6020.

14. J. Guo, et al., *Accelerating methane desorption in lump anthracite modified by electrochemical treatment.* International Journal of Coal Geology, 2014. **131**: p. 392-399.

15. Z. Tang, et al., *Changes to coal pores and fracture development by ultrasonic wave excitation using nuclear magnetic resonance.* Fuel, 2016. **186**: p. 571-578.

16. Y.D. Cai, et al., *Partial coal pyrolysis and its implication to enhance coalbed methane recovery, Part I: An experimental investigation.* Fuel, 2014. **132**: p. 12-19.

17. D. Ritter, et al., *Enhanced microbial coalbed methane generation: a review of research, commercial activity, and remaining challenges.* International Journal of Coal Geology, 2015. **146**: p. 28-41.

18. A. Salmachi and M. Haghighi, *Feasibility Study of Thermally Enhanced Gas Recovery of Coal Seam Gas Reservoirs Using Geothermal Resources.* Energy & Fuels, 2012. **26**(8): p. 5048-5059.

19. M. Maskan, *Microwave/air and microwave finish drying of banana.* Journal of food engineering, 2000. **44**(2): p. 71-78.

20. A. Tahmasebi, et al., *Experimental study on microwave drying of Chinese and Indonesian low-rank coals.* Fuel Processing Technology, 2011. **92**(10): p. 1821-1829.

21. T. Chen, et al., *The relative transparency of minerals to microwave radiation.* Canadian Metallurgical Quarterly, 1984. **23**(3): p. 349-351.

22. X. Cui and R.M. Bustin, *Volumetric strain associated with methane desorption and its impact on coalbed gas production from deep coal seams.* Aapg Bulletin, 2005. **89**(9): p. 1181-1202.

23. C. Pickles, F. Gao, and S. Kelebek, *Microwave drying of a low-rank sub-bituminous coal.* Minerals Engineering, 2014. **62**: p. 31-42.

24. E. Binner, et al., *Factors affecting the microwave coking of coals and the implications on microwave cavity design.* Fuel Processing Technology, 2014. **125**: p. 8-17.

25. E. Jorjani, et al., *Desulfurization of Tabas coal with microwave irradiation/peroxyacetic acid washing at 25, 55 and 85 C.* Fuel, 2004. **83**(7-8): p. 943-949.

26. W. Xia, J. Yang, and C. Liang, *Effect of microwave pretreatment on oxidized coal flotation.* Powder Technology, 2013. **233**: p. 186-189.

27. F. Mushtaq, R. Mat, and F.N. Ani, *Fuel production from microwave assisted pyrolysis of coal with carbon surfaces.* Energy Conversion and Management, 2016. **110**: p. 142-153.

28. F. Mushtaq, R. Mat, and F.N. Ani, *A review on microwave assisted pyrolysis of coal and biomass for fuel production.* Renewable and Sustainable Energy Reviews, 2014. **39**: p. 555-574.

29. E. Lester, S. Kingman, and C. Dodds, *Increased coal grindability as a result of microwave pretreatment at economic energy inputs.* Fuel, 2005. **84**(4): p. 423-427.

30. S. Marland, A. Merchant, and N. Rowson, *Dielectric properties of coal.* Fuel, 2001. **80**(13): p. 1839-1849.

31. T. Uslu and Ü. Atalay, *Microwave heating of coal for enhanced magnetic removal of pyrite.* Fuel Processing Technology, 2004. **85**(1): p. 21-29.

32. H. Li, et al., *Evolution of Coal Petrophysical Properties under Microwave Irradiation Stimulation for Different Water Saturation Conditions.* Energy & Fuels, 2017. **31**(9): p. 8852-8864.

33. S. Mutyala, et al., *Microwave applications to oil sands and petroleum: A review.* Fuel Processing Technology, 2010. **91**(2): p. 127-135.

34. R. Bhandavat, et al., *Synthesis of polymer-derived ceramic Si (B) CN-carbon nanotube composite by microwave-induced interfacial polarization.* ACS applied materials & interfaces, 2011. **4**(1): p. 11-16.

35. J. Huang, et al., *A coupled electromagnetic irradiation, heat and mass transfer model for microwave heating and its numerical simulation on coal.* Fuel Processing Technology, 2018. **177**: p. 237-245.

36. J. Pan, et al., *Coalbed methane sorption related to coal deformation structures at different temperatures and pressures.* Fuel, 2012. **102**: p. 760-765.

37. P.J. Crosdale, T.A. Moore, and T.E. Mares, *Influence of moisture content and temperature on methane adsorption isotherm analysis for coals from a low-rank, biogenically-sourced gas reservoir.* International Journal of Coal Geology, 2008. **76**(1-2): p. 166-174.

38. J.H. Levy, S.J. Day, and J.S. Killingley, *Methane capacities of Bowen Basin coals related to coal properties.* Fuel, 1997. **76**(9): p. 813-819.

39. L. Ge, et al., *Effects of microwave irradiation treatment on physicochemical characteristics of Chinese low-rank coals.* Energy conversion and management, 2013. **71**: p. 84-91.

40. H. Li, et al., *Experimental study on the petrophysical variation of different rank coals with microwave treatment.* International Journal of Coal Geology, 2016. **154**: p. 82-91.

41. J. Cheng, et al., *Improvement of coal water slurry property through coal physicochemical modifications by microwave irradiation and thermal heat.* Energy & Fuels, 2008. **22**(4): p. 2422-2428.

42. E. Lester and S. Kingman, *The effect of microwave pre-heating on five different coals.* Fuel, 2004. **83**(14-15): p. 1941-1947.

43. E. Lester and S. Kingman, *Effect of microwave heating on the physical and petrographic characteristics of a UK coal.* Energy & fuels, 2004. **18**(1): p. 140-147.

44. S. Marland, et al., *The effect of microwave radiation on coal grindability.* Fuel, 2000. **79**(11): p. 1283-1288.

45. S. Kingman, G. Corfield, and N. Rowson, *Effects of microwave radiation upon the mineralogy and magnetic processing of a massive Norwegian ilmenite ore.* Physical Separation in Science and Engineering, 1999. **9**(3): p. 131-148.

46. M.B. Chanaa, M. Lallemant, and A. Mokhlisse, *Pyrolysis of Timahdit, Morocco, oil shales under microwave field.* Fuel, 1994. **73**(10): p. 1643-1649.

47. H. Kumar, et al., *Inducing fractures and increasing cleat apertures in a bituminous coal under isotropic stress via application of microwave energy.* International Journal of Coal Geology, 2011. **88**(1): p. 75-82.

48. T.A. Moore, *Coalbed methane: a review.* International Journal of Coal Geology, 2012. **101**: p. 36-81.

49. Y. Yao, et al., *Assessing the Water Migration and Permeability of Large Intact Bituminous and Anthracite Coals Using NMR Relaxation Spectrometry.* Transport in Porous Media, 2015. **107**(2): p. 527-542.

50. Z. Pan, et al., *Effects of matrix moisture on gas diffusion and flow in coal.* Fuel, 2010. **89**(11): p. 3207-3217.

51. D. Chen, et al., *Modeling and simulation of moisture effect on gas storage and transport in coal seams.* Energy & Fuels, 2012. **26**(3): p. 1695-1706.

52. H. Wang, R. Rezaee, and A. Saeedi, *Preliminary study of improving reservoir quality of tight gas sands in the near wellbore region by microwave heating.* Journal of Natural Gas Science and Engineering, 2016. **32**: p. 395-406.

53. G. Li, Y. Meng, and H. Tang. *Clean up water blocking in gas reservoirs by microwave heating: laboratory studies*. in *International Oil & Gas Conference and Exhibition in China*. 2006. Society of Petroleum Engineers.

54. F. Vermeulen and B. McGee, *In-situ electromagnetic heating for hydrocarbon recovery and environmental remediation.* Journal of Canadian Petroleum Technology, 2000. **39**(08).

55. M.S. Seehra, A. Kalra, and A. Manivannan, *Dewatering of fine coal slurries by selective heating with microwaves.* Fuel, 2007. **86**(5): p. 829-834.

56. J. Huang, et al., *The development of microstructure of coal by microwave irradiation stimulation.* Journal of Natural Gas Science and Engineering, 2019. **66**: p. 86-95.

57. A. Bera and T. Babadagli, *Status of electromagnetic heating for enhanced heavy oil/bitumen recovery and future prospects: A review.* Applied Energy, 2015. **151**: p. 206-226.

58. A.K. Datta, *Handbook of microwave technology for food application*. 2001: CRC Press.

59. G. Hu, et al., *Experimental investigation on variation of physical properties of coal particles subjected to microwave irradiation.* Journal of Applied Geophysics, 2017. **150**: p. 118-125.

60. K.E. Haque, *Microwave energy for mineral treatment processes—a brief review.* International Journal of Mineral Processing, 1999. **57**(1): p. 1-24.

61. H. Wang, R. Rezaee, and A. Saeedi, *Evaporation Process and Pore Size Distribution in Tight Sandstones: A Study Using NMR and MICP.* Procedia Earth and Planetary Science, 2015. **15**: p. 767-773.

62. J.-Z. Liu, et al., *Pore structure and fractal analysis of Ximeng lignite under microwave irradiation.* Fuel, 2015. **146**: p. 41-50.

63. H. Xu, et al., *A precise measurement method for shale porosity with low-field nuclear magnetic resonance: A case study of the Carboniferous-Permian strata in the Linxing area, eastern Ordos Basin, China.* Fuel, 2015. **143**: p. 47-54.

64. V. Cnudde and M.N. Boone, *High-resolution X-ray computed tomography in geosciences: A review of the current technology and applications.* Earth-Science Reviews, 2013. **123**: p. 1-17.

65. C.Ö. Karacan and G.D. Mitchell, *Behavior and effect of different coal microlithotypes during gas transport for carbon dioxide sequestration into coal seams.* International Journal of Coal Geology, 2003. **53**(4): p. 201-217.

66. S. Mazumder, et al., *Application of X-ray computed tomography for analyzing cleat spacing and cleat aperture in coal samples.* International Journal of Coal Geology, 2006. **68**(3-4): p. 205-222.

67. H. Wang, et al., *Data-constrained modelling of an anthracite coal physical structure with multi-spectrum synchrotron X-ray CT.* Fuel, 2013. **106**: p. 219-225.

68. A. Ul-Hamid, *A Beginners' Guide to Scanning Electron Microscopy*. 2018: Springer.

69. F. Zhou, et al., *Upgrading Chinese Shengli lignite by microwave irradiation for slurribility improvement.* Fuel, 2015. **159**: p. 909-916.

70. B. Sahoo, S. De, and B. Meikap, *Improvement of grinding characteristics of Indian coal by microwave pre-treatment.* Fuel Processing Technology, 2011. **92**(10): p. 1920-1928.

71. F. Fu, L. Lin, and E. Xu, *Functional pretreatments of natural raw materials*, in *Advanced High Strength Natural Fibre Composites in Construction*. 2017, Elsevier. p. 87-114.

72. I. Chatterjee and M. Misra, *Dielectric properties of various ranks of coal and numerical modeling under electromagnetic irradiation.* MRS Online Proceedings Library Archive, 1990. **189**.

73. I. Chatterjee and M. Misra, *Electromagnetic and thermal modeling of microwave drying of fine coal.* Mining, Metallurgy & Exploration, 1991. **8**(2): p. 110-114.

74. J. Clemens and C. Saltiel, *Numerical modeling of materials processing in microwave furnaces.* International Journal of Heat and Mass Transfer, 1996. **39**(8): p. 1665-1675.

75. Z. Peng, et al., *Numerical analysis of heat transfer characteristics in microwave heating of magnetic dielectrics.* Metallurgical and Materials Transactions A, 2012. **43**(3): p. 1070-1078.

76. A.A. Salema and M.T. Afzal, *Numerical simulation of heating behaviour in biomass bed and pellets under multimode microwave system.* International Journal of Thermal Sciences, 2015. **91**: p. 12-24.

77. R.H. Vaz, et al., *Simulation and uncertainty quantification in high temperature microwave heating.* Applied Thermal Engineering, 2014. **70**(1): p. 1025-1039.

78. S. Gadkari, B. Fidalgo, and S. Gu, *Numerical investigation of microwave-assisted pyrolysis of lignin.* Fuel Processing Technology, 2017. **156**: p. 473-484.

79. N. Yoshikawa and Y. Tokuyama, *Numerical Simulation of Temperature Distribution in Multi-Phase Materials as a Result of Selective Heating by Microwave Energy.* Journal of Microwave Power and Electromagnetic Energy, 2008. **43**(1): p. 27-33.

80. Y.-d. Hong, et al., *Three-dimensional simulation of microwave heating coal sample with varying parameters.* Applied Thermal Engineering, 2016. **93**: p. 1145-1154.

81. B. Lin, et al., *Sensitivity analysis on the microwave heating of coal: A coupled electromagnetic and heat transfer model.* Applied Thermal Engineering, 2017. **126**: p. 949-962.

82. D. Salvi, et al., *Numerical modeling of continuous flow microwave heating: a critical comparison of COMSOL and ANSYS.* Journal of Microwave Power and Electromagnetic Energy, 2010. **44**(4): p. 187-197.

83. H. Li, et al., *A fully coupled electromagnetic-thermal-mechanical model for coalbed methane extraction with microwave heating.* Journal of Natural Gas Science and Engineering, 2017. **46**: p. 830-844.

84. H. Wang, et al., *Numerical modelling of microwave heating treatment for tight gas sand reservoirs.* Journal of Petroleum Science and Engineering, 2017. **152**: p. 495-504.

85. D. Whittles, S. Kingman, and D. Reddish, *Application of numerical modelling for prediction of the influence of power density on microwave-assisted breakage.* International Journal of Mineral Processing, 2003. **68**(1-4): p. 71-91.

86. J.C. Jaeger, N.G. Cook, and R. Zimmerman, *Fundamentals of rock mechanics*. 2009: John Wiley & Sons.

87. T. Teng, et al., *A thermally sensitive permeability model for coal-gas interactions including thermal fracturing and volatilization.* Journal of Natural Gas Science and Engineering, 2016. **32**: p. 319-333.

88. Y.-d. Hong, et al., *Effect of microwave irradiation on petrophysical characterization of coals.* Applied Thermal Engineering, 2016. **102**: p. 1109-1125.

89. I.T. Union, *Radio Regulations.* Radiocommunication Sector. ITU-R. Geneva, 2016.

90. P. Harrison, *A fundamental study of the effects of 2.45 GHz microwave radiation on the properties of minerals.* The University of Birmingham, Birmingham, UK, 1997.

91. C. Balanis, W. Rice, and N. Smith, *Microwave measurements of coal.* Radio Science, 1976. **11**(4): p. 413-418.

92. C.A. Balanis. *Electrical properties of coal at microwave frequencies for monitoring*. in *AIP Conference Proceedings*. 1981. AIP.

93. S. McGill and J. Walkiewicz, *Applications of microwave energy in extractive metallurgy.* Journal of Microwave Power and Electromagnetic Energy, 1987. **22**(3): p. 175-177.

94. J. Walkiewicz, G. Kazonich, and S. McGill, *Microwave heating characteristics of selected minerals and compounds.* Minerals & metallurgical processing, 1988. **5**(1): p. 39-42.

95. S. Kingman, *Recent developments in microwave processing of minerals.* International materials reviews, 2006. **51**(1): p. 1-12.

96. G.-m. Lu, et al., *The influence of microwave irradiation on thermal properties of main rock-forming minerals.* Applied Thermal Engineering, 2017. **112**: p. 1523-1532.

97. S. Kingman, W. Vorster, and N. Rowson, *The influence of mineralogy on microwave assisted grinding.* Minerals engineering, 2000. **13**(3): p. 313-327.

98. D.E. Clark and W.H. Sutton, *Microwave processing of materials.* Annual Review of Materials Science, 1996. **26**(1): p. 299-331.

99. A. Cumbane, *Microwave processing of Minerals.* University of Nottingham, Nottingham, UK, 2003.

100. M.A. Carrizales, *Recovery of stranded heavy oil by electromagnetic heating.* 2010.

101. L. Hardell, *World Health Organization, radiofrequency radiation and health-a hard nut to crack.* International journal of oncology, 2017. **51**(2): p. 405-413.

102. I.C.o.N.-I.R. Protection, *ICNIRP statement on the "Guidelines for limiting exposure to time-varying electric, magnetic, and electromagnetic fields (up to 300 GHz)".* Health Physics, 2009. **97**(3): p. 257-258.

103. S. Banik, S. Bandyopadhyay, and S. Ganguly, *Bioeffects of microwave—a brief review.* Bioresource technology, 2003. **87**(2): p. 155-159.

104. S.M. Hong, J.K. Park, and Y. Lee, *Mechanisms of microwave irradiation involved in the destruction of fecal coliforms from biosolids.* Water Research, 2004. **38**(6): p. 1615-1625.

105. H. Fröhlich, *The biological effects of microwaves and related questions*, in *Advances in electronics and electron physics*. 1980, Elsevier. p. 85-152.

106. A.B. Martínez, *The effects of microwaves on the trees and other plants.* Valladolid, Spain, 2003.

107. R. Kasevich, et al. *Pilot testing of a radio frequency heating system for enhanced oil recovery from diatomaceous earth*. in *SPE Annual Technical Conference and Exhibition*. 1994. Society of Petroleum Engineers.

108. M. Bientinesi, et al., *A radiofrequency/microwave heating method for thermal heavy oil recovery based on a novel tight-shell conceptual design.* Journal of Petroleum Science and Engineering, 2013. **107**: p. 18-30.

109. A. Davletbaev, L. Kovaleva, and T. Babadagli, *Mathematical modeling and field application of heavy oil recovery by Radio-Frequency Electromagnetic stimulation.* Journal of petroleum science and engineering, 2011. **78**(3-4): p. 646-653.

110. M.M. Abdulrahman and M. Meribout, *Antenna array design for enhanced oil recovery under oil reservoir constraints with experimental validation.* Energy, 2014. **66**: p. 868-880.

111. D.J. Black, N.I. Aziz, and R.M. Florentin. *Assessment of factors impacting coal seam gas production*. in *International Coalbed and Shale Gas Symposium*. 2010. University of Alabama Tuscaloosa, AL.

112. Y.-d. Hong, et al., *Influence of Microwave Energy on Fractal Dimension of Coal Cores: Implications from Nuclear Magnetic Resonance.* Energy & Fuels, 2016. **30**(12): p. 10253-10259.

113. J.-F. Zhu, et al., *Thin-layer drying characteristics and modeling of Ximeng lignite under microwave irradiation.* Fuel Processing Technology, 2015. **130**: p. 62-70.

114. H. Li, et al., *Assessing the moisture migration during microwave drying of coal using low-field nuclear magnetic resonance.* Drying Technology, 2018. **36**(5): p. 567-577.

115. J. Huang, et al., *Simulation of microwave's heating effect on coal seam permeability enhancement.* International Journal of Mining Science and Technology, 2018.

116. S. Sang, et al., *Stress relief coalbed methane drainage by surface vertical wells in China.* International Journal of Coal Geology, 2010. **82**(3): p. 196-203.

117. Q. Ye, et al., *Experimental study on the influence of wall heat effect on gas explosion and its propagation.* Applied Thermal Engineering, 2017. **118**: p. 392-397.

118. T. Teng, et al., *How moisture loss affects coal porosity and permeability during gas recovery in wet reservoirs?* International Journal of Mining Science and Technology, 2017. **27**(6): p. 899-906.

119. Q. Ye, et al., *Similarity simulation of mining-crack-evolution characteristics of overburden strata in deep coal mining with large dip.* Journal of Petroleum Science and Engineering, 2018. **165**: p. 477-487.

120. K. Pitchai, et al., *A microwave heat transfer model for a rotating multi-component meal in a domestic oven: development and validation.* Journal of Food Engineering, 2014. **128**: p. 60-71.

121. B. Wang, K. Xia, and G.-W. Wei, *Second order method for solving 3D elasticity equations with complex interfaces.* Journal of computational physics, 2015. **294**: p. 405-438.

122. C. Zhang, et al., *Permeability evolution model of mined coal rock and its numerical simulation.* Rock and Soil Mechanics, 2015. **36**(8): p. 2409-2418.

123. H. Chen, B.P. Marks, and R.Y. Murphy, *Modeling coupled heat and mass transfer for convection cooking of chicken patties.* Journal of Food Engineering, 1999. **42**(3): p. 139-146.

124. L. Liu, et al., *Relationship between moisture and dielectric properties of coal at terahertz band electromagnetic radiation.* Journal of China Coal Society, 2016. **41**(02): p. 497-501.

125. D. Peng and Q. Zhao, *Study on thermal conductivity of coal and rock.* Mining Safety & Environmental Protection, 2000. **27**(6): p. 16-18.

126. D. Bangham and R.E. Franklin, *Thermal expansion of coals and carbonised coals.* Transactions of the Faraday Society, 1946. **42**: p. B289-B294.

127. H. Li, et al., *Pore structure and multifractal analysis of coal subjected to microwave heating.* Powder Technology, 2019.

128. G. Xu, et al., *Calibration of Mine Ventilation Network Models Using the Non-Linear Optimization Algorithm.* Energies, 2017. **11**(1): p. 31.

129. H. Kumar, et al., *Optimizing enhanced coalbed methane recovery for unhindered production and CO2 injectivity.* International Journal of Greenhouse Gas Control, 2012. **11**: p. 86-97.

130. G. Hu, et al., *Evolution of shale microstructure under microwave irradiation stimulation.* Energy & Fuels, 2018.

131. X. Fu, et al., *Evaluation of gas content of coalbed methane reservoirs with the aid of geophysical logging technology.* Fuel, 2009. **88**(11): p. 2269-2277.

132. J. Zhao, et al., *High production indexes and the key factors in coalbed methane production: A case in the Hancheng block, southeastern Ordos Basin, China.* Journal of Petroleum Science and Engineering, 2015. **130**: p. 55-67.

133. M.B.D. Aguado and C.G. Nicieza, *Control and prevention of gas outbursts in coal mines, Riosa–Olloniego coalfield, Spain.* International Journal of Coal Geology, 2007. **69**(4): p. 253-266.

134. G. Yin, et al., *A new experimental apparatus for coal and gas outburst simulation.* Rock Mechanics and Rock Engineering, 2016. **49**(5): p. 2005-2013.

135. L.B. Colmenares and M.D. Zoback, *Hydraulic fracturing and wellbore completion of coalbed methane wells in the Powder River Basin, Wyoming: Implications for water and gas production.* AAPG bulletin, 2007. **91**(1): p. 51-67.

136. C. Cai, et al., *Experiment of coal damage due to super-cooling with liquid nitrogen.* Journal of Natural Gas Science and Engineering, 2015. **22**: p. 42-48.

137. S.L. Brantley, et al., *Water resource impacts during unconventional shale gas development: The Pennsylvania experience.* International Journal of Coal Geology, 2014. **126**: p. 140-156.

138. H. Boudet, et al., *"Fracking" controversy and communication: Using national survey data to understand public perceptions of hydraulic fracturing.* Energy Policy, 2014. **65**: p. 57-67.

139. M.L. Finkel and J. Hays, *The implications of unconventional drilling for natural gas: a global public health concern.* Public Health, 2013. **127**(10): p. 889-893.

140. D.A. Jones, et al., *Microwave heating applications in environmental engineering—a review.* Resources, conservation and recycling, 2002. **34**(2): p. 75-90.

141. S.W. Kingman, *Recent developments in microwave processing of minerals.* International materials reviews, 2006. **51**(1): p. 1-12.

142. G. Yin, et al., *An experimental study on the effects of water content on coalbed gas permeability in ground stress fields.* Transport in porous media, 2012. **94**(1): p. 87-99.

143. G. Ni, et al., *Experimental study on removing water blocking effect (WBE) from two aspects of the pore negative pressure and surfactants.* Journal of Natural Gas Science and Engineering, 2016. **31**: p. 596-602.

144. W. Guan, Y. Wen, and H. Chen, *Permeability enhancement method of microwave steam explosion for low permeability coal reservoir*. 2017: Google Patents.

145. Z. Rui, et al., *A quantitative oil and gas reservoir evaluation system for development.* Journal of Natural Gas Science and Engineering, 2017. **42**: p. 31-39.

146. Z. Rui, et al., *A realistic and integrated model for evaluating oil sands development with Steam Assisted Gravity Drainage technology in Canada.* Applied Energy, 2018. **213**: p. 76-91.

147. J. Zeng, et al., *Composite linear flow model for multi-fractured horizontal wells in heterogeneous shale reservoir.* Journal of Natural Gas Science and Engineering, 2017. **38**: p. 527-548.

148. Y.L. Zheng, Q.B. Zhang, and J. Zhao, *Effect of microwave treatment on thermal and ultrasonic properties of gabbro.* Applied Thermal Engineering, 2017. **127**: p. 359-369.

149. Z. Liu, et al., *Surface Properties and Pore Structure of Anthracite, Bituminous Coal and Lignite.* Energies, 2018. **11**(6): p. 1502.

150. W. Kenyon, *Nuclear magnetic resonance as a petrophysical measurement.* Nuclear Geophysics, 1992. **6**(2): p. 153-171.

151. G.R. Coates, L. Xiao, and M.G. Prammer, *NMR logging: principles and applications*. Vol. 344. 1999: Haliburton Energy Services Houston.

152. Y. Yao, et al., *Petrophysical characterization of coals by low-field nuclear magnetic resonance (NMR).* Fuel, 2010. **89**(7): p. 1371-1380.

153. A. Ranathunga, M. Perera, and P. Ranjith, *Deep coal seams as a greener energy source: a review.* Journal of Geophysics and Engineering, 2014. **11**(6): p. 063001.

154. J.C. Kurnia, A.P. Sasmito, and A.S. Mujumdar, *CFD simulation of methane dispersion and innovative methane management in underground mining faces.* Applied Mathematical Modelling, 2014. **38**(14): p. 3467-3484.

155. M.N. Heriawan and K. Koike, *Coal quality related to microfractures identified by CT image analysis.* International Journal of Coal Geology, 2015. **140**: p. 97-110.

156. S. Yang, et al., *Spontaneous combustion influenced by surface methane drainage and its prediction by rescaled range analysis.* International Journal of Mining Science and Technology, 2018. **28**(2): p. 215-221.

157. Y. Wu, et al., *Evaluation of gas production from multiple coal seams: A simulation study and economics.* International Journal of Mining Science and Technology, 2018.

158. D.K. Murray, *Coal bed methane; natural gas resources from coal seams.* Geology in Coal Resource Utilization. United States: Tech Books, 1991: p. 97-103.

159. W. Zhu, et al., *A model of coal–gas interaction under variable temperatures.* International Journal of Coal Geology, 2011. **86**(2-3): p. 213-221.

160. S. Brunauer, *The Adsorption of Gases and Vapors Vol I-Physical Adsorption*. Vol. 1. 2008: Brunauer Press.

161. J.-S. Bae, et al., *Pore accessibility of methane and carbon dioxide in coals.* Energy & Fuels, 2009. **23**(6): p. 3319-3327.

162. J.I. Joubert, C.T. Grein, and D. Bienstock, *Sorption of methane in moist coal.* Fuel, 1973. **52**(3): p. 181-185.

163. A. Tahmasebi, et al., *A kinetic study of microwave and fluidized-bed drying of a Chinese lignite.* Chemical Engineering Research and Design, 2014. **92**(1): p. 54-65.

164. S. Mesroghli, et al., *Evaluation of microwave treatment on coal structure and sulfur species by reductive pyrolysis-mass spectrometry method.* Fuel Processing Technology, 2015. **131**: p. 193-202.

165. N. Rowson and N. Rice, *Desulphurisation of coal using low power microwave energy.* Minerals Engineering, 1990. **3**(3-4): p. 363-368.

166. K. Pitchai, et al., *Coupled electromagnetic and heat transfer model for microwave heating in domestic ovens.* Journal of Food Engineering, 2012. **112**(1-2): p. 100-111.

167. T. Ciacci, A. Galgano, and C. Di Blasi, *Numerical simulation of the electromagnetic field and the heat and mass transfer processes during*

microwave-induced pyrolysis of a wood block. Chemical Engineering Science, 2010. **65**(14): p. 4117-4133.

168. G. Brodie, *The influence of load geometry on temperature distribution during microwave heating.* Transactions of the ASABE, 2008. **51**(4): p. 1401-1413.

169. H. Li, et al., *A fully coupled electromagnetic, heat transfer and multiphase porous media model for microwave heating of coal.* Fuel Processing Technology, 2019. **189**: p. 49-61.

170. H. Li, et al., *Pore structure and multifractal analysis of coal subjected to microwave heating.* Powder Technology, 2019. **346**: p. 97-108.

171. L. Tang, et al., *Exploration on the action mechanism of microwave with peroxyacetic acid in the process of coal desulfurization.* Fuel, 2018. **214**: p. 554-560.

172. L. Han, et al., *Application of transmission/reflection method for permittivity measurement in coal desulfurization.* Progress In Electromagnetics Research, 2013. **37**: p. 177-187.

173. R. Simpkin, *Derivation of Lichtenecker's logarithmic mixture formula from Maxwell's equations.* IEEE Transactions on Microwave Theory and Techniques, 2010. **58**(3): p. 545-550.